

**Parallel genetic adaptations to antibiotics, nutrients, and lifestyle by *Pseudomonas aeruginosa***

by

**Michelle Rachel Scribner**

Bachelor of Science, Alma College, 2016

Submitted to the Graduate Faculty of the  
School of Medicine in partial fulfillment  
of the requirements for the degree of  
Doctor of Philosophy

University of Pittsburgh

2021

UNIVERSITY OF PITTSBURGH

SCHOOL OF MEDICINE

This dissertation was presented

by

**Michelle Rachel Scribner**

It was defended on

November 9, 2021

and approved by

Jennifer M. Bomberger, PhD, Associate Professor, Department of Microbiology and Molecular Genetics

Anthony R. Richardson, PhD, Associate Professor, Department of Microbiology and Molecular Genetics

Robert M.Q. Shanks, PhD, Associate Professor, Department of Ophthalmology and Department of Microbiology and Molecular Genetics

Dissertation Director: Vaughn S. Cooper, PhD, Professor, Department of Microbiology and Molecular Genetics

Copyright © by Michelle Rachel Scribner

2021

## Parallel genetic adaptations to antibiotics, nutrients, and lifestyle by *Pseudomonas aeruginosa*

Michelle Rachel Scribner, PhD

University of Pittsburgh, 2021

Microbial evolution has critical implications for human health, from the increasing prevalence of antimicrobial resistance to the pathoadaptation of microbial populations during infection. The evolution of opportunistic pathogen *Pseudomonas aeruginosa* within the respiratory tract of people with cystic fibrosis is a prime example. Though ubiquitous within the environment, *P. aeruginosa* evolves new traits *in vivo* which contribute to reduced clearance of infection and consequent morbidity and mortality. Elucidating the mechanisms and dynamics by which pathogens, including *P. aeruginosa*, evolve is central to the efficacy of attempts to predict and control pathogen evolution.

In this work, we used evolution experiments to examine the influence of genetic background and environmental factors on adaptation of *P. aeruginosa*. We investigated the impact of three factors at play within the host environment: antibiotic pressure, nutrient availability, and biofilm lifestyle on selected genes and their evolutionary dynamics. *P. aeruginosa* populations were propagated in media mimicking the nutrient environment of the cystic fibrosis airways and analyzed using longitudinal whole genome sequencing of evolved populations. First, we determined the evolutionary pathways through which *P. aeruginosa* evolves resistance to the aminoglycoside antibiotic tobramycin and examined how genetic background affects evolution of drug resistance by comparing with results from identical experiments with *Acinetobacter baumannii*. In both species, we studied the impact of lifestyle on evolutionary dynamics by propagating populations in both planktonic (well-mixed) and biofilm environments. Populations

evolved through strikingly parallel adaptations across lineages, lifestyles, and even species with subtle, but notable, distinctions associated with biofilm lifestyle. In addition, parallel adaptations arose in replicate *P. aeruginosa* lineages propagated in the absence of drug that changed social interactions in several ways, including altered biofilm formation, quorum sensing, and prophage induction. Remarkably, every environment we examined selected for mutations in pathways commonly mutated during chronic human infection. These findings reveal that the evolution of persistence to stressors, including antibiotics, and rapid genetic and phenotypic diversification are not specific to host conditions. Ultimately, we have learned that *P. aeruginosa* adaptations to specific host conditions are rapid, somewhat predictable, and generate complex ecological interactions through mutations to regulators of biofilm, quorum sensing, and prophage.

## Table of Contents

Preface.....	xv
<b>1.0 Introduction.....</b>	<b>1</b>
<b>1.1 <i>Pseudomonas aeruginosa</i>.....</b>	<b>1</b>
1.1.1.1 Antibiotic resistance .....	3
1.1.1.2 Tobramycin .....	4
1.1.2 Biofilm .....	7
1.1.2.1 Biofilm regulation .....	7
1.1.2.2 Antibiotic tolerance of biofilms .....	10
1.1.3 Quorum sensing.....	12
1.1.4 Bacteriophage .....	13
<b>1.2 <i>P. aeruginosa</i> in the cystic fibrosis airways .....</b>	<b>16</b>
1.2.1 <i>In vivo</i> adaptation of <i>P. aeruginosa</i> .....	18
1.2.2 Clinical genomes of <i>P. aeruginosa</i> .....	19
<b>1.3 Microbial evolution experiments.....</b>	<b>22</b>
1.3.1 Using microbes to understand evolutionary processes .....	22
1.3.2 Evolution experiments as models of infection .....	25
<b>1.4 Goals of dissertation .....</b>	<b>27</b>
<b>2.0 Parallel evolution of tobramycin resistance across species and environments .....</b>	<b>29</b>
2.1 Project summary .....	30
2.2 Introduction .....	31
2.3 Results.....	33

2.3.1 Parallel evolution of TOB resistance phenotypes and genotypes .....	33
2.3.2 Environment-associated adaptations to TOB selection .....	43
2.3.3 Population-genetic dynamics of TOB resistance evolution .....	48
2.3.4 Parallelism of aminoglycoside resistance mechanisms across species.....	52
2.4 Discussion .....	57
2.5 Methods .....	61
2.5.1 Strains and media.....	61
2.5.2 Evolution experiment.....	62
2.5.3 Minimum inhibitory concentration assays .....	63
2.5.4 Biofilm assays .....	64
2.5.5 Genome sequencing and analysis.....	64
2.5.6 Resistance loci alignment and mutation mapping .....	67
2.5.7 Data availability .....	68
<b>3.0 The nutritional environment is sufficient to select coexisting biofilm and quorum</b>	
<b>sensing mutants of <i>Pseudomonas aeruginosa</i>.....</b>	<b>69</b>
3.1 Project summary .....	70
3.2 Introduction .....	71
3.3 Results.....	73
3.3.1 Genetic targets of evolution in CF nutrients mimic <i>in vivo</i> adaptation .....	73
3.3.2 Mutations in <i>lasR</i> , <i>morA</i> , and <i>wspF</i> underlie rapid morphological and	
phenotypic diversification .....	79
3.3.3 <i>morA</i> mutations produce adaptations specific to high nutrient concentration	
.....	85

3.3.4 <i>lasR</i> mutations are beneficial in the absence of a competitor .....	88
3.3.5 Ecological interactions between <i>morA</i> and <i>lasR</i> mutants facilitate the maintenance of diversity .....	91
3.4 Discussion .....	93
3.5 Methods .....	99
3.5.1 Evolution experiment.....	99
3.5.2 Whole genome sequencing and analysis.....	101
3.5.3 Analysis of <i>morA</i> mutations detected in laboratory and clinical environments .....	102
3.5.4 Morphology.....	103
3.5.5 Motility and biofilm assays.....	103
3.5.6 Fitness assays .....	104
3.5.7 Growth curves .....	104
3.5.8 Nutrient analysis .....	105
3.5.9 Statistical analysis .....	106
3.5.10 Data availability .....	106
<b>4.0 Prophage induction and rapid coevolution during laboratory propagation of <i>P.</i> <i>aeruginosa</i> .....</b>	<b>107</b>
<b>4.1 Project summary .....</b>	<b>108</b>
<b>4.2 Introduction .....</b>	<b>109</b>
<b>4.3 Results.....</b>	<b>113</b>
<b>4.3.1 Prophage Pf5 is induced at low levels during growth in CF nutrients.....</b>	<b>113</b>
<b>4.3.2 Mutant Pf5 genotypes invaded two evolved populations .....</b>	<b>114</b>

4.3.3 <i>pf5r</i> mutations stimulate Pf5 induction and replication of an uncharacterized element .....	117
4.3.4 Prophage induction is costly for fitness, but costs vary with genetic background.....	122
4.3.5 Mutant Pf5 rapidly evolves and infects neighboring cells.....	125
4.3.6 Pf5 induction increases the relative fitness of host cells even while decreasing absolute fitness.....	127
4.4 Discussion .....	129
4.5 Methods .....	133
4.5.1 Bacterial strains and culture conditions .....	133
4.5.2 Whole genome sequence analysis.....	134
4.5.3 qPCR .....	135
4.5.4 Growth curves .....	136
4.5.5 Fitness assays.....	136
4.5.6 Statistical analysis .....	137
4.5.7 Data availability .....	137
5.0 Conclusions.....	138
5.1 Parallelism is predictable.....	139
5.2 Simple is sufficient .....	142
5.3 Prophage are precarious .....	145
5.4 Future directions .....	146
5.5 Limitations .....	150
Appendix A Supplemental Material.....	153

<b>Appendix B List of Abbreviations .....</b>	<b>154</b>
<b>Bibliography .....</b>	<b>156</b>

## List of Tables

<b>Table 1. Evolved mutant clones genotyped by WGS demonstrate increased TOB resistance relative to the ancestral clone.....</b>	<b>42</b>
<b>Table 2. Evolved mutant clones genotyped by WGS demonstrate increased tobramycin resistance in a biofilm environment relative to the ancestral clone. ....</b>	<b>42</b>
<b>Table 3. Datasets of <i>P. aeruginosa</i> clinical isolates were analyzed to reveal gene and residue-level parallelism within the aminoglycoside resistance loci observed in this study..</b>	<b>57</b>
<b>Table 4. Genotypes isolated from evolved populations in Chapter 3.....</b>	<b>100</b>
<b>Table 5. Populations propagated in CF nutrients evolved mutations within Pf5. ....</b>	<b>114</b>
<b>Table 6. <i>pf5r</i> mutations induce Pf5 excision and circularization.....</b>	<b>119</b>
<b>Table 7. Primers used for quantification of Pf5 excision and circularization by qPCR. ...</b>	<b>121</b>
<b>Table 8. Average read depth of PA14 and Pf5 genomes for isolated clones.....</b>	<b>122</b>
<b>Table 9. Mutant Pf5 rapidly superinfects ancestral <i>P. aeruginosa</i>, evolves, and integrates at new sites. ....</b>	<b>126</b>

## List of Figures

<b>Figure 1. Parallel evolution of tobramycin resistance level across species and environment.</b> .....	<b>35</b>
<b>Figure 2. Minimum inhibitory concentration of <i>P. aeruginosa</i> evolved populations on day twelve in the minimal media used in the evolution experiment and Mueller Hinton Broth.....</b>	<b>37</b>
<b>Figure 3. Population sequencing reveals interspecies parallelism and lifestyle-dependence of molecular targets of evolution.....</b>	<b>38</b>
<b>Figure 4. Population sequencing reveals molecular adaptations to tobramycin and biofilm selection.....</b>	<b>39</b>
<b>Figure 5. MICs and biofilm production of <i>P. aeruginosa fusA1</i>, <i>fusA1 orfN</i>, and <i>ptsP</i> mutants compared to the ancestral genotype.....</b>	<b>43</b>
<b>Figure 6. Allele frequency plots of three populations from each treatment.....</b>	<b>47</b>
<b>Figure 7. Evolutionary dynamics of bacterial populations in increasing concentrations of tobramycin.....</b>	<b>50</b>
<b>Figure 8. Parallelism of mutations in genetic loci associated with aminoglycoside resistance across species .....</b>	<b>55</b>
<b>Figure 9. Propagation of <i>P. aeruginosa</i> in nutrients present in the CF airway rapidly selects for mutations in regulators of quorum sensing and cyclic-di-GMP.....</b>	<b>76</b>
<b>Figure 10. Parallel evolution of mutations in <i>lasR</i> and <i>morA</i> reveal sites under strong selection.....</b>	<b>77</b>

Figure 11. Mutated residues within MorA detected in this experiment, other laboratory experiments and clinical isolates are illustrated on the structure of the PAO1 MorA DGC and PDE domains (PDB 4RNF).....	78
Figure 12. Mutations in the <i>lasR</i> , <i>morA</i> , and <i>wspF</i> genes produce rapid morphological diversity over short timescales. ....	81
Figure 13. Mutations in <i>lasR</i> and in multiple cyclic-di-GMP regulators produce coexisting subpopulations with distinct biofilm and motility phenotypes. ....	83
Figure 14. Decreased swarming motility of all clones isolated from evolved populations..	84
Figure 15. Environment-specific fitness advantages of <i>lasR</i> and <i>morA</i> mutants. ....	86
Figure 16. Growth curves of evolved clones in different carbon sources reveal distinct growth advantages for mutants with <i>morA</i> and <i>lasR</i> alterations. ....	87
Figure 17. <i>lasR</i> mutations increase growth yield in independent culture.....	89
Figure 18. HPLC analysis of supernatants from a <i>lasR</i> R216Q mutant and the ancestral strain reveal that nutrients are consumed at similar rates between the two genotypes. ....	90
Figure 19. Relative fitness of <i>lasR</i> and <i>morA</i> mutants is greater when in the minority. ....	92
Figure 20. The negative frequency dependence relationship between <i>lasR</i> and <i>morA</i> mutants persists across similar genotypes. ....	93
Figure 21. Excision and circularization of Pf5, a prophage within <i>P. aeruginosa</i> strain PA14, can be detected by deep whole genome sequencing. ....	112
Figure 22. Increased replication of Pf5 in planktonic population 5. ....	116
Figure 23. Increased replication of a truncated Pf5 genome in biofilm population 1. ....	117

**Figure 24. *pf5r* mutations increase replication of Pf5 and an uncharacterized circular element. .... 120**

**Figure 25. Increased Pf5 excision and circularization was confirmed for *pf5r* mutants by qPCR. .... 121**

**Figure 26. *pf5r* mutations are costly to the host cell. .... 124**

**Figure 27. Mutant Pf5 superinfects ancestral *P. aeruginosa* and increases Pf5 induction. 127**

**Figure 28. Strains with mutant *pf5r* outcompete those with WT *pf5r*. .... 129**

## Preface

This dissertation could not have been completed without the encouragement and mentorship of several individuals. I would like to thank my thesis advisor, Dr. Vaughn Cooper, for coaching me through the process of graduate school and the unexpected hurdle of completing my degree during a pandemic. Over the last several years I have received the training and flexibility I needed to pursue the topics that I am passionate about, for which I am truly grateful. I am also thankful for my committee: Dr. Jen Bomberger, Dr. Tony Richardson, and Dr. Rob Shanks. Their time and attention are valuable resources, and my project has benefitted enormously from their involvement. I am also thankful for the mentors that introduced me to research as an undergraduate and made it possible for me to pursue graduate training: Dr. Laura Machesky, Dr. Emma Woodham, Dr. Tim Keeton, and Prof. Murray Borrello. I would also like to thank my current and former labmates for their support, advice, inspiration, and comradery, especially Caroline, Chris, Alfonso, and Eisha for showing me the ropes during my grad school “lag phase”. I am also grateful for the lab mates and MMG colleagues who challenged and encouraged me over the last several years, including those I worked with for the projects described in my dissertation: Alfonso, Chris Marshall, Chris Deitrick, Brayan, Justin, Nanami, and Amie.

Finally, I am thankful for the family and friends who have supported me during my time in graduate school and all the stages of life leading up to it. I am fortunate to have been raised by a small army of parents and grandparents who did everything in their power to create opportunities for me. I know that I could not have accomplished this, or anything else prior, without you. To my sisters: having you in my life has pulled me through the hardest of times, and I feel so lucky to share this and all our other life events with you. And of course, thank you to the friends that have

encouraged me over the last several years, particularly my quilt contributors, my pandemic pod, the Black Hole, Drew, Alec, and Goose. To all my family and friends: thank you for believing that I could reach this point and helping me to believe it too.

## 1.0 Introduction

### 1.1 *Pseudomonas aeruginosa*

*Pseudomonas aeruginosa* is a ubiquitous Gram-negative bacterium known for its ability to thrive in a diverse range of niches, from environmental sources to humans with immune deficiencies (Moradali et al., 2017). Metabolic and pathogenic versatility is a hallmark of the species. Contributing to this versatility is its large and plastic genome (5-7 Mbp), which harbors a genetic repertoire sufficient for survival in many environments, including intrinsic resistance to antibiotics and growth in diverse nutrient conditions (Mathee et al., 2008). In addition, *P. aeruginosa* possesses a high proportion of regulatory genes (~10% of genes in strain PAO1) that enable transient changes in the presence of stressors (Stover et al., 2000). Among the most clinically relevant of these changes are the induction of antibiotic efflux and biofilm formation (Ciofu and Tolker-Nielsen, 2019). *P. aeruginosa* also demonstrates further adaptation to harsh conditions by evolving multidrug resistance through the acquisition of new genetic material and mutations (Pang et al., 2019).

*P. aeruginosa* acts as an opportunistic pathogen that produces persistent infections in lungs, wounds, the urinary tract, and blood. The incidence of multidrug resistant *P. aeruginosa* is increasing, thus it is classified as an ESKAPE pathogen and serious antimicrobial resistance (AMR) threat by the CDC (Centers for Disease Control and Prevention (U.S.), 2019; De Oliveira et al., 2020). In 2017, multidrug resistant *P. aeruginosa* was responsible for 32,600 hospitalizations and 2,700 deaths in the United States (Centers for Disease Control and Prevention (U.S.), 2019).

It is particularly detrimental to life expectancy for people with the genetic disease cystic fibrosis (CF), thus motivating the choice of cystic fibrosis respiratory infections as a focus of this thesis.

Phylogenetic analysis of *P. aeruginosa* isolates generally indicates that most genomes cluster into two groups (Freschi et al., 2019; Ozer et al., 2019). The two most frequently used laboratory strains of *P. aeruginosa*, PAO1 (Holloway, 1955) and UCBPP-PA14 (PA14) (Rahme et al., 1995; Schroth et al., 2018), are representative of these two groups (Ozer et al., 2019; Wiehlmann et al., 2007). Both strains were initially isolated from wound infections (Holloway, 1955; Rahme et al., 1995). Though many differences exist between clusters, several distinguishing traits are the effector proteins secreted by the type III secretion system, O antigen biosynthesis genes (Ozer et al., 2019), and exopolysaccharides secreted during biofilm formation (Colvin et al., 2011; Lee et al., 2006). Both groups are detected from environmental and clinical sources, and do not cluster by geography (Ozer et al., 2019). However, strains from the PAO1 cluster are overrepresented in respiratory infections in people with cystic fibrosis, whereas strains from the PA14 cluster make up the majority of those detected in infections of the eye, ear, and nose (Ozer et al., 2019). PA14 is the strain used for all *P. aeruginosa* experiments described in this work. PA14 is a virulent burn wound isolate with two pathogenicity islands that are not present in PAO1 (108kb PAPI-1 and 11kb PAPI-2) (He et al., 2004). Though it may seem counterintuitive to examine adaptation to the CF environment using a strain that is less representative of CF isolates, evolution of a strain that is less adapted to the CF environment reveals the adaptations that are critical to fitness in this environment. This strain was also used for previous investigations of how the biofilm lifestyle affects evolution in our laboratory (Flynn et al., 2016; Harris et al., 2021), and is a frequent model for studies of biofilm formation (Ha et al., 2014a; O'Toole and Kolter, 1998) and biofilm-associated infection (Gloag et al., 2019; Marshall et al., 2021).

### 1.1.1.1 Antibiotic resistance

The evolution of antimicrobial resistance is an increasingly concerning problem in *P. aeruginosa* (Pang et al., 2019). As in other bacterial pathogens, antimicrobial resistance is generally conferred by alterations in the target of the antibiotic, interference with the antibiotic itself, increased efflux, or reduced cell permeability (Blair et al., 2015; Pang et al., 2019). Alternatively, resistance can be categorized by intrinsic, adaptive, or acquired mechanisms. *P. aeruginosa* has high levels of intrinsic resistance due to low outer membrane permeability, high expression of efflux pumps, and production of drug inactivating enzymes like beta-lactamases (Breidenstein et al., 2011). *P. aeruginosa* also produces adaptive mechanisms, or alterations in gene and protein expression that promote survival, through the formation of biofilms, as discussed in the next section. Acquired mechanisms encapsulate both resistance genes acquired from the environment and *de novo* mutations, the former of which is relevant *in vivo* but not the focus of this work.

Many mutations that confer antimicrobial resistance in *P. aeruginosa* have been established. A few representative examples include mutations which induce overexpression of efflux pumps (*nalD*, *mexZ*, *nfxB*) to confer resistance to aminoglycosides, beta lactams, and fluoroquinolones (Cabot et al., 2016). Also, mutations which impair porins (OprD) can increase resistance to drugs which require porins to enter the cell (Fang et al., 2014). Mutations that alter the target of a drug have also been detected, the most frequent of which are mutations in DNA gyrase for fluoroquinolone resistance (Ahmed et al., 2018; Feng et al., 2016), penicillin binding proteins for beta-lactam resistance (Moyá et al., 2012), and two component regulatory systems (PhoPQ and PmrAB) for polymyxin resistance (Moskowitz et al., 2012). Finally, mutations causing overexpression of drug inactivating enzymes (*ampC* beta-lactamase) have been reported for beta-

lactam resistance (Berrazeg et al., 2015). These findings derive from transposon mutagenesis screens, evolution experiments in the presence of antibiotic, and sequence analysis of clinical isolates. However, our knowledge of the spectrum of resistance mechanisms in *P. aeruginosa* is biased in favor of transposon mutagenesis screens and other loss of function mutations at the expense of *de novo* mutations like single nucleotide substitutions (SNPs) and structural rearrangements, which likely contribute significantly to resistance *in vivo*.

Development of new drugs to treat bacterial infection is lagging considerably behind the rate at which pathogens acquire resistance, therefore, optimizing use of existing drugs is a key goal. For example, resistance to one antibiotic may produce fitness costs that increase sensitivity to other antibiotics, a phenomenon termed collateral sensitivity (Imamovic and Sommer, 2013). Alternatively, cross resistance can occur, or the development of resistance to one antibiotic that produces resistance to another antibiotic (Jansen et al., 2016). Identifying and exploiting collateral sensitivity networks in the drugs used to treat cystic fibrosis could serve to optimize drug efficacy without increasing drug concentration or dosage. The underlying mechanisms of antimicrobial resistance determine the predictability and nuances of these relationships, therefore better understanding of the mutations that confer resistance to frequently used drugs is key to improving treatment efficacy. Here, we aim to reveal the genetic and phenotypic mechanisms that may be worthy of consideration for *P. aeruginosa* treatment strategies, particularly regarding aminoglycosides.

### **1.1.1.2 Tobramycin**

A variety of antibiotics as well as modes of delivery are prescribed for *P. aeruginosa* infections in people with cystic fibrosis, including intravenous, oral, and inhaled drugs (Cystic

Fibrosis Patient Registry, 2019). The use of inhaled antibiotics has become a common treatment strategy as they allow for delivery of high concentrations of drug to the site of infection without systemic administration (Saiman et al., 1996). For example, inhaled tobramycin and aztreonam are used to treat *P. aeruginosa* (Maselli et al., 2017). As a result, we chose tobramycin, a bactericidal aminoglycoside antibiotic that kills bacterial cells by disrupting translation, as the primary antibiotic to examine for this work.

Tobramycin can inhibit translation by binding to the A site of the ribosome at helix 44 of the 16S rRNA, which impairs both tRNA selection and translocation (Gutierrez et al., 2013). Aminoglycosides have also been shown to bind helix 69 of the 23S rRNA and prevent ribosome recycling (Borovinskaya et al., 2007). Importantly, unlike beta-lactams or fluoroquinolones, aminoglycosides must bind to the negatively-charged lipopolysaccharides of the outer membrane for active transport into the cell (Hancock et al., 1981; Krause et al., 2016; Peterson et al., 1985). Binding of aminoglycosides to the outer membrane in this manner may also induce cell killing (Bulitta et al., 2015; Kadurugamuwa et al., 1993).

Several mechanisms of resistance to tobramycin are currently known for *P. aeruginosa* (Bolard et al., 2017; Doi et al., 2016; Schurek et al., 2008). Aminoglycoside modifying enzymes may be acquired during infections to confer high levels of resistance (Poole, 2005). However, impermeability and efflux have been reported to be a more prevalent mode of aminoglycoside resistance in isolates from cystic fibrosis (Hurley et al., 1995; MacLeod et al., 2000). Further, efflux pump overexpression, most frequently observed for the MexXY efflux pump due to mutations to the *mexZ* gene, have been observed previously (López-Causapé et al., 2017; Prickett et al., 2017). Mutations to the target site in ribosomal RNA genes have also been reported, but infrequently (Garneau-Tsodikova and Labby, 2016). Mutations in *fusA1*, encoding elongation

factor G, are detected in clinical isolates from people with CF and have been shown to confer resistance to tobramycin *in vitro* (Bolard et al., 2017). Elongation factor G is a GTPase that catalyzes translocation during translation and binds where these helices form a bridge to catalyze separation of the two subunits. However, the full spectrum of resistance mechanisms to this antibiotic and the dynamics of resistance evolution, including their order, combination, and associated fitness costs remain unknown. In addition, adaptive resistance through increased expression of biofilm or transition to anaerobic growth, which may interfere with aminoglycoside uptake, are also critical to treatment failure (Karlowsky et al., 1997), and the impact of these processes on resistance evolution is incompletely understood.

For people with cystic fibrosis, tobramycin is frequently prescribed in cyclic treatments in which tobramycin is administered for four weeks followed by a four week hiatus (Vázquez-Espinosa et al., 2015). This approach is motivated by the finding that cyclical drug treatments are effective in improving patient outcomes (Ramsey et al., 1999) and is intended to reduce evolution of drug resistance by allowing susceptible organisms to increase in frequency during periods without antibiotic treatment (Gilligan, 1991). The underlying assumption of this strategy is that antibiotic resistance mechanisms produce fitness costs in the absence of drug and will be outcompeted by susceptible organisms in the absence of antibiotic pressure (Andersson and Hughes, 2010). However, while many antibiotic resistance mechanisms are costly, others have been shown to produce little or no cost (Melnyk et al., 2015, 2017). Furthermore, resistant bacteria can acquire compensatory mutations which increase the fitness of resistant subpopulations in the absence of drug (Dunai et al., 2019). The fitness of antibiotic resistance mutations is unknown in most strains and antibiotic combinations; therefore, it is unclear to what extent drug cycling regimes are advantageous for slowing the spread of resistance. As a result, characterizing the

mutations acquired during antimicrobial treatment and their impact on subsequent evolution is critical to improving treatment regimens and antibiotic stewardship.

### **1.1.2 Biofilm**

Biofilms, or communities of bacteria within an extracellular matrix, are a major mechanism of tolerance to stresses for bacteria, including *P. aeruginosa* populations. Biofilms are frequently described as surface-associated communities, though aggregates encased in exopolysaccharides detected in CF sputum suggest that non-surface-associated communities are prevalent *in vivo* (Jennings et al., 2021). *P. aeruginosa* biofilms are composed of polysaccharides, protein, and exogenous DNA (Ma et al., 2009). The primary protein within the biofilm matrix of many *P. aeruginosa* strains is CdrA, an adhesin (Reichhardt et al., 2020). *P. aeruginosa* is capable of producing multiple polysaccharides including Psl, Pel, and alginate, however, the primary polysaccharide within the biofilm matrix varies by strain (Colvin et al., 2011; Ryder et al., 2007). Although Psl plays an important role in attachment for PAO1, PA14 is incapable of producing Psl, thus Pel is the primary polysaccharide within its biofilms (Colvin et al., 2011, 2012). Likewise, isolates from people with cystic fibrosis often express high levels of alginate due to mutations acquired during infection, thus are referred to as mucoid (Govan and Deretic, 1996), but many strains, including PAO1 and PA14, are non-mucoid.

#### **1.1.2.1 Biofilm regulation**

Several complex and interconnected regulatory systems are associated with regulation of biofilm formation in *P. aeruginosa* (Fazli et al., 2014). Two second messenger systems are known

to influence biofilm formation: cyclic diguanosine-5'-monophosphate (cyclic-di-GMP) and cyclic adenosine monophosphate (cyclic-AMP). Cyclic-di-GMP influences a number of cell processes and is regarded as one of the primary regulators of biofilm lifestyle (Ha and O'Toole, 2015; Jenal et al., 2017). Increased cyclic-di-GMP is associated with increased production of extracellular matrix components and decreased expression of flagellar genes (Ha and O'Toole, 2015). This messenger acts through a number of mechanisms, including, transcriptional, post-transcriptional, and post-translational (Ha and O'Toole, 2015). Cyclic-di-GMP levels are controlled by diguanylate cyclases (DGC) and phosphodiesterases (PDE), which increase and decrease levels, respectively. These domains are present in about 40 different genes within *P. aeruginosa* and can occur within the same proteins (Ha et al., 2014a). Several of these proteins have been shown to influence biofilm formation, particularly the DGCs SadC, WspR, and YfiN and the PDE BifA (Chang, 2018). Quorum sensing systems, which are regulatory systems in which cells secrete and sense signaling molecules to coordinate gene regulation with cell density, also regulate pathways associated with biofilm formation, and will be discussed in greater detail in a subsequent section. Other pathways, particularly those involving GacA/GacS and RetS, which influence the expression of small RNAs, are also involved in biofilm regulation (Fazli et al., 2014; Gloag et al., 2019).

The ability of bacteria to sense and respond to surfaces is an active area of research in which *P. aeruginosa* is a prominent model organism (Chang, 2018). *P. aeruginosa* engages in initial, reversible attachment via extracellular appendages (flagella and type IV pili), followed by activation of signaling pathways that enable irreversible attachment (Lee et al., 2020). The Wsp and Pil-Chp systems represent two pathways which contribute to biofilm initiation. The Wsp system involves WspA, a chemoreceptor which modulates levels of cyclic-di-GMP via WspR, a diguanylate cyclase domain-containing protein (Güvener and Harwood, 2007; O'Connor et al.,

2012). In addition, surface sensing occurs via type IV pili through the Pil-Chp system (Luo et al., 2015). Polarly-localized type IV pili transmit a signal to CyaB, which increases cyclic-AMP. Subsequently, cyclic-AMP results in production of PilY1, which increases cyclic-di-GMP production through SadC (Luo et al., 2015).

Recent studies have shown that *P. aeruginosa* strains exhibit different behavior during initiation of biofilm formation (Kasetty et al., 2021). The Wsp system is known to play an integral role in biofilm formation in PAO1 (Armbruster et al., 2019), whereas surface sensing is thought to predominately occur through the Pil-Chp system in PA14 (Luo et al., 2015). This, combined with the absence of Psl polysaccharide in PA14, results in distinct characteristics of biofilm formation between PAO1 and PA14-like strains (Colvin et al., 2011; Friedman and Kolter, 2004). In addition, recent work suggests that PAO1 and PA14 are best suited for biofilm formation under distinct conditions and therefore may inhabit different ecological niches (Kasetty et al., 2021). Specifically, in direct competition of PAO1 and PA14, PAO1 was shown to possess an advantage in early biofilms that is dependent on Psl, whereas PA14 was more adept at invading preformed biofilms (Kasetty et al., 2021).

In addition to its intrinsic ability to form biofilms, *P. aeruginosa* can acquire *de novo* mutations that further increase biofilm production. Mutations that alter the function of regulators that overexpress biofilm production are among these genotypes detected both *in vivo* and *in vitro* (Flynn et al., 2016; Gloag et al., 2019; Harrison et al., 2020; Häussler et al., 1999; Marshall et al., 2021). For instance, mutations which increase levels of cyclic-di-GMP have been shown to increase biofilm, particularly mutations to the Wsp pathway (Gloag et al., 2019). Mutations to other genetic architecture, including flagellar genes, can also increase biofilm formation (Harrison et al., 2020). High-biofilm variants are frequently identified due to altered colony morphology,

including the rugose small colony variant phenotype (RSCV) (Gloag et al., 2019; Starkey et al., 2009).

### **1.1.2.2 Antibiotic tolerance of biofilms**

Biofilms can produce tolerance to a number of stresses, including antimicrobial stress, through multifactorial mechanisms (Billings et al., 2013; Ciofu and Tolker-Nielsen, 2019; Costerton et al., 1999; Walters et al., 2003). Biofilm can produce a physical barrier delaying antibiotic from reaching the cell if the antibiotic is unable to penetrate the biofilm. This has been demonstrated for charged antibiotics, like aminoglycosides, but is less pertinent for non-charged drugs (Tseng et al., 2013). Biofilms may also contribute to resistance to beta-lactam drugs if secreted beta-lactamases within a biofilm inactivate a drug before it is able to penetrate to the cell (Ciofu et al., 2000). Biofilms also produce nutrient gradients that permit a bacterial population to exist in multiple physiological states. Many classes of antimicrobials induce cell killing only in metabolically active cells, therefore cells within a biofilm may be tolerant to antimicrobials (Høiby et al., 2010). Oxygen gradients, for instance, cause the inner regions of a biofilm to have low oxygen concentrations or become anaerobic, the metabolic effects of which may induce antibiotic tolerance (Walters et al., 2003; Werner et al., 2004). Slow growth rate may be a particularly relevant mechanism of survival of *P. aeruginosa* in the CF lung environment, as slow growth phenotypes were reported from biofilms within CF sputum (Bjarnsholt, 2013; Ciofu et al., 2015; Yang et al., 2008). Finally, biofilms may produce transcriptional changes that increase tolerance. *P. aeruginosa* mutants with alterations that overexpress biofilm may be particularly tolerant to antimicrobial treatment (Goltermann and Tolker-Nielsen, 2017).

Biofilms also have the potential to alter the evolution of antimicrobial resistance for several reasons. For instance, the strength of antibiotic selection perceived by cells within a biofilm can differ from that of cells in a well-mixed environment due to the factors described above, like producing a physical barrier to antibiotic penetration or altered metabolic states (Billings et al., 2013; Tseng et al., 2013; Walters et al., 2003). As a result, different mechanisms of resistance may be advantageous within biofilms than in well-mixed environments. In addition, the spatially structured nature of biofilms could influence the evolutionary dynamics of resistance through two mechanisms. First, whereas cells in a well-mixed environment must compete against all other cells in the population, resulting in selection of the most fit haplotype, spatial separation of cells within a biofilm means that cells must compete only with neighboring cells, which may allow less fit haplotypes to persist in the population. This process is known as clonal interference, and may slow the rate of fixation and thus produce evolution of greater diversity in biofilms than in well-mixed environments (France et al., 2019). Second, the spatial structure of biofilms may produce distinct ecological environments within bacterial populations (Poltak and Cooper, 2011), in which different mechanisms of antibiotic resistance may confer greater fitness advantage. This may also facilitate the evolution of diversity. While studies from our laboratory and others have demonstrated that growth in a biofilm lifestyle alters the dynamics and mechanisms of antibiotic resistance (Ahmed et al., 2018; France et al., 2019; Santos-Lopez et al., 2019), the impact of biofilms on evolution of resistance remains untested in most combinations of bacterial species and antibiotics.

### 1.1.3 Quorum sensing

*P. aeruginosa*, like many bacterial species, uses quorum sensing to coordinate gene regulation with cell density (Papenfort and Bassler, 2016). Quorum sensing systems function through the secretion of signaling molecules called autoinducers, which are sensed by other bacteria to trigger expression of specific genes at high cell densities. As a result, quorum sensing enables sensing of the local density of “self” for bacterial populations. *P. aeruginosa* harbors multiple interconnected quorum sensing systems that regulate gene expression. It possesses two *N*-acyl-homoserine-lactone (AHL) systems: LasI-LasR and RhlI-RhlR (Gambello and Iglewski, 1991; Pearson et al., 1995). LasI and RhlI catalyze the production of diffusible signals, 3OC12-HSL and C4-HSL, respectively, which enter neighboring cells and bind the receptor portion of these systems, LasR and RhlR (Schuster et al., 2013; Waters and Bassler, 2005). The receptor proteins are then able to alter the expression of genes within their massive regulons (Schuster et al., 2003; Whiteley et al., 1999). *P. aeruginosa* was later discovered to produce a third quorum sensing signal, 2-heptyl-3-hydroxy-1H-quinolin-4-one, named *Pseudomonas* quinolone signal (PQS) (Pesci et al., 1999). Enzymes which synthesize PQS and its precursor 2-heptyl-1H-quinolin-4-one (HHQ) are encoded by the *pqsA-E* operon. Both signals are released from cells and induce transcriptional changes in neighboring cells through binding to the regulator PqsR (also referred to as MvfR) (Cao et al., 2001; Déziel et al., 2004).

These quorum systems are highly interconnected and influence each other in several ways. The LasIR system was previously thought to be the top of the quorum sensing hierarchy, as LasR can regulate the expression of *lasI*, *rhlI*, and *rhlR* (Gilbert et al., 2009; Pesci et al., 1997). LasR was later discovered to regulate the expression of MvfR, and PqsE able to regulate RhlR (Groleau et al., 2020; Mukherjee et al., 2018). The genes within each regulon have also been shown to be

highly overlapping. These genes include virulence factors like proteases (Gambello et al., 1993), elastase (Rust et al., 1996), rhamnolipids (Pearson et al., 1997), phenazines (Higgins et al., 2018), and hydrogen cyanide (Pessi and Haas, 2000).

Many of the virulence factors controlled by these quorum sensing systems are regarded as public goods because they are secreted factors that benefit the entire population. The presence of public goods renders populations susceptible to “cheaters”, or members of the population that utilize the public goods produced by other cells without producing them themselves (Smith and Schuster, 2019). Cells that are defective in quorum sensing, like those with loss of function mutations in *lasR*, are therefore examples of cheaters, and have been found to readily evolve in microbial populations (Chen et al., 2019; Sandoz et al., 2007). However, the quorum sensing regulons also include a number of genes that are not directly related to virulence factor expression, including stress response genes and genes associated with metabolism (D’Argenio et al., 2007). Therefore, it stands to reason that quorum sensing mutants may be selected for reasons other than cheating. Regardless, the evolution of mutations in quorum sensing regulators has potential to substantially alter the physiology of their populations. However, the fitness effects of quorum sensing mutants in *P. aeruginosa* are incompletely understood.

#### **1.1.4 Bacteriophage**

Many *P. aeruginosa* isolates (~36-52%) harbor filamentous prophage of the Inoviridae family, called Pf1-like phage (Burgener et al., 2019). Phage may be either lytic, meaning that they lyse their bacterial host following infection, or temperate, meaning that they can integrate their genomes into the host chromosome through a process called lysogeny. Following lysogeny, temperate phages can spontaneously induce phage excision and replication. Alternatively,

temperate phage can replicate their genomes extrachromosomally as an episome (Mai-Prochnow et al., 2015). Filamentous phages are temperate and have circular, single-stranded DNA genomes (Mai-Prochnow et al., 2015). Those of the Inoviridae family exist in both Gram-negative and Gram-positive bacterial species (Roux et al., 2019), and certain examples are well studied, including the CTX $\phi$  phage in *Vibrio cholera* (Davis et al., 2002) and Ff phage in *E. coli* (Hay and Lithgow, 2019). Phages in the Inoviridae family are unique in that they can extrude virions from the cell without lysis of the host (Hay and Lithgow, 2019). They also may harbor virulence factors that play critical roles in host fitness, including cholera toxin in the case of CTX $\phi$ .

The first filamentous phage described in *P. aeruginosa* was Pf1 in strain K (PAK) (Takeya and Amako, 1966). Pf1 is maintained as an episome, whereas PAO1 and PA14 harbor phages Pf4 and Pf5 as integrated prophage, respectively (Mooij et al., 2007). The Pf1-like prophage within *P. aeruginosa* are thought to derive from an ancestral prophage that evolved strain specificity due to differentiation of their type-IV pili receptors (Mai-Prochnow et al., 2015). Pf5 is 10.6 kbp in length and is integrated at nucleotide 4,345,126 within the PA14 strain. Like other Pf1-like phage, it harbors genes encoding an integrase, replication initiation protein, excisionase, repressor, single stranded DNA binding protein, and coat proteins (Li et al., 2019). These phage require host polymerases to replicate. Lysogeny is maintained by expression of the prophage repressor, which inhibits the expression of the excisionase. As a result, loss of function mutations to the repressor gene of Pf4 (*pf4r*) derepress excision and produce high levels of prophage activation (Li et al., 2019; McElroy et al., 2014).

Filamentous phage begin their lifecycle by attaching to the host cell through host surface receptors, including type IV pili in the case of *P. aeruginosa* (Castang and Dove, 2012). In *E. coli*, retraction of the pili draws the virion into the periplasm, where it interacts with TolA for entry into

the cytoplasm (Riechmann and Holliger, 1997). Host polymerases then synthesize the complementary strand of DNA to form the double stranded genome, which can either insert into the host chromosome or form the circular replicative form (Higashitani et al., 1997). To integrate, filamentous phage must possess an *attP* site with homology to *attB* sites within the host chromosome. Subsequently, Pf phages sense host stress, particularly oxidative stress, to either maintain lysogeny or induce the lytic cycle (Hui et al., 2014).

Several environmental factors associated with triggers inducing lysis versus lysogeny have been characterized in *P. aeruginosa* strains. In PAO1, exposure to agents that induce production of reactive oxygen and nitrogen species including mitomycin C, H<sub>2</sub>O<sub>2</sub>, and nitric oxide increase Pf4 phage production (Hui et al., 2014). A possible mechanism by which Pf phage sense the cellular environment is through OxyR, a transcriptional regulator induced by oxidative stress that controls expression of a number of downstream genes (Zheng et al., 1998) and binds to genes within Pf4 (Wei et al., 2012). The increased oxidative stress within a biofilm environment (Webb et al., 2003) may therefore contribute to the high levels of Pf phage gene expression in biofilms (Whiteley et al., 1999). A few other pathways have also been associated with Pf phage induction, including the protein DppA1, which induces Pf5 replication when inactivated (Lee et al., 2018), and the MvaT and MvaU DNA-binding proteins in the H-NS family, in which inactivation also induces prophage replication (Li et al., 2009a). While the prophage repressor gene normally provides protection from infection by exogenous phage, or superinfection, high levels of phage can overcome these defenses and enable superinfection (McElroy et al., 2014).

The induction of filamentous phage can have important consequences for bacterial populations. Pf genes are among the most highly induced genes in *P. aeruginosa* biofilms (Whiteley et al., 1999), and Pf virions are detected at high levels in biofilms (McElroy et al., 2014;

Rice et al., 2009; Webb et al., 2003). Deletion of Pf4 from PAO1 reduces cell death in *P. aeruginosa* microcolonies (Rice et al., 2009), suggesting that Pf phage play a role in cell lysis in bacterial populations. Release of DNA from cells due to this lysis may facilitate biofilm formation, as extracellular DNA adds structural integrity to biofilms (Whitchurch et al., 2002). In addition, Pf phage themselves play an important role in structural integrity of the biofilm matrix by aligning to form a liquid crystalline structure (Secor et al., 2015). Their contribution to biofilm formation may increase tolerance to stresses, including reduced disruption by detergent, resistance to desiccation, and resistance to antibiotics (Rice et al., 2009; Secor et al., 2015). Specifically, Pf phage increase tolerance to positively charged antibiotics (Secor et al., 2015), likely due to sequestration by their negatively-charged filaments. Naturally, they can also lyse competing cells that do not have the prophage, altering pathogen evolution. Pf virions are present at high densities in CF expectorated sputum (Burgener et al., 2019; Secor et al., 2015) and 36-44% of strains isolated from people with CF are Pf positive (Burgener et al., 2019). Furthermore, isolates from later in a person's life tend to be colonized by strains with Pf more than earlier isolates (Burgener et al., 2019). In people with CF, the presence of Pf phage was correlated with a marker of airway destruction, elastase (Burgener et al., 2017), consistent with the finding that Pf is important for virulence during chronic infection (Secor et al., 2016).

## **1.2 *P. aeruginosa* in the cystic fibrosis airways**

Cystic fibrosis (CF) is the most common genetic disease in Caucasians (Feigelman et al., 2017), affecting about 30,000 people in the United States (Cystic Fibrosis Patient Registry, 2019). CF is caused by mutations to the cystic fibrosis transmembrane conductance regulator (CFTR)

gene, a chloride and bicarbonate ion transport channel protein expressed in many epithelial cell types. As a result, people with cystic fibrosis experience symptoms related to defective ion transport in multiple organ systems throughout the body (Cutting, 2015). The dysregulated immunity within the respiratory tract of people with CF renders them more susceptible to pulmonary infection (Malhotra et al., 2019). Ultimately, chronic pulmonary infections are a leading cause of morbidity and mortality in people with CF (Carmody et al., 2013; Nixon et al., 2001).

Several bacterial pathogens frequently colonize people with CF, including *Staphylococcus aureus*, *Haemophilus influenzae*, *Pseudomonas aeruginosa*, and *Burkholderia cenocepacia* complex (Cystic Fibrosis Patient Registry, 2019; Muhlebach et al., 2018). The composition of the CF lung microbiome is associated with several factors, including age. *S. aureus* and *H. influenzae* are the most frequently detected bacterial pathogens during early childhood (Cystic Fibrosis Patient Registry, 2019). However, as people with CF near adulthood, *P. aeruginosa* is the most frequently detected pathogen (LiPuma, 2010). Infections in the CF lung can also be polymicrobial, particularly in the case of *S. aureus* and *P. aeruginosa*. In 2019, 44% of people with CF cultured positive for *P. aeruginosa*, and it was the most common pathogen in adults with CF (Cystic Fibrosis Patient Registry, 2019).

People with CF typically initially experience acute transient infections with *P. aeruginosa* in childhood followed by a transition to a chronic infection later in life (Burns et al., 2001). Although multiple *P. aeruginosa* strains may infect people with CF during acute infection, chronic infections are thought to derive from a single strain (LiPuma, 2010; Winstanley et al., 2016). People with CF frequently acquire *P. aeruginosa* from environmental sources, but person to person transmission has also been reported, particularly for the drug resistant Liverpool Epidemic Strain

(LES) (Cheng et al., 1996; Salunkhe et al., 2005). Use of antibiotics to treat *P. aeruginosa* infections has been shown to delay the decline in lung function and increase life expectancy, however, these treatments often fail to clear the infection (Sherrard et al., 2014). Ultimately, *P. aeruginosa* infections are associated with increased morbidity and mortality for people with CF (Henry et al., 1992; Kosorok et al., 2001).

### **1.2.1 *In vivo* adaptation of *P. aeruginosa***

While *P. aeruginosa* produces infections in multiple body sites, its extensive adaptation to the CF respiratory environment motivates its use in studies of microbial evolution, including the work described in this thesis. The CF respiratory environment places new stresses upon *P. aeruginosa* upon colonization, including intra and interspecies competition, nutrient availability, antibiotic treatment, immune pressure, and oxygen limitation (Palmer et al., 2005). Longitudinal sampling of isolates from the sputum of people infected with *P. aeruginosa* has revealed that it undergoes relatively well-described and predictable adaptations (Rossi et al., 2020). These adaptations are frequently associated with survival in the presence of antibiotic and immune pressure and coincide with the transition from acute to chronic infection.

Among the best characterized adaptations associated with the transition to chronic infection are increased biofilm formation due to the overproduction of exopolysaccharides (Häussler et al., 1999; Malone, 2015) and loss of motility (Mahenthiralingam et al., 1994). For example, conversion to a mucoid phenotype due to increased production of the polysaccharide alginate is commonly detected (Flynn and Ohman, 1988; Govan and Deretic, 1996; Winstanley et al., 2016). Increased production of exopolysaccharides Pel and Psl can also manifest as diverse colony types, including the hyper biofilm-forming rugose small colony variant (RSCV) morphology, which is

frequently detected in chronic *P. aeruginosa* infections (Pesttrak et al., 2018; Starkey et al., 2009). Increased resistance to antibiotics administered to patients, including aminoglycosides, betalactams, fluoroquinolones, and polymyxins (Caballero et al., 2018) and altered production of virulence factors associated with quorum sensing, like proteases, type III secretion (Jain et al., 2004), and pyoverdine (Nguyen et al., 2014) are also commonly reported. In addition, metabolic rewiring can occur during *in vivo* adaptation for *P. aeruginosa* (La Rosa et al., 2018). Isolates have been shown to have loss of metabolic pathways, possibly due to the nutrient richness of the host environment compared to soil and water (Barth and Pitt, 1996; Rohmer et al., 2011).

Although chronic infections are frequently dominated by a single strain, *P. aeruginosa* is known to diversify during infection. The drivers of this diversity are still unclear, but spatial isolation within the lung and environmental heterogeneity have previously been suggested (Jorth et al., 2015; Markussen et al., 2014). This is thought to have critical repercussions for treatment due to the presence of many clone types of varying levels of resistance and persistence within the microbial population at any given time (Clark et al., 2018; Winstanley et al., 2016). In addition, it renders obtaining representative samples of the pulmonary *P. aeruginosa* population and analysis of longitudinal samples more challenging.

### **1.2.2 Clinical genomes of *P. aeruginosa***

Whole genome sequencing of isolates from people with CF has also revealed a number of mutations acquired during chronic infection (Armbruster et al., 2021; Caballero et al., 2015; Chung et al., 2012; Gabrielaite et al., 2020; Klockgether et al., 2018; Markussen et al., 2014; Marvig et al., 2013, 2015; Smith et al., 2006; Yang et al., 2011). Although mutations can differ considerably between patients and between samples taken from the same patient, many genes have been found

to be mutated in parallel, suggesting that they confer traits under selection (Marvig et al., 2015). One of the most common adaptations is altered quorum sensing through mutations to the *lasR* gene (Hoffman et al., 2009; Winstanley and Fothergill, 2009). In addition, alginate overproduction is frequently conferred by mutations to the *algU* and *mucABCD* gene cluster (Boucher et al., 1997). Although *P. aeruginosa* intrinsically forms robust biofilms, mutations that overexpress biofilm are also frequently enriched during infections (Marvig et al., 2015; Winstanley et al., 2016). Among the genes frequently mutated that confer increased biofilm are those in the Wsp pathway (Gloag et al., 2019; Smith et al., 2006), *retS* (Marvig et al., 2015), and flagellar genes (*morA*, *fleQ*) (Harrison et al., 2020). Mutations to PDEs and DGCs can also confer alterations to biofilm and motility phenotypes (Starkey et al., 2009). While certain traits associated with these mutations are known, the interconnected regulatory networks influencing biofilm production cloud our ability to predict their fitness benefit *in vivo*. For instance, flagellar mutations were previously proposed to reduce expression of flagella to evade host immune response or reduce energetic costs of flagellar biosynthesis, but recent work suggests that these mutations also contribute to elevated levels of exopolysaccharides (Harrison et al., 2020).

Clinical genomes also reflect the evolution of hypermutability during chronic infection of the lungs, and more recently, the sinuses of people with cystic fibrosis (Armbruster et al., 2021; Cramer et al., 2011; Feliziani et al., 2014; Jorth et al., 2015; Mena et al., 2008; Oliver et al., 2000). While hypermutability is frequently conferred through mutations to genes encoding DNA repair proteins (*mutS/mutL*), gene disruptions due to the transposition of IS elements also appear to accelerate evolution *in vivo* (Armbruster et al., 2021). In addition, Armbruster et al. discovered that hypermutability was correlated with smaller aggregate sizes and increased pathoadaptation for isolates from the sinuses of people with CF, suggesting that growth in aggregates with small

population sizes may enrich for mutators *in vivo*. In addition, mutator phenotypes coincided with signatures of genome degradation, suggesting host restriction (Armbruster et al., 2021).

Whole genome sequencing of *P. aeruginosa* isolates has also revealed mutations associated with the evolution of antimicrobial resistance. While mechanisms of resistance through horizontally acquired elements is possible, chromosomally encoded mechanisms are reported to predominate during CF infection (Clark et al., 2018). Notable examples include regulators of beta-lactamase genes (*ampC*, *ampD*) and efflux pumps (*mexR*, *mexT*, *mexZ*, *nalB*, *nfxB*), target site modifications (*gyrAB*, *ftsI*, *fusA1*, *parC*), outer membrane porins (*oprD*), and other regulators (*pmrB*, *phoQ*) (Clark et al., 2018; Marvig et al., 2013, 2015).

Although certain genotypes and phenotypes evolve in parallel across patients and isolates, and this provides strong evidence that they are adaptive, the fitness advantages contributing to their selection remain unclear. This is in part because mutations detected during chronic infection in people with CF frequently occur in pleiotropic regulators of gene expression (Yang et al., 2011). For instance, although metabolic rewiring is associated with adaptation to the CF lung environment, mutations to genes that cause metabolic shifts, particularly the *lasR* gene, also alter production several products associated with virulence (D'Argenio et al., 2007; Hoffman et al., 2010). Therefore, the extent to which metabolic adaptations are directly selected versus byproducts of selection for altered production of virulence factors is unknown (La Rosa et al., 2018). In addition, phenotypes like increased biofilm formation of rugose small colony variants are associated with several traits that could produce fitness advantages *in vivo*, therefore it is difficult to discern which selective pressures most impact pathogen evolution. As a result, evolution experiments using models of CF infection are useful to test the effect of specific selective pressures to adaptation.

### **1.3 Microbial evolution experiments**

Microbial evolution experiments consist of propagation of microbial populations in controlled conditions to test various hypotheses related to evolutionary biology, however, the questions these studies investigate can vary considerably. For instance, evolutionary biologists use microbial populations as model systems to investigate evolutionary processes, but these experiments do not necessarily test hypotheses related to microbial traits such as pathogenesis. Rather, these experiments examine the rate and dynamics of adaptation, as well as the contributions of epistasis, strength of selection, heterogeneity and mutation rate on evolution (Adams and Rosenzweig, 2014; Lenski, 2017; McDonald, 2019). On the other hand, evolution experiments are also used by microbiologists to test the impact of factors relevant to infection on pathogen evolution, including propagating microbes in environments that simulate infection (Gloag et al., 2019; Schick and Kassen, 2018). Although at one time the fields of evolutionary biology and microbiology were viewed as relatively distinct, fortunately, the findings of microbial evolution experiments are increasingly recognized as synergistic (Adams and Rosenzweig, 2014). In this work, we investigated the roles of genetic background and environment on adaptation of *P. aeruginosa* with the aim of appreciating the implications of our findings within both evolutionary biology and infection.

#### **1.3.1 Using microbes to understand evolutionary processes**

Microbial populations are optimal model systems for the study of evolutionary processes due to several key characteristics (Adams and Rosenzweig, 2014; Cooper, 2018; McDonald, 2019). First, the short generation times of microbes enable us to examine hundreds or even

thousands of generations of adaptation over relatively short periods of time (Lenski et al., 1991). Furthermore, entire populations may be frozen at any timepoint and reconstituted at a later date, which permits researchers to “restart” evolution from archived populations. The increased popularity of whole genome sequencing also enables affordable investigation of mutations responsible for adaptations observed in evolved microbial populations.

While all microbial evolution experiments consist of propagation in a selective medium to allow naturally occurring mutations to develop, the design of these experiments can be modified to address specific questions related to evolution. These experiments can vary in length from brief experiments examining only first step mutations to the famous long term evolution experiment (LTEE) lead by Richard Lenski, which has propagated lineages of *E. coli* in the laboratory for over 70,000 generations (Wiser et al., 2013). Researchers can tailor the evolutionary parameters of their experiments to best address their research questions, including manipulating population size, genetic background of the ancestral strain, mutation rate, and environmental characteristics. In this regard, different methods of propagating lineages are useful in different contexts. Serial dilution of liquid culture, the mechanism of transfer utilized in the Lenski LTEE and many other evolution experiments, generates large effective population sizes which increases the strength of selection during the experiment, and is useful for identifying the genetic targets of selection (Cooper, 2018). Studies have utilized this model to identify the dynamics of evolution (Good et al., 2017), mutation rate (Sniegowski et al., 1997), genome dynamics (Barrick and Lenski, 2013), and the predictability of evolution (Bailey et al., 2015). Alternatively, forcing populations through repeated bottlenecks can minimize the force of selection because the success of mutations becomes random, which can be useful to study mutation rate and spectrum (Dillon et al., 2015). In either case, evolution experiments have been used to test the contributions of these parameters. For example, the roles

of history, chance, and selection in adaptation have been experimentally examined to determine their relative contributions to evolution (Santos-Lopez et al., 2021; Travisano et al., 1995).

As microbial evolution experiments have gained popularity, new approaches have been designed to ask questions of greater detail and complexity. Barcoding of microbial populations has enabled high resolution lineage tracking beyond the capabilities of WGS (Blundell and Levy, 2014; Jahn et al., 2018). Evolution experiments have also been utilized to examine the impact of ecological factors on evolution, including spatial and temporal heterogeneity (Flynn et al., 2016; Rainey and Travisano, 1998; Turner et al., 2018, 2020). Furthermore, microbes enable the investigation of relationships between parasites and their hosts (Koskella and Brockhurst, 2014; Shapiro et al., 2016).

Ultimately, several key observations are consistently reported across evolution experiments. First, evolution often precedes by parallel mechanisms at the phenotypic or genetic level (Cooper et al., 2003; Herron and Doebeli, 2013; Lang et al., 2013; McDonald et al., 2009). These instances attract interest because they reveal the contexts in which evolution is, to a certain extent, predictable. Therefore, there is considerable motivation to continue to examine the genetic and environmental factors that result in parallelism, as well as the phenotypes that are repeatedly observed. Secondly, experiments have demonstrated diminishing returns epistasis, or the decrease in advantage for mutations as populations become more fit in their environment (Barrick et al., 2009; Kryazhimskiy et al., 2014; Wisser et al., 2013). However, the Lenski LTEE lines have demonstrated that even after 50,000 generations, populations continued to accumulate fitness advantages (Lenski, 2017). Finally, the evolution of complexity has been repeatedly observed in both short and long term experiments, be it through the evolution of the ability of *E. coli* to consume citrate in the LTEE (Blount et al., 2008) or rapid evolution of ecological interactions in

biofilms (Flynn et al., 2016; Rainey and Travisano, 1998). In any case, evolution of distinct ecological types within these models can alter the conditions of the experiment in ways that alter subsequent evolution.

### **1.3.2 Evolution experiments as models of infection**

Experimental evolution of microbial populations need not relate to pathogenesis, but many recent studies have combined evolution experiments with models of the host environment to forecast adaptation during or leading to infection (Brockhurst, 2015). This is an appealing avenue of study because the host environment is generally highly complex, making it is impossible to determine the selective pressures contributing to pathogen evolution. However, evolution experiments can isolate specific aspects of the host environment to examine their impact on adaptation (Brockhurst, 2015). For instance, propagation of a microbial population with antimicrobial treatment, followed by phenotypic analysis or whole genome sequencing, can reveal dynamics and mechanisms of resistance (Ahmed et al., 2020; Barbosa et al., 2017). Microbial populations can also be propagated in highly complex models that aim to encapsulate as many relevant features of the host environment as possible, including *in vivo* models of infection (Cooper et al., 2020; Gloag et al., 2019; Green et al., 2021; Marshall et al., 2021). Models of cystic fibrosis infection have previously been utilized for studies of *P. aeruginosa*, including propagation in synthetic cystic fibrosis media (SCFM) (Davies et al., 2017; Palmer et al., 2007; Schick and Kassen, 2018; Wright et al., 2013).

Biofilms are thought to be the most prevalent growth lifestyle during chronic infection, therefore many evolution experiments have been performed with selection for the biofilm lifestyle (Steenackers et al., 2016; Traverse et al., 2013). A number of models for biofilm growth have been

characterized, including biofilms formed at the air-liquid interface of cultures (Rainey and Travisano, 1998), on agar surfaces (Ahmed et al., 2018, 2020), and flow cell biofilms (McElroy et al., 2014). Our laboratory designed a bead-based model in which populations must undergo the entire biofilm lifecycle over 24 hours (Flynn et al., 2016; Harris et al., 2021; Poltak and Cooper, 2011; Traverse et al., 2013; Turner et al., 2018, 2020). Cells must first colonize a polystyrene bead, then, upon transfer to fresh experimental medium, disperse and colonize a new bead.

Antibiotic resistance is one of the greatest threats to human health and few new drugs are in development, therefore better understanding of evolution of resistance to existing antimicrobials is a critical priority (Hughes and Andersson, 2017). Evolution experiments have been used particularly frequently to identify mechanisms and dynamics of antimicrobial resistance. These have been performed in many combinations of drugs and species and vary considerably in the questions they seek to address. Most aim to provide a screen of resistance mechanisms available to pathogens by performing whole genome sequencing of microbial strains following treatment with drug (Feng et al., 2016; Sanz-García et al., 2018). Many also seek to examine the impact of environmental conditions on the evolution of resistance, including biofilm lifestyle (Ahmed et al., 2018, 2018; Santos-Lopez et al., 2019; Wong et al., 2012) and other spatial variation (Baym et al., 2016). Others examine the role of genetic background of a strain on evolution of resistance (Card et al., 2021; Jorth et al., 2017; Lukačičinová et al., 2020; Vogwill et al., 2016; Yen and Papin, 2017). A major aim of several studies is to identify opportunities to exploit collateral sensitivity networks, in which a strain's genetic background might endanger it to drug sensitivities in subsequent treatments (Barbosa et al., 2017; Imamovic and Sommer, 2013). Others have examined various treatment regimes, like the strength, duration, and consistency of antibiotic treatment in order to characterize the impact on evolution (Jahn et al., 2017; Kim et al., 2014; Melnyk et al.,

2017; Vestergaard et al., 2016) or altered evolutionary parameters to examine their impact on the trajectory toward resistance, including mutation supply (Cabot et al., 2016; Dijk et al., 2017; Ibacache-Quiroga et al., 2018).

Ultimately, we have learned from screens of resistance adaptations for a few bacterial species and drug combinations, particularly for frequently used model organisms like *E. coli*. However, we do not know the extent to which findings from certain drugs and strains might be relevant to other pathogens, so examinations of parallelism between species remains a subject worthy of study. Also, while the potential of biofilm to impact evolution of resistance is becoming clear (Ahmed et al., 2018; Santos-Lopez et al., 2019), different types of antimicrobials are known to exhibit distinct physiological properties and ability to penetrate a biofilm matrix (Tseng et al., 2013), so it is important to examine evolution of drug resistance using additional experiments across species and drug types.

#### **1.4 Goals of dissertation**

The focus of this dissertation is the evolution of *P. aeruginosa* in the clinically relevant selective pressures of tobramycin, biofilm, and CF nutrients. Although other factors likely play critical roles in microbial adaptation *in vivo* including immune response and microbial competition, we have chosen these selective pressures due to their demonstrated impact on persistence during host infection. We examined the adaptation of *P. aeruginosa* populations using evolution experiments with whole population genome sequencing to identify all mutations that were selected in a particular environment and track their evolution within replicate populations over time. In Chapter 2, we examined the evolutionary dynamics of tobramycin resistance for *P.*

*aeruginosa* in both planktonic and biofilm environments. We also examined the impact of genetic background on adaptation by comparing with identical evolution experiments in *A. baumannii*. In Chapters 3 and 4, we turned our attention to the adaptations that were selected in the absence of drug, focusing on quorum sensing and biofilm alterations in Chapter 3, and the unexpected evolution of prophage induction in Chapter 4.

## 2.0 Parallel evolution of tobramycin resistance across species and environments

This chapter is adapted from the published manuscript:

**Michelle R. Scribner<sup>a,b</sup>**, Alfonso Santos-Lopez<sup>a,b</sup>, Christopher W. Marshall<sup>a,b\*</sup>, Christopher Deitrick<sup>a,b</sup>, and Vaughn S. Cooper<sup>a,b</sup>

Parallel evolution of tobramycin resistance across species and environments. (2020). *MBio* 11, (3). DOI: 10.1128/mBio.00932-20

Copyright © 2020 Scribner et al..

<sup>a</sup>Department of Microbiology and Molecular Genetics, University of Pittsburgh, Pittsburgh, Pennsylvania, USA

<sup>b</sup>Center for Evolutionary Biology and Medicine, University of Pittsburgh, Pittsburgh, Pennsylvania, USA

\*Current address: Department of Biological Sciences, Marquette University, Milwaukee, Wisconsin, USA

## 2.1 Project summary

Different species exposed to a common stress may adapt by mutations in shared pathways or in unique systems, depending on how past environments have molded their genomes. Understanding how diverse bacterial pathogens evolve in response to an antimicrobial treatment is a pressing example of this problem, where discovery of molecular parallelism could lead to clinically useful predictions. Evolution experiments with pathogens in environments containing antibiotics, combined with periodic whole-population genome sequencing, can be used to identify many contending routes to antimicrobial resistance. We separately propagated two clinically relevant Gram-negative pathogens, *Pseudomonas aeruginosa* and *Acinetobacter baumannii*, in increasing concentrations of tobramycin in two different environments each: planktonic and biofilm. Independently of the pathogen, the populations adapted to tobramycin selection by parallel evolution of mutations in *fusAI*, encoding elongation factor G, and *ptsP*, encoding phosphoenolpyruvate phosphotransferase. As neither gene is a direct target of this aminoglycoside, mutations to either are unexpected and underreported causes of resistance. Additionally, both species acquired antibiotic resistance-associated mutations that were more prevalent in the biofilm lifestyle than in the planktonic lifestyle; these mutations were in electron transport chain components in *A. baumannii* and lipopolysaccharide biosynthesis enzymes in *P. aeruginosa* populations. Using existing databases, we discovered site-specific parallelism of *fusAI* mutations that extends across bacterial phyla and clinical isolates. This study suggests that strong selective pressures, such as antibiotic treatment, may result in high levels of predictability in molecular targets of evolution, despite differences between organisms' genetic backgrounds and environments.

## 2.2 Introduction

The notion that evolution can be forecasted at the level of phenotype, gene, or even amino acid is no longer a fantasy in the post-genomic era (Lässig et al., 2017). Most forecasting efforts rely on history to anticipate the future, and the explosive growth of whole-genome sequencing (WGS) now sets the stage to resolve evolutionary phenomena in action and determine probabilities of the next selected path. Among the best examples, bacterial populations exposed to strong selection like antibiotics and analyzed by WGS are likely to identify genotypes that produce resistance and increased fitness (Ahmed et al., 2018; Cooper, 2018; Feng et al., 2016; Palmer and Kishony, 2013; Wardell et al., 2019). Repeated instances of the same antibiotic selection may enrich the same types of mutations and ultimately enable some measure of predictability (Ibacache-Quiroga et al., 2018; Wong et al., 2012). For instance, we can be confident that exposing different bacteria to high doses of fluoroquinolones like ciprofloxacin selects for substitutions in residues 83 or 87 of the drug target, DNA gyrase A (Fàbrega et al., 2009; Wong and Kassen, 2011). Furthermore, drug resistance phenotypes have been predicted from genome sequence data for certain bacterial species (Bradley et al., 2015; Tamma et al., 2019). These successful predictions likely result from an underlying genetic constraint, where relatively few single mutations can achieve high-level resistance, as well as population-genetic power, where strong selection acts on populations with ample mutation supply (Ibacache-Quiroga et al., 2018).

Yet predicting evolution may be hampered when these conditions are not met, or when antibiotic selection produces species or environment-specific outcomes. Evolution experiments in environments containing antibiotics have demonstrated that subjecting different bacterial strains to the same antibiotic treatment regime (Gifford et al., 2018; Vogwill et al., 2014, 2016), or the same strains to different environments (Ahmed et al., 2018; Santos-Lopez et al., 2019) can select

for different drug resistance levels as well as molecular targets. We can test the potential for predicting evolved levels and genetic causes of drug resistance by studying the evolution of resistance in different environments and across different species with inherently different genetic backgrounds.

*Acinetobacter baumannii* and *Pseudomonas aeruginosa* are ESKAPE pathogens that are responsible for multidrug-resistant infections (Santajit and Indrawattana, 2016). These species are members of the Moraxellaceae and Pseudomonadeae families, respectively, and the genomes of the species differ in size by approximately 2.7Mb, or more than 40%. Infections with these two opportunistic pathogens are often associated with a biofilm mode of growth (Eze et al., 2018; Mulcahy et al., 2014), where the bacteria grow in aggregates on surfaces and are protected from antimicrobials by a number of mechanisms. This biofilm protection may occur from secreted substances like polysaccharides, proteins, or eDNA that limit diffusion or by slowing growth and rendering the bacteria much less susceptible to an antibiotic (Hall and Mah, 2017; Høiby et al., 2010). Given the lifestyle differences between cells growing in a biofilm compared to free-living cells, we asked whether evolution of tobramycin (TOB) resistance could proceed by different mechanisms between these two environments. TOB is an aminoglycoside antibiotic commonly used to treat infections caused by Gram-negative pathogens. Aminoglycosides are actively transported into the cell following binding to the outer membrane, and subsequently can cause cell death by binding the ribosome and disrupting translation (Bulitta et al., 2015; Kohanski et al., 2010). Resistance to aminoglycosides can occur by several mechanisms including alteration of translation machinery, reduced uptake, increased drug efflux, and enzymatic inactivation of the drug (Bolard et al., 2017; Krause et al., 2016; Wistrand-Yuen et al., 2018). However, the prevalence of these resistance strategies in different environments is incompletely understood.

Here, we experimentally propagated two bacterial species from different families, *A. baumannii* and *P. aeruginosa*, in increasing concentrations of the aminoglycoside TOB in both planktonic and biofilm environments. We performed whole population genome sequencing at regular intervals for each lineage to identify the range of molecular mechanisms of resistance available in these species and environments. Furthermore, we aimed to examine the evolutionary dynamics of adaptation – what mutations are favored at each drug concentration in each environment – in the presence of TOB. The success of the available molecular mechanisms of resistance is determined by the order in which causative mutations occurred (Wistrand-Yuen et al., 2018), the fitness imposed by those mechanisms at a given drug concentration in the selective environment (MacLean and Buckling, 2009), and the combinations of these mutations that are selectively tolerated (Knopp and Andersson, 2018). This study depicts both marked gene- and even domain-level parallelism in evolved genotypes as well as genetic differences between lifestyles that indicate shifts in the mode of action of TOB with potentially important clinical consequences.

## **2.3 Results**

### **2.3.1 Parallel evolution of TOB resistance phenotypes and genotypes**

We used TOB-sensitive ancestral clones of *A. baumannii* ATCC 17978 and *P. aeruginosa* strain PA14 to inoculate five replicate, single-species lineages for each of four treatments: planktonic without drug, planktonic with drug, biofilm without drug, and biofilm with drug. The evolution experiment was performed using a previously described protocol in which planktonic populations were propagated through a 1:100 dilution into fresh media every 24 hours, and biofilm

populations through the transfer of a colonized 7mm polystyrene bead (Santos-Lopez et al., 2019; Traverse et al., 2013; Turner et al., 2018). This produces similar transfer sizes for both planktonic and biofilm treatments: approximately  $1 \times 10^7$  CFU/transfer for *A. baumannii* and  $2 \times 10^8$  CFU/transfer for *P. aeruginosa*. Populations undergo approximately 6.64 generations/day, producing at least an estimated  $10^6$  new mutations each day (Cooper, 2018; Santos-Lopez et al., 2019). Populations were initially exposed to 0.5X MIC and antibiotic concentrations were subsequently doubled every 72 hours. We propagated populations for twelve days and periodically froze samples for later sequencing and phenotypic analysis. The experimental design is illustrated in Figure 1.

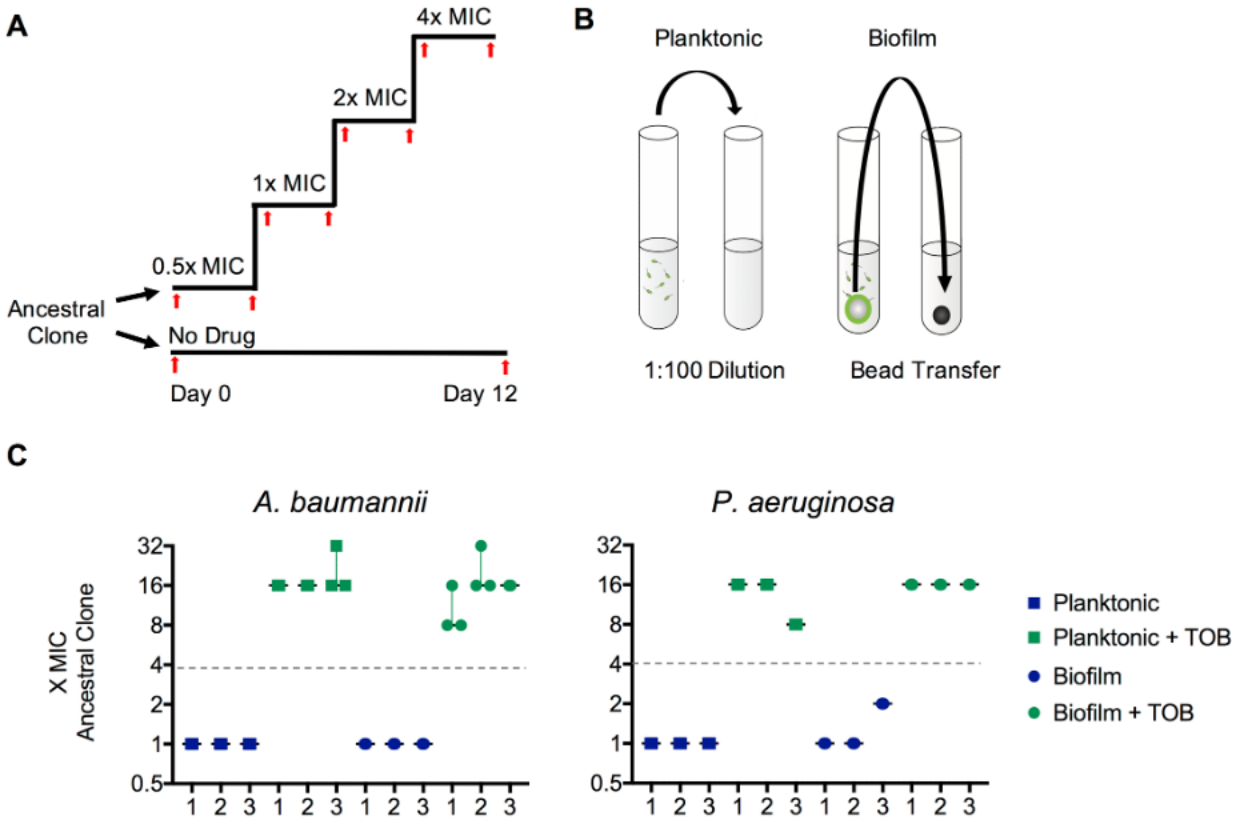


**Figure 1. Parallel evolution of tobramycin resistance level across species and environment.**

Populations of *A. baumannii* and *P. aeruginosa* were propagated in minimal media with either increasing concentrations of tobramycin or no drug and either planktonic or biofilm lifestyle. Five replicate populations were propagated per treatment. (A) Populations were either propagated for twelve days in no antibiotic or inoculated into half the minimum inhibitory concentration of tobramycin with doubling concentrations every 72 hours. Samples of each population were archived for later phenotypic analysis and sequencing periodically throughout the experiment (red arrows). (B) Populations were propagated with either selection for planktonic growth through a daily 1:100 dilution or biofilm growth through a daily bead transfer that forces cells to undergo the entire biofilm lifecycle of attachment, growth, dispersion and reattachment every 24 hours as described in previous work (79). (C). Tobramycin resistance level relative to the ancestral clone for three randomly chosen populations per treatment after twelve days of evolution. MICs were determined by microdilution in Mueller Hinton Broth according to CLSI guidelines. Fold change in MIC of three replicates per population is shown with median fold change and range indicated. *A. baumannii* ancestral MIC = 1.0 mg/L, *P. aeruginosa* ancestral MIC = 0.5 mg/L in Mueller Hinton Broth.

Populations must acquire resistance to 4x the MIC of the ancestral strain in order to survive the experiment (gray dashed line).

For a population to survive to the end of the experiment, it must evolve resistance to at least four times (4x) the TOB concentration that would kill the ancestral clone. Previous evolution experiments in antibiotics show that replicate populations may acquire different levels of resistance in response to the same antibiotic treatment regime when evolving in different environments (Gifford et al., 2018; Santos-Lopez et al., 2019; Trampari et al., 2019). While resistance levels did not change during the experiment for populations not exposed to antibiotics, populations propagated under TOB selection demonstrated resistance levels 8-32x MIC of the ancestral clone (Figure 1C and D). These gains in resistance correspond to an increase from sensitive to intermediate or resistant levels according to CLSI breakpoints (CLSI, 2019). In *P. aeruginosa*, MICs of TOB differed when measured in Muller Hinton Broth compared to the experimental minimal medium but reflect similar fold changes in MIC relative to the ancestral clone (Figure 2).

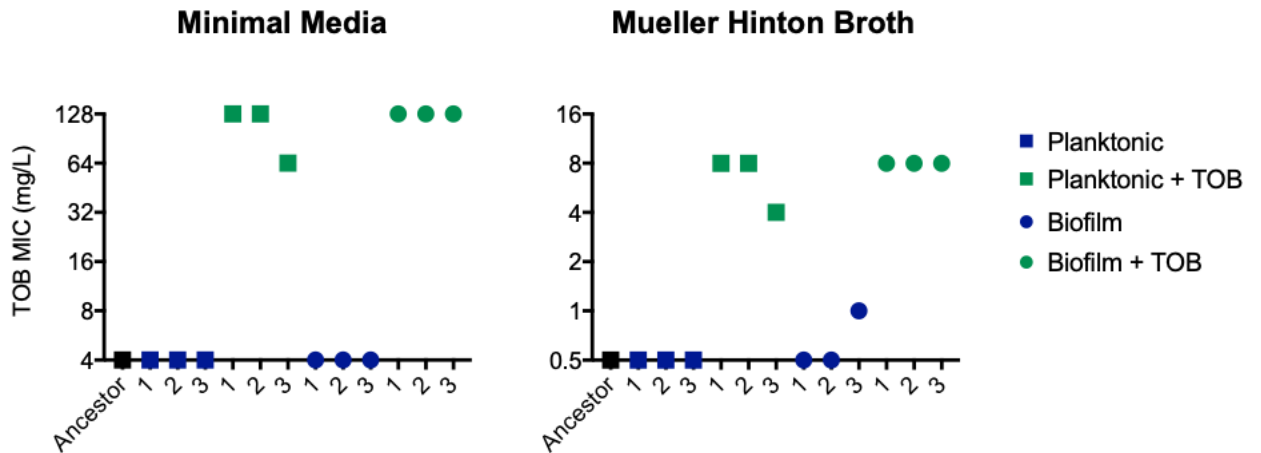


**Figure 2. Minimum inhibitory concentration of *P. aeruginosa* evolved populations on day twelve in the minimal media used in the evolution experiment and Mueller Hinton Broth.**

MICs were performed according to CLSI guidelines with the exception of media used. The median of at least three replicate MIC assays per population is shown and error bars represent range of measured values.

Prior mutant screens have indicated that as many as 135 genes can produce low level resistance to aminoglycosides, suggesting that TOB resistance might arise by mutations in diverse molecular targets (Schurek et al., 2008). Instead, whole genome sequencing of the twenty TOB-treated populations at day twelve revealed that mutations in only a few loci rose to high frequencies (Figure 3). The large effective population sizes ( $>10^7$ ) of these experiments ensure that mutations occurred in nearly every position across the genome, and often multiple times (Cooper, 2018; Santos-Lopez et al., 2019). Further, the large sizes of these populations despite strong drug selection greatly empowers selection relative to effects of drift or mutation pressure (Cooper, 2018; Desai and Fisher, 2007). Therefore, mutations identified by population-wide WGS, which in our case reliably detects those  $\geq 5\%$  frequency, represent the fittest resistant genotypes among many contenders. Mutations in the same genes selected in parallel across antibiotic-treated populations provide clear evidence of their fitness benefits in the presence of TOB, and their absence in drug-

free populations indicates they were not simply selected by other experimental conditions (Figure 4). In the unlikely possibility that these particular loci experienced significantly higher mutation rates in the presence of TOB, only selection would have driven them to these frequencies within 3-12 days (Cooper, 2018).

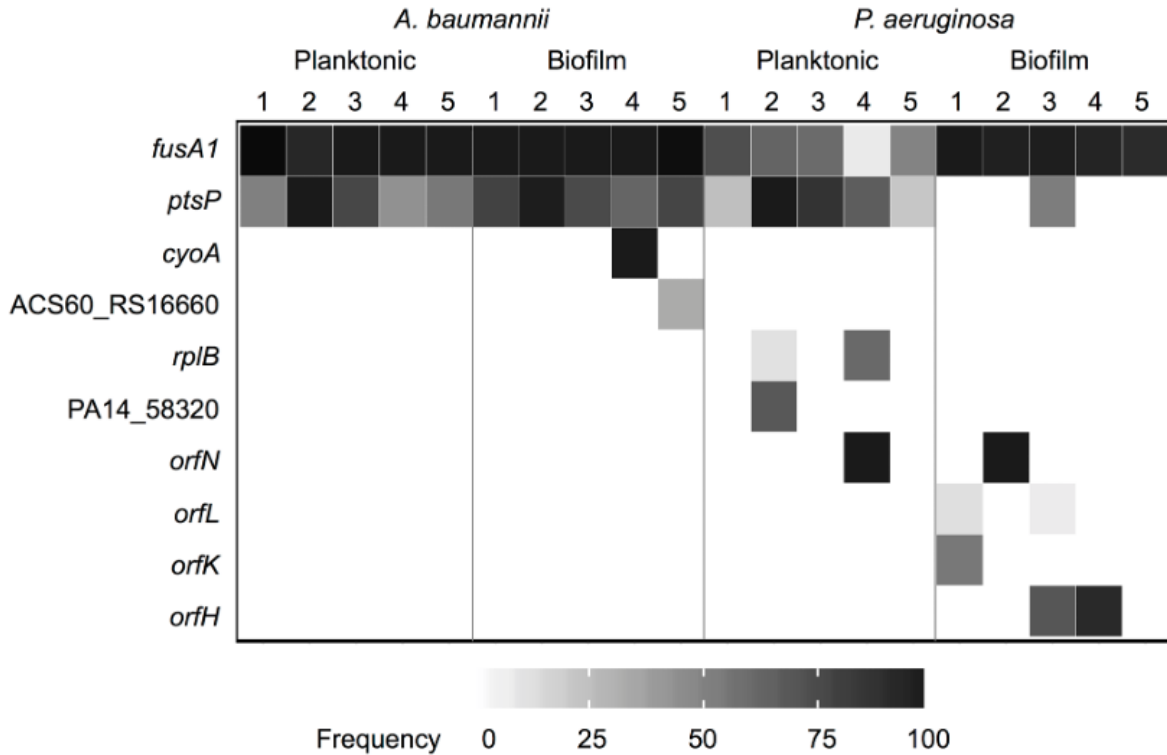


**Figure 3. Population sequencing reveals interspecies parallelism and lifestyle-dependence of molecular targets of evolution.**

Tobramycin-associated mutations identified by whole population genome sequencing of *A. baumannii* and *P. aeruginosa*. Five populations per treatment were sequenced after 12 days of experimental evolution. Shading indicates the total frequency of all mutations in each gene within a population at day twelve.

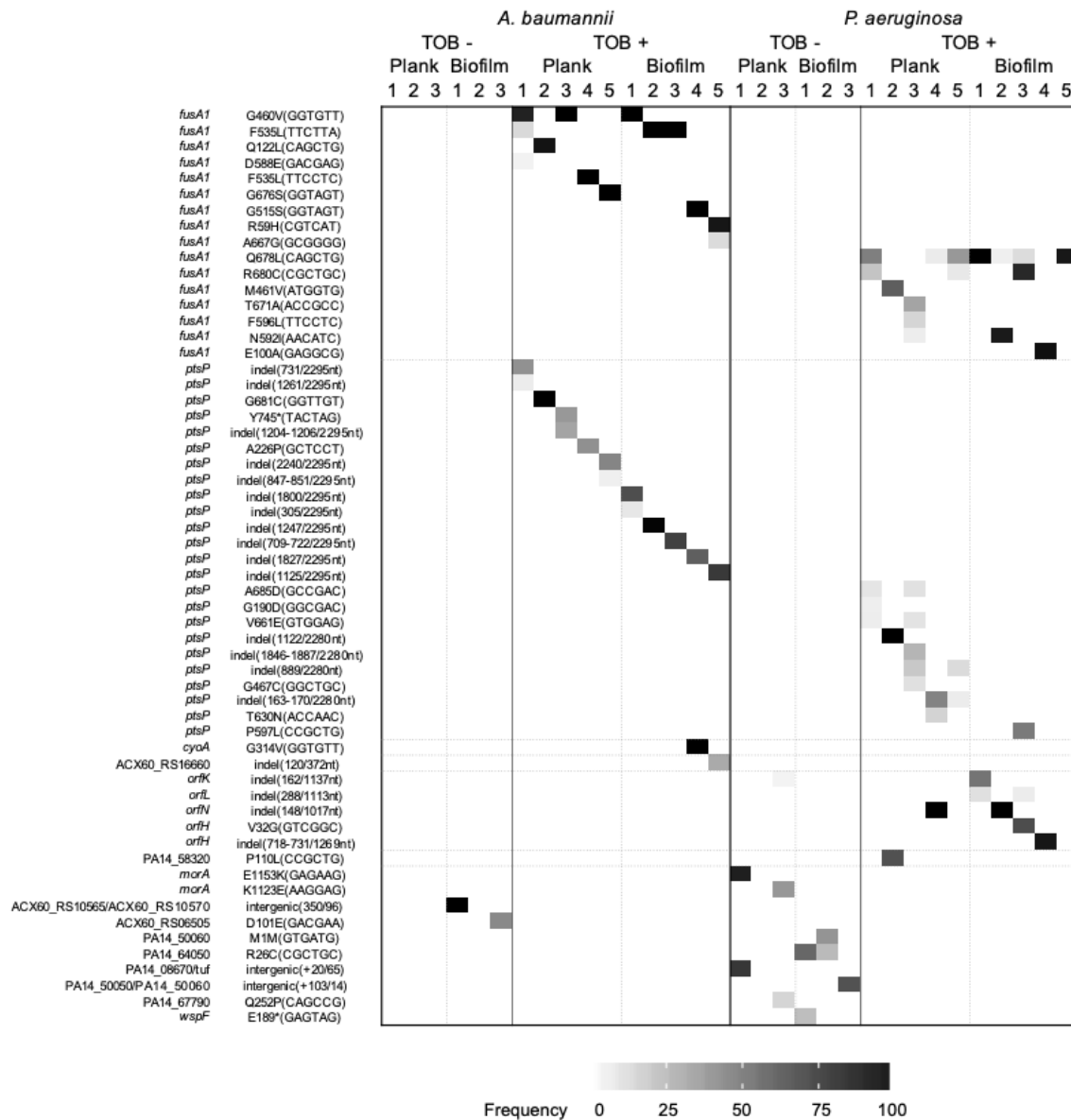


**Figure 4. Population sequencing reveals molecular adaptations to tobramycin and biofilm selection.**

Three populations per treatment for no antibiotic lineages and five populations per treatment for antibiotic lineages were sequenced at the day twelve timepoint for each species. Shading indicates the total frequency of the mutations in each locus at day twelve. SNPs and stop codon mutations are denoted by the gene name or locus tag, amino acid change, then nucleotide change in parentheses. Indels are indicated by the gene name or locus tag followed by “indel” and the nucleotide position of the indel within the affected gene.

Despite the many differences between *A. baumannii* and *P. aeruginosa*, both species frequently acquired mutations in *fusAI* and *ptsP* (Figure 3). The *fusAI* gene encodes elongation factor G (EF-G), an essential protein which functions in catalyzing translocation and ribosome recycling during translation (Savelsbergh et al., 2009). While *A. baumannii* has one copy of *fusAI*, *P. aeruginosa* and other *Pseudomonas* species also encode the paralogous gene *fusA2* (Palmer et al., 2013). Mutations to EF-G have received little attention as a mechanism of TOB resistance in *P. aeruginosa* and no previous reports in *A. baumannii* to the best of our knowledge (Bolard et al., 2017; Sanz-García et al., 2018). EF-G is also not known to be a binding target of TOB, however, this protein is the direct binding target of other antibiotics including fusidic acid and argyrisin B (Johanson and Hughes, 1994; Jones et al., 2017). The exact mechanism by which mutations in EF-G confer aminoglycoside resistance is currently unknown but this study demonstrates it is an important resistance determinant. The *ptsP* gene encodes phosphoenolpyruvate phosphotransferase protein, which is part of the nitrogen phosphotransferase system and has been identified as a target of TOB resistance for *P. aeruginosa*, but not *A. baumannii* to the best of our knowledge (Sanz-García et al., 2018; Schurek et al., 2008). The mechanism by which mutations in *ptsP* confer resistance to TOB is also unknown. However, the nitrogen phosphotransferase system has been shown to regulate the GigA and GigB pathway that functions in coordinating the antibiotic stress response, suggesting a link between the nitrogen phosphotransferase system and coordinating the transcriptional response to antibiotic pressure (Gebhardt and Shuman, 2017). Therefore, despite as many as 135 genes in which mutations confer reduced susceptibility, mutations in two genes, *fusAI* and *ptsP*, appear to be most fit in the presence of TOB across species and environments.

To distinguish the specific contributions of these mutations to TOB resistance, we obtained isogenic mutants by isolating clones from evolved *A. baumannii* and *P. aeruginosa* populations and genotyping them by WGS. We measured TOB MICs by broth microdilution for seven isogenic *fusAI* mutants including R59H and G460V in *A. baumannii* and Q129H, N592I, F596L, Q678L, R680C in *P. aeruginosa* (Table 1). Regardless of species or amino acid change, *fusAI* mutations conferred a 2-4x increase in TOB resistance relative to the MIC of the ancestor. We also measured the resistance levels of two *ptsP* mutants ( $\Delta 42\text{bp}$ : 1846-1887/2295nt,  $\Delta 14\text{bp}$ : 1296-1309/2295nt) in *P. aeruginosa* and found these to produce a similar increase in resistance (2 and 3x ancestor MIC, respectively). Mutants with both *fusAI* and *ptsP* alterations generally exhibited higher resistance to TOB in both species than *fusAI* or *ptsP* mutations alone (4-8x ancestral clone), at a level that is consistent with an additive effect of these two mutations on MIC. To examine if these mutations produced increased resistance in a biofilm environment, we treated polystyrene beads colonized with *fusAI*, *ptsP*, and *fusAI+ptsP* mutants with TOB. Biofilms of evolved mutants survived at least 3x higher concentrations of TOB than biofilms composed of the ancestral genotype (Table 2), suggesting that these mutations also increase TOB resistance in a biofilm environment. Mutations in *fusAI* also increased the MIC to other ribosome-targeting antibiotics, including amikacin, gentamicin, and tigecycline; however, mutations in *ptsP* did not produce cross resistance to other antibiotics tested (Figure 5A), suggesting specificity to TOB resistance. While species-specific mutations did occur in several genes discussed below, the parallel evolution of mutations in *fusAI* and *ptsP* across *A. baumannii* and *P. aeruginosa* indicates that regardless of genetic background, mutations to these two genes are among the few that jointly increase TOB resistance and fitness in these conditions.

**Table 1. Evolved mutant clones genotyped by WGS demonstrate increased TOB resistance relative to the ancestral clone.**

Species	Genotype	Median MIC (mg/L)	Range (mg/L)	Fold Change
<i>A. baumannii</i>	Ancestor	1.0	1.0-2.0	-
	<i>fusA1</i> R59H	4.0	2.0-4.0	4.0
	<i>fusA1</i> G460V	4.0	4.0-8.0	4.0
	<i>cyoA</i> V53V + <i>ptsP</i> indel 1742/2295nt + ACX60_RS12470 A173D	4.0	2.0-4.0	4.0
	<i>fusA1</i> G460V + <i>ptsP</i> indel 1340-1368/2295nt	8.0	8.0-8.0	8.0
	<i>fusA1</i> G460V + <i>ptsP</i> indel 1788/2295nt	8.0	8.0-8.0	8.0
<i>P. aeruginosa</i>	Ancestor	0.5	0.25-1.0	-
	<i>fusA1</i> Q129H	1.5	1.0-2.0	3.0
	<i>fusA1</i> N592I	2.0	2.0-2.0	4.0
	<i>fusA1</i> F596L	2.0	1.0-2.0	4.0
	<i>fusA1</i> Q678L	2.0	1.0-2.0	4.0
	<i>fusA1</i> R680C	1.0	1.0-2.0	2.0
	<i>ptsP</i> Δ42bp 1846-1887/2280nt	1.0	1.0-2.0	2.0
	<i>ptsP</i> Δ14bp 1296-1309/2280nt	1.5	1.0-2.0	3.0
	<i>fusA1</i> Q678L + <i>ptsP</i> R301C	4.0	1.0-4.0	8.0
	<i>fusA1</i> T456A + <i>ptsP</i> V661E	2.0	1.0-4.0	4.0
	<i>fusA1</i> Q563L + <i>ptsP</i> E335*	4.0	2.0-4.0	8.0
	<i>fusA1</i> R680C + <i>ptsP</i> E335*	4.0	2.0-4.0	8.0
	<i>fusA1</i> T671A + <i>ptsP</i> Δ1bp 1122/2280nt	4.0	2.0-8.0	8.0
	<i>fusA1</i> N592I + <i>orfN</i> Δ1bp 148/1017nt	2.0	2.0-4.0	4.0

**Table 2. Evolved mutant clones genotyped by WGS demonstrate increased tobramycin resistance in a biofilm environment relative to the ancestral clone.**

Species	Genotype	Median MIC (mg/L)	Range	Fold Change
<i>A. baumannii</i>	Ancestor	≤16	16-16	-
	<i>fusA1</i> G460V	96	32-128	≥6
	<i>fusA1</i> G460V + <i>ptsP</i> indel 1788/2295nt	48	32-64	≥3
<i>P. aeruginosa</i>	Ancestor	≤16	16-16	-
	<i>fusA1</i> N592I	96	32-128	≥6
	<i>ptsP</i> Δ42bp 1846-1887/2280nt	64	64-64	≥4
	<i>fusA1</i> R680C + <i>ptsP</i> E335*	64	32-64	≥4
	<i>fusA1</i> N592I + <i>orfN</i> Δ1bp 148/1017nt	64	32-128	≥4

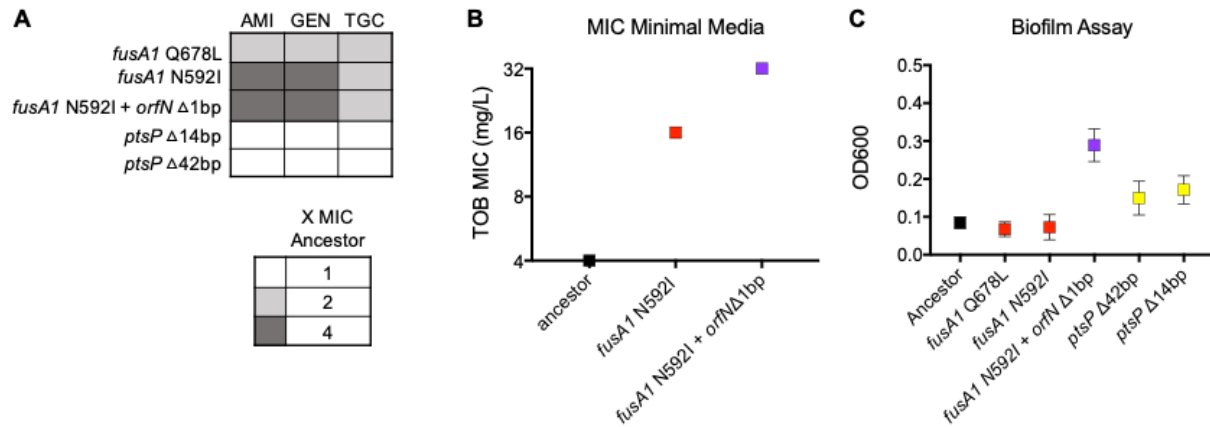


**Figure 5. MICs and biofilm production of *P. aeruginosa fusA1*, *fusA1 orfN*, and *ptsP* mutants compared to the ancestral genotype.**

A) Change in MIC of ribosome-targeting antibiotics for mutants isolated from evolved populations was determined by microdilution in Mueller Hinton Broth using Sensititre plates. Shading indicates the fold increase in MIC relative to the ancestral clone based on the median of three replicates. Ancestral MICs: amikacin (AMI) = 8mg/L, gentamicin (GEN) = 2mg/L, tigecycline (TGC) = 1mg/L. B) MICs of TOB for mutants isolated from evolved populations was determined by macrodilution using the experimental minimal media to mimic the conditions of the evolution experiment. Median of four replicates is shown. C) Biofilm production was measured by crystal violet biofilm assay. Mean of at least four replicates is shown, error bars represent 95% confidence intervals. *fusA1* N592I *orfN* Δ1bp corresponds to a genotype with a *fusA1* N592I mutation and deletion at nucleotide 148/1017 of *orfN*. *ptsP* Δ14bp corresponds to a genotype with a deletion from nucleotides 1296-1309/2280 of the *ptsP* gene, and *ptsP* Δ42bp corresponds to a genotype with a deletion from nucleotides 1846-1887/2280 of the *ptsP* gene.

### 2.3.2 Environment-associated adaptations to TOB selection

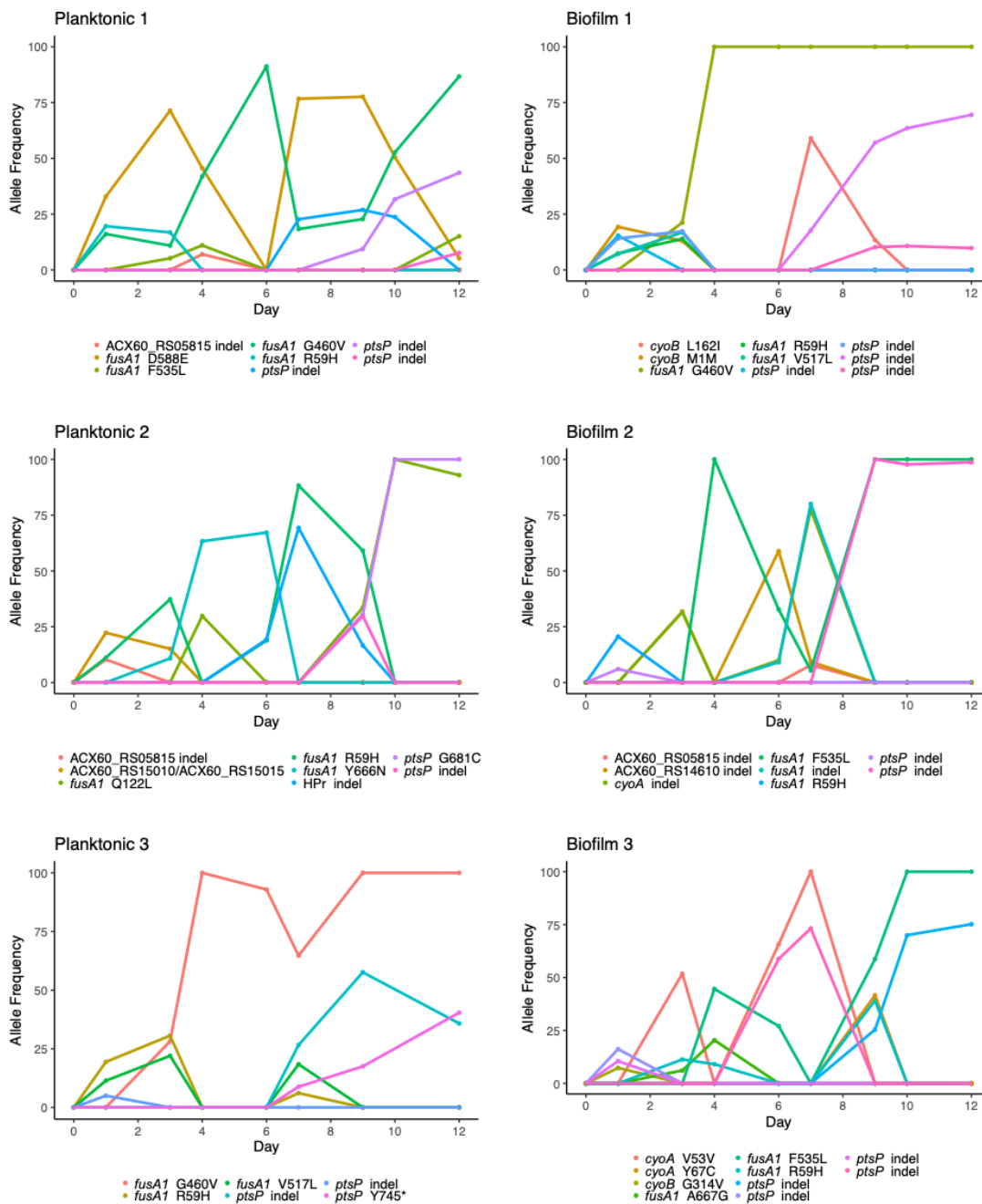
Bacterial growth in different environments often involves distinct physiological processes, including nutrient uptake, metabolic pathways, growth rates, and investment in defenses (Mah and O’Toole, 2001). Consequently, the stresses produced by a given antibiotic may vary in different environments. Evolution experiments in both planktonic and biofilm conditions allow us to test if

the genetic pathways of adaptation depend on the external environment. TOB selection enriched multiple mutations in *fusAI* within each population regardless of the environment, but their frequencies differed with lifestyle. For *P. aeruginosa*, *fusAI* mutations dominated biofilm populations in the final sample (mean 95.4%, standard deviation  $\pm 3.7$ ) but their frequencies varied in planktonic populations (mean 50.4%, standard deviation  $\pm 25.7$ ) (Figure 3). Furthermore, twelve distinct mutations in *ptsP* rose to detectable frequencies in *P. aeruginosa* lineages, eleven of which occurred in planktonic populations, demonstrating strong selection for *ptsP* mutations in the planktonic condition that is less pronounced in biofilm (Figure 6). Meanwhile, *P. aeruginosa* biofilm populations frequently acquired mutations in *orfK*, *orfH*, *orfL*, or *orfN* genes (subsequently referred to jointly as *orfKHLN*), encoding O antigen biosynthesis enzymes, and this locus was only mutated in one of the planktonic populations exposed to TOB (Burrows et al., 1996; Rocchetta et al., 1999). A mutation in *orfK* also occurred at low frequency in a population with no TOB selection, suggesting that these mutations may be beneficial in a variety of conditions, but most beneficial in the combination of biofilm and TOB selection (Figure 4). Indeed, *orfN* mutations together with *fusAI* mutations were more resistant than *fusAI* mutants alone in the experimental media (Figure 5B) and increased biofilm production (Figure 5C).

The genetic targets of resistance were more consistent in *A. baumannii* populations treated with TOB, with *fusAI* and *ptsP* mutations reaching similar frequencies in both biofilm and planktonic treatments by the end of the experiment. However, six independent mutations in *cyoA* and *cyoB* (subsequently referred to jointly as *cyoAB*) encoding components of the electron transport chain rose to detectable frequencies prior to day twelve, all of which occurred in biofilm lineages (Figure 3, Figure 6) (Ibacache-Quiroga et al., 2018). Together, parallel evolution of

mutations in *orfKHLN* and *cyoAB* in biofilm lineages, but not planktonic lineages, indicates that lifestyle may influence the strength of selection for certain TOB resistance mutations.

## *A. baumannii*



***P. aeruginosa***

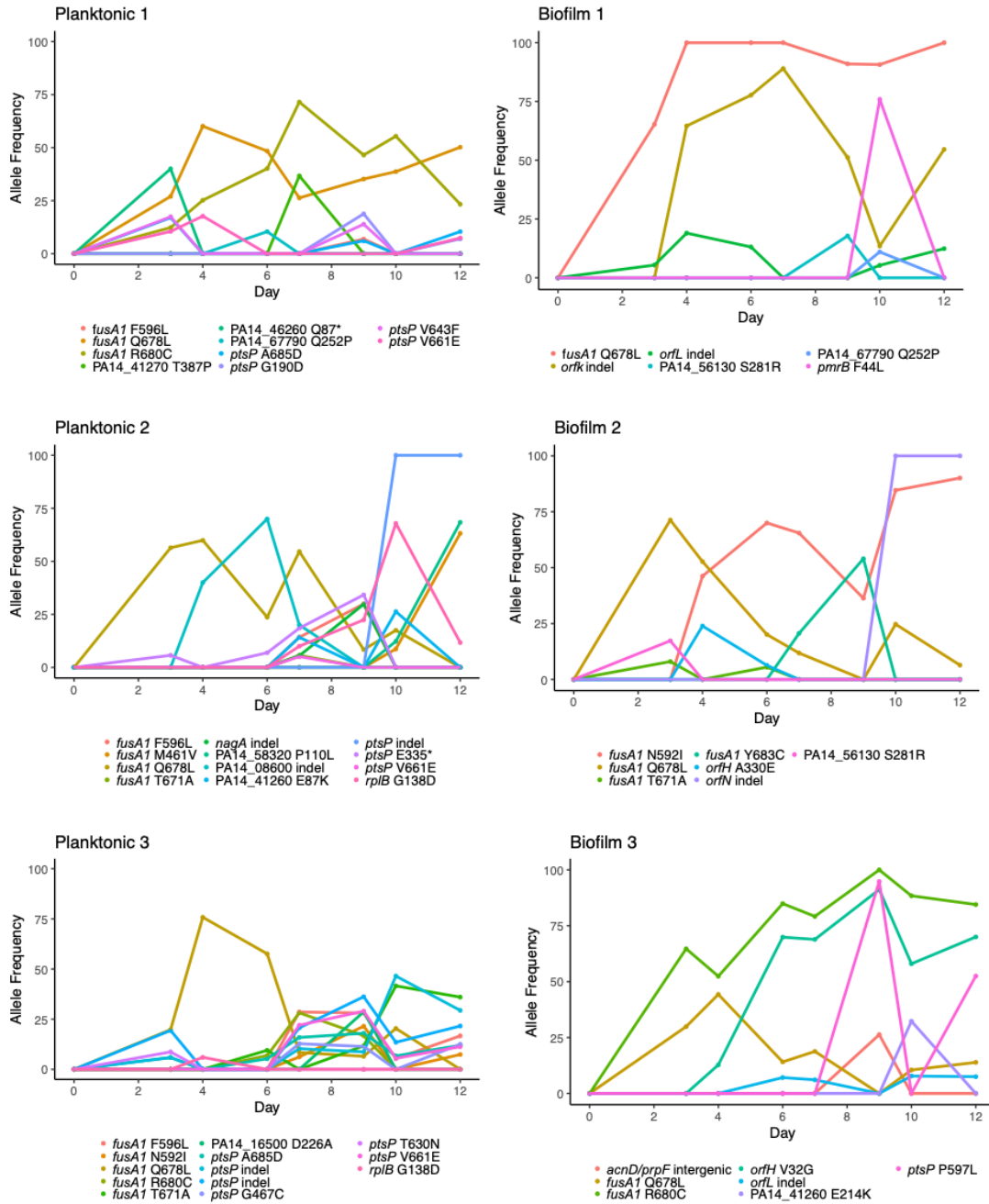


**Figure 6. Allele frequency plots of three populations from each treatment.**

*A. baumannii* (top) and *P. aeruginosa* (bottom) mutations are plotted by their frequency within each population on each day of the experiment in which population sequencing was performed. SNPs are indicated by gene name or locus tag followed by amino acid change. Insertions or deletions are indicated by the gene name or locus tag followed by “indel”.

The parallel evolution of mutations in four genes associated with O antigen biosynthesis in *P. aeruginosa* suggests that selection favors alterations in the outer membrane when biofilm populations are exposed to TOB (Burrows et al., 1996; Tognon et al., 2017; Wong et al., 2012). Consistent with this observation, mutations in *orfN*, a homolog of *wbpL* in PAO1, have been shown to cause loss of O-specific antigen in PA14 LPS, a phenotype which frequently arises during chronic *P. aeruginosa* infection in people with cystic fibrosis (Tognon et al., 2017). This loss of O-specific antigen also increases resistance to aminoglycosides by reducing permeability and binding affinity to the outer membrane (Bryan et al., 1984; Kadurugamuwa et al., 1993). Together, these reports indicate that the selected *orfKHLN* mutations may produce TOB resistance by altering the outer membrane to reduce drug binding or uptake. Similarly, populations of *A. baumannii* evolved with TOB and biofilm selection acquired mutations in the *cyoAB* operon. Mutations in electron transport chain components like *cyoAB* have previously been associated with resistance to aminoglycosides by reducing membrane permeability (Bryan and Kwan, 1983; Damper and Epstein, 1981; Schurek et al., 2008). Therefore, although the biofilm populations of the two species propagated in this experiment evolved mutations in different loci (affecting LPS biosynthesis genes in *P. aeruginosa* and electron transport chain components in *A. baumannii*), these may represent parallelism of a broad strategy to alter membrane structure or permeability under combined biofilm and aminoglycoside selection.

### **2.3.3 Population-genetic dynamics of TOB resistance evolution**

We used longitudinal population sequencing of three lineages per treatment to determine effects of species and environment on the temporal dynamics of evolution in increasing

concentrations of this antibiotic. The frequencies of mutated alleles within a population were plotted over time to display mutation trajectories (Figure 6). To infer genotypes based on allele frequency data, we developed and implemented a novel set of computational tools which applies a hierarchical clustering algorithm to genetic distance metrics. The lineage of genotypes is subsequently inferred using a Bayesian approach. This application then illustrates the observed dynamics of genotypes over the course of evolution through Muller plots (Figure 7, see methods). Genotype frequency is represented by the breadth of shading with colors corresponding to the presence of *fusA1*, *ptsP*, *cyoAB*, and *orfKHLN* mutations within that genotype.

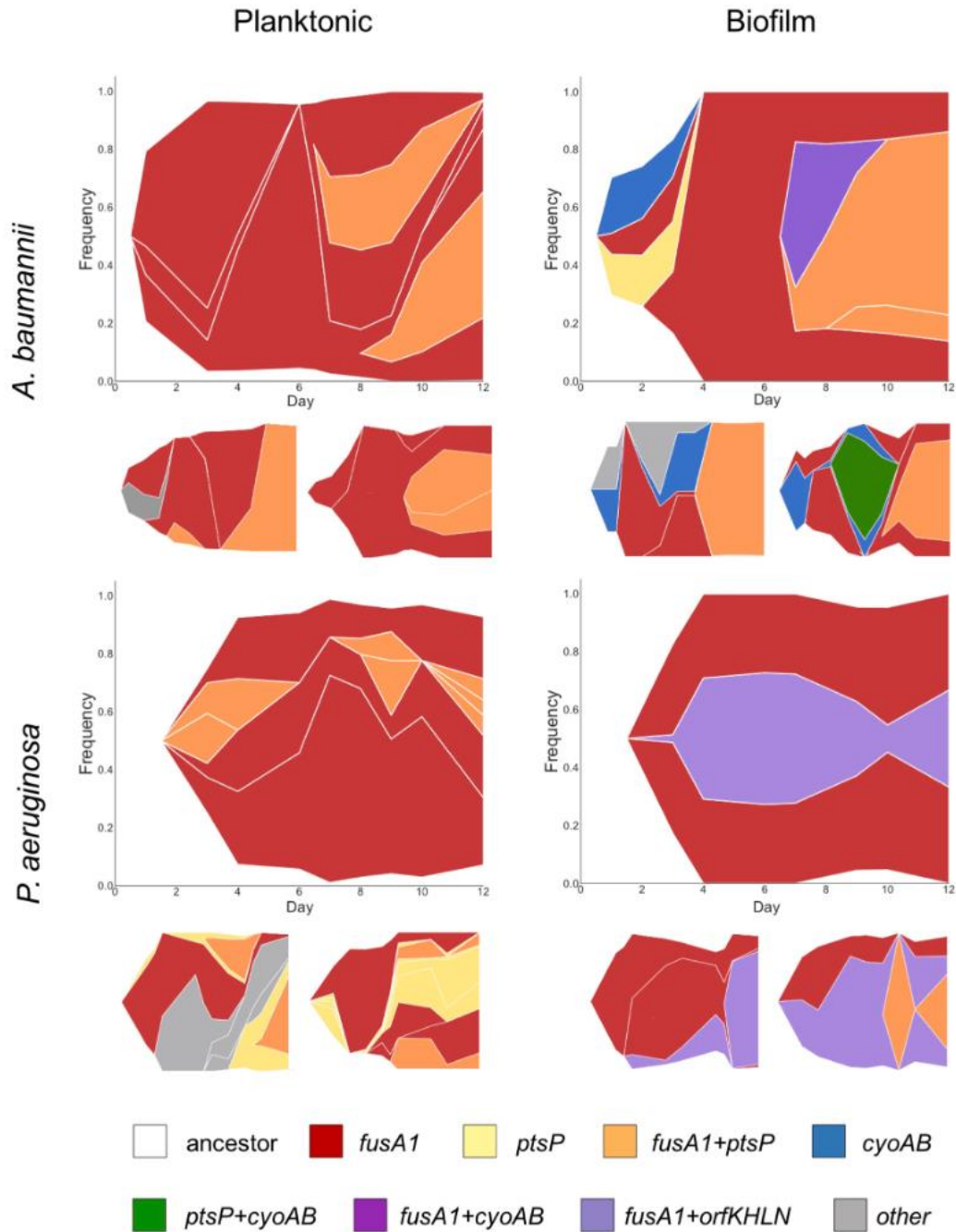


**Figure 7. Evolutionary dynamics of bacterial populations in increasing concentrations of tobramycin.**

Muller diagrams displaying genotype frequencies as a proportion of the population throughout twelve days of evolution for three populations per treatment. Genotypes are shaded by the putative driver loci that are mutated.

Different lineages of the same color represent mutations at different positions within the same loci that are coexisting within the population. The frequency of genotypes at every time point is represented by the height of the

graph that it spans at that time point. In situations where a first mutation arises in the background of the ancestral genotype, the color representing that genotype can be seen beginning from the white background, whereas in situations where a mutation arises in the background of another mutation, thus generating a new genotype, the new color arises in the middle of the existing genotype. Mutations occurring in the background of putative driver mutations are not shown but may be viewed in Figure 6.

In all lineages, regardless of environment, mutations in *fusAI* were detected at either 0.5x MIC or 1.0x MIC and subsequently rose to high frequencies (Figure 7, red). Their rapid rise in frequency in the first few days of the experiment suggests that *fusAI* mutations were the fittest contending mutations at subinhibitory concentrations of TOB. Some *fusAI* mutations, for example *fusAI* G460V, occurred in multiple independent lineages (Figure 4). Given the extensive gene-level parallelism observed in these experiments, these mutations may reflect parallel evolution at the amino acid level, but we cannot exclude the possibility that these mutations were introduced at undetectable frequencies in the starting culture. However, 20 distinct mutations in *fusAI* were selected in lineages treated with TOB and never detected in drug-free lineages, demonstrating that *fusAI* mutations were acquired and highly advantageous under TOB selection (Figure 4). Lineages with different *fusAI* SNPs coexisted in some populations for the duration of the experiment, and secondary mutations were frequently selected on these genotypes in the genes discussed previously (*ptsP*, *orfKHLN*, and *cyoAB*, Figure 7). *A. baumannii* populations tended to become dominated by *fusAI+ptsP* genotypes, but all three biofilm populations also selected *cyoAB* mutants prior to day nine (up to 2x MIC). This *cyoAB* genotype was ultimately outcompeted by a *fusAI+ptsP* genotype at 4x MIC TOB, indicating the superiority of the latter genotype at the higher drug concentration. This result was confirmed by MIC comparisons of *cyoA + ptsP* and *fusAI + ptsP* mutants, which show the former genotype was unable to survive the final antibiotic concentration in the evolution

experiment (Table 1). In planktonic populations of *P. aeruginosa*, *fusAI*, *ptsP*, and *fusAI+ptsP* haplotypes were prevalent throughout the experiment (Figure 7). In contrast, biofilm populations of *P. aeruginosa* repeatedly selected *orfKHLN* mutants on a *fusAI* background. These evolutionary dynamics demonstrate that following initial selection of a *fusAI* mutation, selection favored secondary mutations particular to lifestyle and species.

#### 2.3.4 Parallelism of aminoglycoside resistance mechanisms across species

The repeated evolution of *fusAI* and *ptsP* mutations in both *P. aeruginosa* and *A. baumannii* suggested that these mutations may provide a general mechanism of TOB resistance across diverse species. We tested this hypothesis by searching published datasets and genomes for *fusAI*, *ptsP*, *cyoA*, and *cyoB* mutations (Methods). Mutations in *fusAI* have been reported in several different species including *Eschericia coli*, *Salmonella enterica*, and *Staphylococcus aureus* (Ibacache-Quiroga et al., 2018; Jahn et al., 2017; Johanson and Hughes, 1994; Kim et al., 2014; Mogre et al., 2014; Norström et al., 2007), and all laboratory studies reported these mutations arising either in response to aminoglycoside selection or as a direct cause of aminoglycoside resistance. Mutations in *cyoA* and *cyoB* were also found in *E. coli* and *S. enterica* in these experiments (Ibacache-Quiroga et al., 2018; Jahn et al., 2017; Wistrand-Yuen et al., 2018).

We performed multiple sequence alignments of the proteins encoded by *fusAI* (EF-G), *ptsP*, *cyoA*, and *cyoB* for all of the species that acquired mutations within each loci. We subsequently plotted all of the identified aminoglycoside-associated mutations according to their position in the consensus sequence to examine the distribution of mutations within the proteins (Figure 8). Most selected mutations in *ptsP* were indels producing a frameshift, demonstrating that the fitness advantage conferred by these variants results from loss of function of the product.

Mutations affecting cytochrome components encoded by *cyoAB* acquired frameshift, stop codon, nonsynonymous, and synonymous variants, including an unusual mutation changing the start codon from AUG to AUU (Appendix Table 1). In contrast, mutations in EF-G occurred at 57 distinct amino acid positions and were nearly exclusively nonsynonymous SNPs. Because *fusAI* is an essential gene (Gil et al., 2004; Poulsen et al., 2019) that is highly conserved (44% identity across the five species studied, and much greater similarity), these mutations must presumably both increase fitness in the presence of an aminoglycoside and maintain the essential functions of the protein.

The distribution of mutations within EF-G was similar across species and clustered primarily between amino acids 21 and 184 or between amino acids 327 and 695, with the exception of *E. coli* in which mutations occurred only near the C-terminus (Figure 8A) (Wattam et al., 2017). To test the likelihood that this clustering of mutations within EF-G could occur by chance, we divided EF-G into different bins and then used a Chi Square goodness of fit test to determine if the observed count of mutations within bins differed from expectation based on bin size. The test was significant using three different binning strategies: binning mutations by protein domain (X-squared = 36.956, df = 4, p-value = 1.839e-07), by 100 amino acid intervals (X-squared = 54.175, df = 7, p-value = 2.172e-09), and by five randomly determined bins (X-squared = 41.957, df = 4, p-value = 1.703e-08). Further, ten amino acids of the EF-G consensus sequence repeatedly evolved mutations (amino acids 122, 461, 472, 592, 596, 663, 671, 672, 680, and 681), revealing strong selection on particular sites of EF-G in response to aminoglycoside treatment regardless of genetic background or growth conditions. We visualized mutated positions on the crystal structure of *P. aeruginosa* EF-G (Figure 8B) (Nyfeler et al., 2012) and identified further spatial clustering of the mutated residues. Mutations affected domains I (GTPase), III, IV, and V frequently, but occurred

only once in domain II in these studies, which suggests that mutations to this region are either deleterious to the function of EF-G, do not confer an increase in resistance to aminoglycosides, or fulfill these criteria but produce less advantageous variants than those that rose to high frequencies in these experiments.

When antibiotic resistance occurs through mutations in essential gene products, one might expect that selection would favor peptide alterations that prevent drug action but retain the core functionality of the enzyme or structure. More specifically, selection might select for mutations that alter residues that are more tolerant of variation and vary among extant homologs, rather than strictly conserved residues. We tested whether mutations in EF-G occurred less frequently in amino acid positions that were identical across species. On the contrary, SNPs occurred at positions with identical amino acids across species more frequently than expected by chance for EF-G ( $P = 8.002e-05$ , Fisher's exact test). The mechanism by which these mutations produce aminoglycoside resistance without disrupting its essential functions merits further study. Regardless, the parallel evolution of *fusAI* mutations across species and environments demonstrates the potential utility of this gene as a predictive marker of aminoglycoside resistance.

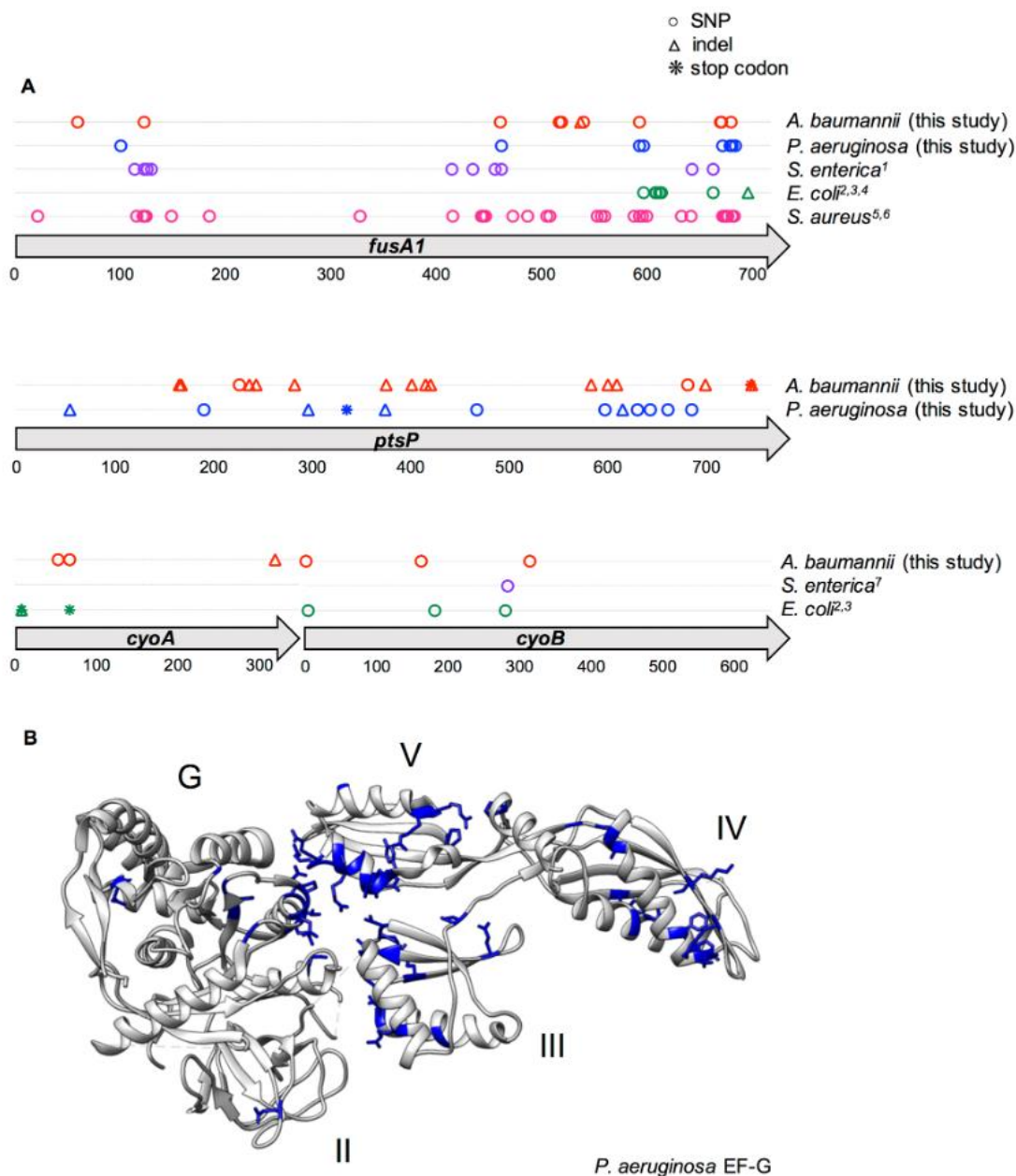


**Figure 8. Parallelism of mutations in genetic loci associated with aminoglycoside resistance across species**

(A) All mutations that occurred at any point in the experiment within the *fusA1*, *ptsP*, *cyoA*, or *cyoB* genes are indicated by a symbol at its position within the consensus amino acid sequence. Mutations reported in previous literature in other species are indicated and color coded by species; these mutations were either selected by aminoglycoside treatment in vitro or selected by another antibiotic and subsequently demonstrated to confer resistance to aminoglycosides. SNPs are indicated by a circle, insertions or deletions (indels) are indicated by a

triangle, and stop codon mutations are indicated by an asterisk. For each gene, the encoded amino acid sequences for all species in which mutations were identified were aligned. Mutations are shown according to their position in the resulting consensus amino acid sequence. (B) Amino acid positions that were mutated in any species are shown in blue on the protein structure of PAO1 EF-G (Nyfeler et al., 2012). Mutations are shown according to their corresponding position in the *P. aeruginosa* EF-G amino acid sequence. Domains G (GTPase), II, III, IV, and V are indicated. Top: *fusAI* gene, Middle: *ptsP* gene, Bottom: *cyoA* and *cyoB* genes. Referenced literature: 1. Johanson and Hughes, 1994, 2. Jahn et al., 2017, 3. Ibacache-Quiroga et al., 2018, 4. Mogre et al., 2014, 5. Kim et al., 2014, 6. Norström et al., 2007, 7. Wistrand-Yuen et al., 2018.

To examine if the precise mutations found in our *in vitro* study also arise in clinical isolates, we searched published genomes of *P. aeruginosa* clinical isolates from people who had likely been treated with aminoglycosides like TOB (Bolard et al., 2017; Chung et al., 2012; López-Causapé et al., 2017, 2018; Markussen et al., 2014). Mutations within *fusAI* and *ptsP* were reported in these genomes, suggesting that these mutations evolve during infections (Table 3). Although it is not possible to distinguish aminoglycoside selection as the driver of these mutations in a clinical setting, the selection of mutations at identical residues in these genes in our evolution experiment suggests that these mutations have potential to produce the same increase in aminoglycoside resistance *in vivo*. Taken together, the parallel evolution of mutations in these genes in clinical isolates suggests that they may contribute to aminoglycoside resistance in clinically relevant genetic backgrounds and environments, including infections of the cystic fibrosis respiratory tract.

**Table 3. Datasets of *P. aeruginosa* clinical isolates were analyzed to reveal gene and residue-level parallelism within the aminoglycoside resistance loci observed in this study.**

Study Authors	Variants	
	<i>fusA1</i>	<i>ptsP</i>
López-Causapé, C., et al. (2017).	V93A, K430E, N482S, K504E, Y552C, P554L, D588G, P618L, T671I*	-
Markussen, T., et al. (2014).	G118S, D467G	L42L, R61H
Chung, J.C.S., et al. (2012).	A418T, V538A, G610V, Q678R*	-
Bolard, A., et al. (2017).	V93A, A555E, T671A*	-

\*Mutations at this amino acid position occurred in populations treated with TOB in this study

## 2.4 Discussion

The rapidly intensifying problem of antimicrobial resistance demands understanding of how antibiotic resistance evolves and which types of mutations or mobile elements are common causes (Brockhurst et al., 2019; MacLean and San Millan, 2019). Genetic screens of mutant collections have revealed potential resistance mechanisms (Schurek et al., 2008), and more recently, evolve-and-resequence experiments have been used to identify the most fit resistance mutations in a given condition (Santos-Lopez et al., 2019; Sanz-García et al., 2018; Wong et al., 2012). However, the broader clinical utility of these screens for predicting the evolution of antibiotic resistance depends upon the relevance of the findings in other strains, species, or environments. This study served the dual purpose of identifying mutations that contribute to TOB resistance in *A. baumannii* and *P. aeruginosa* and demonstrating effects of different environments and species history on the evolutionary dynamics and causes of resistance.

In spite of the many genetic differences between *A. baumannii* and *P. aeruginosa* – the latter genome much larger and containing dozens of additional putative resistance loci – we identified parallel mutations in *fusAI* and *ptsP* following tobramycin selection, a largely unknown combination of mutations conferring high fitness and resistance. Furthermore, we found amino acid-level parallelism of *fusAI* mutations associated with aminoglycoside resistance, including kanamycin, gentamicin, and amikacin, across diverse species including *E. coli*, *S. enterica*, and *S. aureus* (Figure 8). While specific molecular targets of resistance shared by multiple species are known, for example DNA gyrase mutations in response to fluoroquinolones (Wong et al., 2012), the level of predictability of *fusAI* mutations has yet to be appreciated as an example of this phenomena. We report that *fusAI* mutations not only arise during aminoglycoside treatment in at least five diverse species, but also produce resistance to nearly every antibiotic within this clinically useful family of drugs (Krause et al., 2016). Furthermore, the level of parallelism distinguishes this study from merely episodic discoveries of *fusAI* mutations in multiple species – on the contrary, we found at least one *fusAI* mutation in every TOB-treated lineage in our study, making these mutations both widely available and highly predictable. The locations of mutations within EF-G revealed that the distribution of mutations was also similar across species (Figure 8). But unlike other resistance genes that frequently acquire mutations in specific sites or narrow regions (Gruger et al., 2004; Qi et al., 2014; Wong and Kassen, 2011), EF-G mutations are distributed across the length of the protein. Alterations in EF-G have been suggested to produce structural changes that could interfere with aminoglycoside binding to the ribosome (Bolard et al., 2017), but the mechanism(s) by which mutations across much of the protein all produce aminoglycoside resistance and how they alter protein function merit further study. The finding that *fusAI* mutations repeatedly evolve in clinical *P. aeruginosa* isolates from different strains and host

conditions further supports the notion that these mutations are selected in diverse genetic backgrounds and environments, and we predict that *fusA1* mutations may be considerably more prevalent following antibiotic therapy than previously appreciated. EF-G substitutions also produced cross resistance to other ribosome-targeting antibiotics in *P. aeruginosa* (Figure 5), a concerning finding given the frequent use of tobramycin in treating infections of the CF airway (Chmiel et al., 2014).

Bacterial growth in biofilms also demonstrably altered the targets of TOB selection from those in well-mixed cultures in ways that motivate studies of the predominant mechanism of aminoglycoside killing and resistance when bacteria grow on surfaces or in aggregates. The selection of mutations in LPS biosynthesis genes (*orfKHLN*) and electron transport chain components (*cyoAB*) primarily in biofilm populations indicates that resistance may have resulted from altered TOB binding or uptake in this lifestyle. In addition to tobramycin's mode of killing through disrupting translation, it has also been shown to exhibit a second, translation-independent killing mechanism through binding to the membrane (Bulitta et al., 2015; Kadurugamuwa et al., 1993). Furthermore, aminoglycosides have been shown to induce cell killing in various types of non-replicating bacteria (McCall et al., 2019). The enrichment of resistance mechanisms that alter drug binding or uptake in biofilm lineages may imply that slow-growing, sessile cells in a biofilm experience weaker selection for mutations preserving translation but increased demand to prevent tobramycin binding and uptake. More generally, these lifestyle distinctions in resistance traits suggest that the environment may influence the evolutionary dynamics of antimicrobial resistance, in concordance with previous studies (Ahmed et al., 2018; Santos-Lopez et al., 2019; Trampari et al., 2019). Therefore, while genes like *fusA1* represent mechanisms of resistance that are robust across a wide range of species, environments, and host conditions, considering the prevailing mode

of bacterial growth may also improve predictions of other genetic causes of antimicrobial resistance.

The extent of parallelism in molecular evolution in these experiments is surprising and its causes warrant consideration. Why would widely different species evolve to resist tobramycin by *fusAI* mutations, and to a lesser extent *ptsP* mutations, when many causes of aminoglycoside resistance are likely available (Schurek et al., 2008)? Several possible explanations exist that are not mutually exclusive. One possibility is that these genes possess a high local mutation rate and thus acquire mutations more rapidly than other available molecular targets of resistance. However, it is doubtful that these mutations are more available than others, since neither were enriched in studies of mutations accumulated in the near-absence of selection nor are these loci in genome regions shown to have higher mutation rates (Dettman et al., 2016; Long et al., 2014). Another possibility is that the target sizes of *fusAI* and *ptsP* (and to a lesser extent *orfKHLN* and *cyoAB*), in which multiple nonsynonymous mutations produce resistance, increases the likelihood of gene-level parallelism. More likely still is that mutations to *fusAI* and *ptsP* produce the greatest fitness benefit in these conditions and these fitness benefits are robust to different species and environments. Other drugs may have a wider range of targets that produce the same level of fitness benefit, resulting in less parallelism.

It is notable that while *fusAI* and *ptsP* are not direct targets of TOB or other aminoglycosides, the effect of mutations in these enzymes may be conserved across species and is relatively insensitive to the genetic background. Many have appreciated that epistatic interactions can limit parallel evolution of resistance mechanisms (Breen et al., 2012; Hernando-Amado et al., 2019; MacLean et al., 2010; Ward et al., 2009), and hence predictability (Kryazhimskiy et al., 2014; Papp et al., 2011). The gene and nucleotide-level parallelism of molecular targets of

aminoglycoside resistance across species, environments, and clinical isolates holds promise for predicting molecular evolution, improving diagnostics for resistance and informing more rational treatment design.

## 2.5 Methods

### 2.5.1 Strains and media

*Pseudomonas aeruginosa* strain UCBPP-PA14 and *Acinetobacter baumannii* strain ATCC 17978 were the ancestral strains used in the evolution experiments (Baumann et al., 1968; Piechaud and Second, 1951; Rahme et al., 1995). *A. baumannii* ATCC 17978 was propagated for ten days in minimal media to pre-adapt it to the media conditions prior to the evolution experiment. The minimal media used in the evolution experiments consisted of an M9 salt base (0.1 mM CaCl<sub>2</sub>, 1.0 mM MgSO<sub>4</sub>, 42.2 mM Na<sub>2</sub>HPO<sub>4</sub>, 22 mM KH<sub>2</sub>PO<sub>4</sub>, 21.7mM NaCl, 18.7 mM NH<sub>4</sub>Cl), 11.1mM glucose, 20 mL/L MEM essential amino acid solution, 10 mL/L MEM nonessential amino acid solution (Thermofisher 11130051, 11140050), and 1 mL/L each of Trace Elements A, B, and C (Corning 99182CL, 99175CL, 99176CL). In addition, DL-lactate (Sigma-Aldrich 72-17-3) was added to the *P. aeruginosa* medium to a final concentration of 10mM in order to generate the approximate nutrient concentrations present in the cystic fibrosis lung environment (Palmer et al., 2007). All cultures were grown in 18x150mm glass tubes containing 5mL of minimal media and incubated at 37°C in a roller drum (30rpm).

### 2.5.2 Evolution experiment

Evolution experiments in both *P. aeruginosa* and *A. baumannii* were initiated using a single ancestral clone. For *P. aeruginosa*, a single colony was selected and resuspended in PBS, then used to inoculate twenty replicate lineages. For *A. baumannii*, a single colony was selected and grown in minimal medium with no antibiotic for 24 hours, then used to inoculate twenty replicate lineages. Lineages were propagated with either increasing concentrations of TOB or no TOB and either planktonic or biofilm selection, such that five replicate lineages each were propagated for four experimental conditions (planktonic without TOB, planktonic with TOB, biofilm without TOB, and biofilm with TOB) for each organism. Lineages with planktonic selection were propagated through a 1:100 dilution every 24 hours (50uL into 5mL of fresh minimal media), and lineages with biofilm selection were propagated through transferring a colonized polystyrene bead (Cospheric, Santa Barbara, CA) to a tube of fresh media and three fresh beads every 24 hours, as described previously (Palmer et al., 2007; Poltak and Cooper, 2011). *P. aeruginosa* biofilm transfers were performed by transferring a bead directly to the next day's tube, whereas *A. baumannii* biofilm transfers were performed by first rinsing the bead by transferring it to a tube of PBS, then to the next day's tube. Lineages propagated with antibiotic selection were treated with tobramycin sulfate (Alfa Aesar, Wardhill, MA) starting at 0.5X MIC of the ancestral strain in the experimental minimal media (0.5 mg/L for *A. baumannii* and 2.0 mg/L for *P. aeruginosa*), with doubling of the concentration every 72 hours. The experiment was performed for twelve days, with samples collected on days 3, 4, 6, 7, 9, 10, and 12 and frozen at -80°C in either 25% glycerol for *P. aeruginosa* or 9% DMSO for *A. baumannii*. Planktonic lineages were sampled by freezing an aliquot of the liquid culture, and biofilm lineages by sonicating a bead in PBS and freezing an aliquot of the resuspended cells.

### 2.5.3 Minimum inhibitory concentration assays

We determined MICs by broth microdilution in Mueller Hinton Broth according to Clinical Laboratory Standards Institute guidelines (CLSI, 2019). To measure MICs for evolved populations, we revived frozen populations by streaking onto a ½ T-Soy agar plate, resuspended a portion of the resulting bacterial lawn in PBS, and diluted to a 0.5 McFarland standard. We inoculated the suspension into round bottom 96 well plates containing two-fold dilutions of TOB at a final concentration of  $5 \times 10^5$  CFU/mL. *P. aeruginosa* and *A. baumannii* MIC assays were then incubated at 37°C for 16-20 hours or 18-22 hours, respectively, then the MIC was determined as the first well that showed no growth. At least three assays were performed for each population. Clones were measured by the same procedure with the exception that freezer stocks were streaked for isolation and MIC assays were performed using an isolated colony. MICs of other ribosome-targeting antibiotics for the *fusA1* and *ptsP* isogenic mutants were performed using Sensititre plates according to manufacturer specifications (Sensititre GN3F, Trek Diagnostics Inc., 514 Westlake, OH).

Although mutations to *orfKHLN* were frequent in tobramycin-treated populations, only a small increase in MIC was observed by microdilution in Mueller Hinton broth. We therefore measured the MIC of isogenic *fusA1* and *fusA1+orfN* mutants by macrodilution in minimal media to better represent the conditions of the evolution experiment. Two-fold dilutions of TOB in 5mL of minimal media were inoculated with  $5 \times 10^5$  CFU/mL for each genotype, incubated for 18 hours, and MIC was determined by the lowest concentration with no visible growth.

The TOB MIC of evolved clones in a biofilm environment was measured by inoculating tubes contain 5mL of Mueller Hinton broth and 5 polystyrene beads with each isogenic mutant and incubating for 24 hours. Each colonized bead was then transferred to a fresh tube of Mueller

Hinton broth at two-fold dilutions of TOB and treated for 18 hours. Beads were transferred to 1mL PBS and sonicated, then 10uL was transferred to 100uL of fresh media and incubated for 24 hours. The MIC was determined by the lowest concentration of TOB at which no growth occurred ( $OD_{600} < 0.05$ ) after this 24-hour incubation. This MIC reflects the lowest TOB concentration that produced effective killing of the biofilm. MIC is reported as the median value of at least three replicates in all MIC experiments.

#### **2.5.4 Biofilm assays**

Biofilm production of mutants isolated from evolved populations was determined by crystal violet assay using a previously described protocol (O'Toole, 2011). Overnight cultures of the mutants in the experimental minimal media were diluted 1:100 in fresh minimal media to a volume of 200uL in a 96 well dish. Plates were incubated for 24 hours at 37°C then rinsed twice with water. Wells were stained with 250 uL of 0.1% crystal violet, incubated for 15 minutes, rinsed three times with water, then allowed to dry overnight. Crystal violet was solubilized by adding 250  $\mu$ l 95% EtOH solution (95% EtOH, 4.95% dH<sub>2</sub>O, 0.05% Triton X-100) to each well for 15 minutes. Biofilm formation was then visualized by measuring OD<sub>600</sub>. Results are the average of four replicates.

#### **2.5.5 Genome sequencing and analysis**

Whole populations were sequenced periodically throughout the experiment. For TOB-treated lineages, all populations were sequenced on day 12, and 3 lineages from each of the planktonic and biofilm conditions were also sequenced on days 3, 4, 6, 7, 8, 9, and 10 for *P.*

*aeruginosa* and days 1, 3, 4, 6, 7, 9, 10, and 12 for *A. baumannii*. Three no TOB lineages from each of the biofilm and planktonic conditions were also sequenced on days 6 and 12 for *P. aeruginosa* and days 1, 4, 9, and 12 for *A. baumannii*.

Populations were prepared for sequencing by inoculating freezer stocks of the bacterial populations into the same media and antibiotic concentration in which the population was growing in at the time of freezing. Identical growth conditions to the population's growth conditions at the time of freezing were maintained in order to minimize bias in the population structure during the outgrowth process. After 24 hours of growth, populations were sampled by either removing an aliquot of the culture for planktonic populations or transferring beads to PBS, sonicating, and removing an aliquot of the resuspended cells for biofilm populations. DNA was extracted using the DNeasy Blood and Tissue Kit (Qiagen, Hiden, Germany). The sequencing library was prepared as described by Turner and colleagues (30) according to the a previously described protocol (Baym et al., 2015) using the Illumina Nextera kit (Illumina Inc., San Diego, CA) and sequenced using an Illumina NextSeq500. Samples were sequenced to 160x coverage on average for *P. aeruginosa* populations and 309x coverage on average for *A. baumannii* populations.

Sequences were trimmed using the Trimmomatic software v0.36 with the following criteria: LEADING:20 TRAILING:20 SLIDINGWINDOW:4:20 MINLEN:70 (Bolger et al., 2014). The breseq software v0.31.0 was used to call variants using the default parameters and the -p flag when analyzing population sequences (Deatherage and Barrick, 2014). These parameters call mutations only if they are present at least 5% frequency within the population and are in at least 2 reads from each strand. The *A. baumannii* ATCC 17978-mff genome (NZ\_CP012004) and plasmid NZ\_CP012005 sequences were downloaded from RefSeq. Two additional plasmids were found to exist in our working strain and were added to this reference genome: NC009083 and

NC\_009084. The *P. aeruginosa* UCBPP-PA14 genome was downloaded from RefSeq (NC\_008463). Mutations were removed if they were also found in the ancestor's sequence when mapped to the reference genome. Mutations that did not reach at least 25% cumulative frequency across all populations at all timepoints were removed, and mutations were also manually curated to remove biologically implausible mutations. A mutation was determined biologically implausible if it occurred either *i*) at trajectories that were not possible given the trajectories of the putative driver mutations, *ii*) at only the ends of reads, only reads with many other mutations, or at only low coverage (<10 reads), indicating poor read mapping at that region. When high-quality mutations in loci related to the putative driver loci or ribosome machinery were reported in New Junction Evidence by breseq, these mutations were also included in the analysis. Mutations fitting these criteria included mutations to 23S rRNA in *P. aeruginosa*, and mutations to *ptsP*, HPr, and NADH quinone oxidoreductase in *A. baumannii*. Filtering, allele frequencies, and plotting were done in R v3.5.3 with the packages ggplot2 v2.2.1 (R Core Team, 2021; Wickham et al., 2019). Muller plots were generated using the lolipop package by CD (<https://github.com/cdeitrick/lolipop>) v0.5.2 using default parameters. These scripts predict genotypes and lineages based on the trajectories of mutations over time using a hierarchical clustering method and implement filtering criteria to eliminate singletons that do not comprise prevalent genotypes. Muller plots were manually color coded by the presence of putative driver mutations within each genotype. Additional mutations that occurred on the background of putative driver mutations can be viewed in the allele frequency plots in Figure 6 but were not shown in Muller plots.

### 2.5.6 Resistance loci alignment and mutation mapping

Mutations in putative resistance loci (*fusA1*, *ptsP*, *cyoA*, and *cyoB*) were identified in previous literature reporting that these mutations arose in response to aminoglycoside selection or directly conferred an increase in aminoglycoside resistance by MIC assay. Amino acid sequences of the encoded proteins for these species were obtained by searching the “Features” section of PATRIC for these genes in the genomes specified in these experiments (Wattam et al., 2017). The amino acid sequences were aligned in PATRIC and mutations reported in each study were determined according to the corresponding position in the sequence alignment. We tested whether the SNPs identified in each of these genes occur in conserved positions more frequently than expected considering the frequency of conserved positions within the genes using a Fisher’s exact test. The protein structure of EF-G for *P. aeruginosa* strain PAO1 (4FN5) was obtained from the Protein Data Bank (Berman et al., 2000; Nyfeler et al., 2012). All mutations associated with aminoglycoside resistance were colored in blue according to the relative position of the mutation in the *P. aeruginosa* EF-G protein sequence using UCSF Chimera (Pettersen et al., 2004). Mutations in these genes in clinical isolates were found by searching for whole genome sequencing studies of *P. aeruginosa* isolates from cystic fibrosis patients that reported these mutations. Studies that reported increased aminoglycoside resistance *in vitro* for mutants with identical SNP changes as those identified in clinical isolates were also included (Bolard et al., 2017).

### **2.5.7 Data availability**

All sequencing reads were deposited in NCBI under BioProjects PRJNA595915 and PRJNA485123. Detailed methods regarding data processing can be found at [https://github.com/michellescribner/tobramycin\\_analysis\\_code](https://github.com/michellescribner/tobramycin_analysis_code).

**3.0 The nutritional environment is sufficient to select coexisting biofilm and quorum sensing mutants of *Pseudomonas aeruginosa***

This chapter is adapted from the following manuscript under review:

**Michelle R. Scribner<sup>a,b</sup>**, Amelia C. Stephens<sup>a</sup>, Justin L. Huong<sup>a,b</sup>, Anthony R. Richardson<sup>a</sup>,  
Vaughn S. Cooper<sup>a,b</sup>

**The nutritional environment is sufficient to select coexisting biofilm and quorum sensing mutants of *Pseudomonas aeruginosa***

<sup>a</sup>Department of Microbiology and Molecular Genetics, University of Pittsburgh, Pittsburgh, Pennsylvania, USA

<sup>b</sup>Center for Evolutionary Biology and Medicine, University of Pittsburgh, Pittsburgh, Pennsylvania, USA

### 3.1 Project summary

The evolution of bacterial populations during infections can be influenced by various factors including available nutrients, the immune system, and competing microbes, rendering it difficult to identify the specific forces that select on evolved traits. The genomes of *Pseudomonas aeruginosa* isolated from the airway of people with cystic fibrosis (CF), for example, have revealed commonly mutated genes, but which phenotypes led to their prevalence is often uncertain. Here, we focus on effects of nutritional components of the CF airway on genetic adaptations by *P. aeruginosa* grown in either well-mixed (planktonic) or biofilm-associated conditions. After only 80 generations of experimental evolution in a simple medium with glucose, lactate, and amino acids, all planktonic populations diversified into lineages with mutated genes common to CF infections: *morA*, encoding a regulator of biofilm formation, or *lasR*, encoding a quorum sensing regulator that modulates the expression of virulence factors. Although mutated quorum sensing is often thought to be selected *in vivo* due to altered virulence phenotypes or social cheating, isolates with *lasR* mutations demonstrated increased fitness when grown alone and outcompeted the ancestral PA14 strain. Nonsynonymous SNPs in *morA* increased fitness in a nutrient concentration-dependent manner during planktonic growth and surprisingly also increased biofilm production. Populations propagated in biofilm conditions also acquired mutations in loci associated with chronic infections, including *lasR* and cyclic-di-GMP regulators *roeA* and *wspF*. These findings demonstrate that nutrient conditions and biofilm selection are sufficient to select mutants with problematic clinical phenotypes including increased biofilm and altered quorum sensing.

### 3.2 Introduction

During infection, a subset of spontaneous mutations in the pathogen population may produce dangerous clinical consequences including resistance to antimicrobial treatment and immune clearance (Gatt and Margalit, 2021; Lieberman et al., 2014; Marvig et al., 2015; Winstanley et al., 2016). These become more probable with increasing generations of growth as populations expand or persist (Cooper, 2018; Cooper et al., 2020; Hughes and Andersson, 2017). It is therefore critical to characterize adaptations that are selected *in vivo*, the causative mutations, and the environmental factors that contribute to their selection. Longitudinal *Pseudomonas aeruginosa* isolates from many people with cystic fibrosis (CF) commonly share several evolved traits, including high biofilm phenotypes (Smith et al., 2006), increased antimicrobial resistance (Greipel et al., 2016), loss of O-antigen (Hancock et al., 1983), and increased alginate production (Boucher et al., 1997). These traits also often vary among isolates within patients and this diversity is thought to contribute to ineffective clearing by treatment (Clark et al., 2018; Jorth et al., 2015) and ultimately increased morbidity and mortality (Caverly et al., 2015; Emerson et al., 2002). Whole-genome sequencing (WGS) of these isolates has identified convergent mutations in certain genes that persist within the CF respiratory environment (Marvig et al., 2015; Smith et al., 2006). One of the most commonly mutated genes is *lasR*, encoding a transcriptional regulator of quorum sensing, and mutations in regulators of biofilm production are also common, among others (Feltner et al., 2016; Marvig et al., 2015; Wilder et al., 2009). However, numerous factors could select for phenotypic and genotypic diversity in the CF airway (Jorth et al., 2015; Markussen et al., 2014), making it challenging to infer causes of the prevalence of these mutations and phenotypes.

Evolution experiments in models of host systems can clarify which factors most influence pathogen fitness *in vivo*. The nutritional environment is increasingly appreciated as a major

selective pressure, which motivated development of an artificial sputum medium that approximates the nutrient concentrations found in CF sputum and produces similar growth phenotypes and transcriptional responses as actual sputum (Palmer et al., 2005, 2007; Cornforth et al., 2020). Evolution experiments with *P. aeruginosa* have been conducted in this medium to identify beneficial mutations in particular conditions, including antibiotic pressure (Wong et al., 2012), biofilm lifestyle (Azimi et al., 2020), and presence of mucins (Schick and Kassen, 2018; Wong et al., 2012). Several observations are consistent across these studies, particularly the rapid diversification of biofilm, motility, and colony phenotypes. Mutations in certain genes have also been identified repeatedly including *lasR* and genes within the Wsp pathway (Azimi et al., 2020; Schick and Kassen, 2020; Wong et al., 2012).

Because these common mutations produce broad pleiotropic effects, determining which phenotypes were initially adaptive within the host remains unresolved. For instance, the *lasR* gene encodes the transcriptional regulator of the LasRI acyl-homoserine lactone (AHL) quorum sensing system which regulates the expression of hundreds of genes, including other quorum sensing systems (RhlRI and PQS). Loss-of-function *lasR* mutations reduce production of extracellular proteases (Passador et al., 1993), improve fitness in microoxia (Clay et al., 2020), increase resistance to ceftazidime (Azimi et al., 2020), improve growth in amino acids (D'Argenio et al., 2007), and produce a “lysis and sheen” colony morphology (D'Argenio et al., 2007). LasR mutants are frequently described as social cheaters because they can use public goods such as proteases produced by competitors without undergoing the cost of producing these products themselves (Chen et al., 2019; Sandoz et al., 2007), although recent findings suggest that *lasR* mutants actually overproduce these public goods when co-cultured with a LasR+ strain (Mould et al., 2020). In addition, mutations in regulators of cyclic-di-GMP, a second messenger that promotes biofilm and

suppresses motility when upregulated, may also produce a wide range of effects on cell cycle, virulence, and motility (Ha and O'Toole, 2015; Jenal et al., 2017). These mutations may be selected for the complete suite of new phenotypes they cause or perhaps only one of them. Modeling specific subsets of the infection environment is therefore required to quantify contributions of different selective pressures to pathogen evolution.

We sought to identify which adaptations to the CF airway may be related to the nutrient environment by performing an evolution experiment of *P. aeruginosa* strain PA14 in a defined medium containing carbon sources prevalent in CF sputum. Replicate populations were propagated either by serial broth dilution or in a biofilm model using beads to study the influence of lifestyle on mutant selection (Traverse et al., 2013). We performed whole population genome sequencing of each lineage and sequenced isolated clones to infer population structure and to link evolved phenotypes to genotypes. We also characterized the consequences of these mutations on clinically relevant phenotypes including biofilm production and motility to examine how these adaptations could influence pathogenesis.

### **3.3 Results**

#### **3.3.1 Genetic targets of evolution in CF nutrients mimic *in vivo* adaptation**

To examine the role of nutrients in *P. aeruginosa* adaptation to the CF airway, strain PA14 was propagated in substrates found to be prevalent in the cystic fibrosis respiratory tract (11mM glucose, 10mM LD-lactate, and 4mM amino acids) for 12 days. The concentrations of these carbon sources differ from those in an established synthetic CF medium (SCFM; 3.2mM glucose, 9.3mM lactate, and 19mM amino acids), but are within the range previously reported for CF sputum with

the exception of increased glucose (Palmer et al., 2007). Populations were propagated with either planktonic selection through a 1:100 dilution into fresh medium every 24 hours or biofilm selection by transferring a colonized polystyrene bead to fresh medium every 24 hours as previously described (Scribner et al., 2020). Although other factors associated with our culture conditions also influence selection, we can identify mutations associated with growth in CF nutrients by comparing adaptations in this medium with previous experiments from our laboratory, which used different medium but an identical ancestral strain and transfer protocol (Harris et al., 2021). Population transfer sizes were  $\sim 10^8$  cells in both planktonic and biofilm transfer methods, producing approximately 6.6 generations/day and 80 generations over the course of the experiment. We estimate that approximately  $10^6$  new mutations occur each day in this experiment based on reported mutation rates of this and related strains (Dettman et al., 2016; Flynn et al., 2016; Harris et al., 2021; Heilbron et al., 2014), but these large effective population sizes ensure that only the fittest mutants within each population will rise to a detectable frequency within this short time frame (Santos-Lopez et al., 2019). Thus, the mutations reported here almost certainly produce adaptations.

We performed whole genome sequencing of five evolved planktonic and five evolved biofilm populations to read depths of 86-254X to identify selected genotypes (Figure 9). After only twelve days, mutations in *lasR* (PA14\_45960) and *morA* (PA14\_60870) evolved within four of five planktonic populations. Mutations in *lasR* included large deletions encompassing both *lasR* and *lasI* genes (PA14\_45920 to PA14\_46440  $\Delta 49,133$  and PA14\_45800 to PA14\_46240  $\Delta 40,707$ ), nonsynonymous SNPs, and nonsense mutations (Figure 10A). The *lasR* and *lasI* genes encode the regulator and autoinducer synthesis proteins, respectively, of the Las quorum sensing system (Kostylev et al., 2019). The *morA* gene encodes a protein with both diguanylate cyclase

(DGC) and phosphodiesterase (PDE) domains, which produce and degrade second messenger cyclic di-GMP, respectively (Ha and O'Toole, 2015). Nonsynonymous substitutions occurred at five different residues within *morA* (A1109V, K1123E, N1124K, E1153K, and L1155Q), indicating that they arose independently and were selected in parallel (Figure 10B). Mutations in *morA* and *lasR* are two of the most frequently mutated genes in CF clinical isolates (D'Argenio et al., 2007; Marvig et al., 2015; Smith et al., 2006), and strikingly, this experiment selected mutations in some of the same residues altered during CF infections, including *lasR* P117 and A231 (Smith et al., 2006). We also identified multiple instances of residue and domain-level parallelism between *morA* mutations detected in this experiment, other evolution experiments in SCFM or rich media, and clinical isolates (Figure 10B, Figure 11) (Marvig et al., 2015; Sanz-García et al., 2018; Wong et al., 2012). This convergent evolution demonstrates that the nutrients found in CF sputum are sufficient to select for similar mutations as identified in clinical isolates.

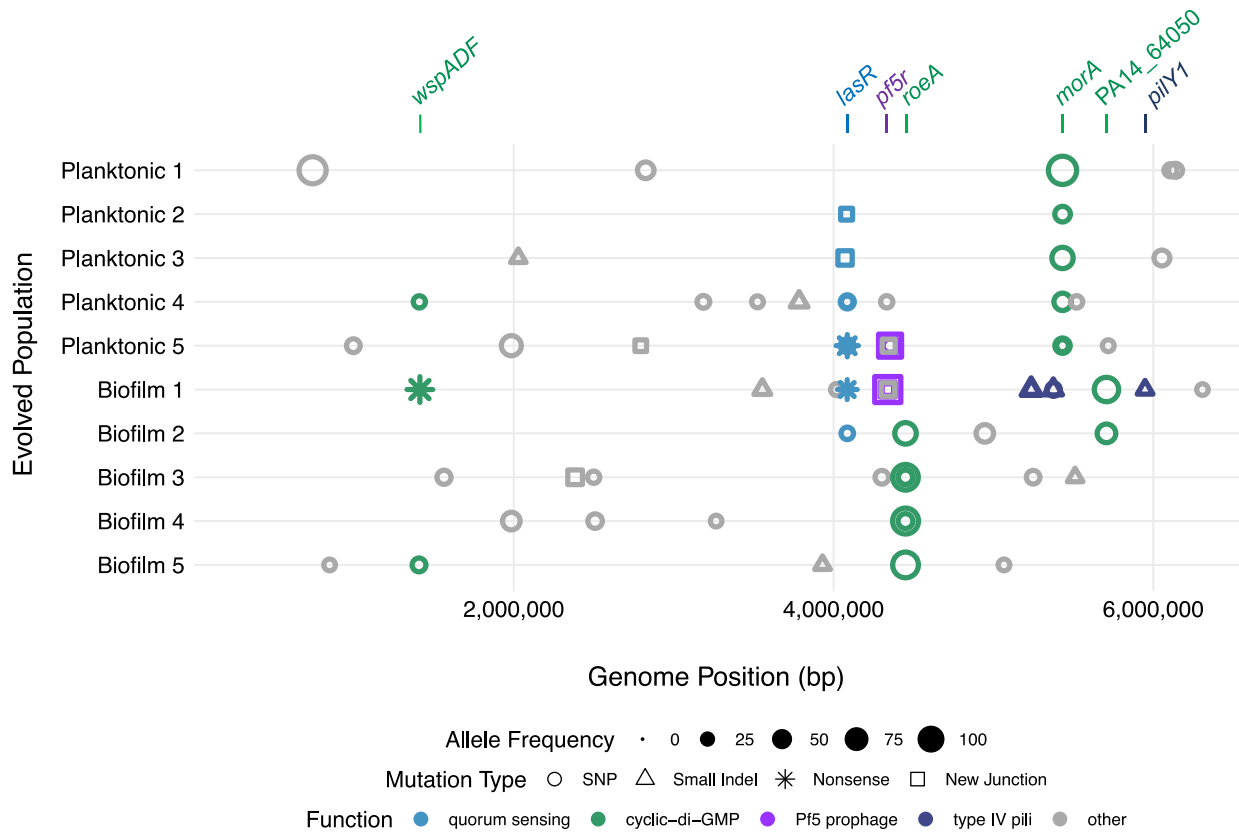


**Figure 9. Propagation of *P. aeruginosa* in nutrients present in the CF airway rapidly selects for mutations in regulators of quorum sensing and cyclic-di-GMP.**

Mutations were inferred from whole genome sequencing of evolved populations after 12 days of selection. All mutations detected by population WGS are indicated, and genes that acquired multiple mutations are labeled. A list of detected variants is in Appendix Table 2. Allele frequency for each mutation is indicated by symbol size, mutation type by symbol shape, and function of the impacted loci by symbol color. Mutations detected by new junction evidence, which include insertions, large deletions, and structural rearrangements, are indicated at the position of the most upstream side of the junction.

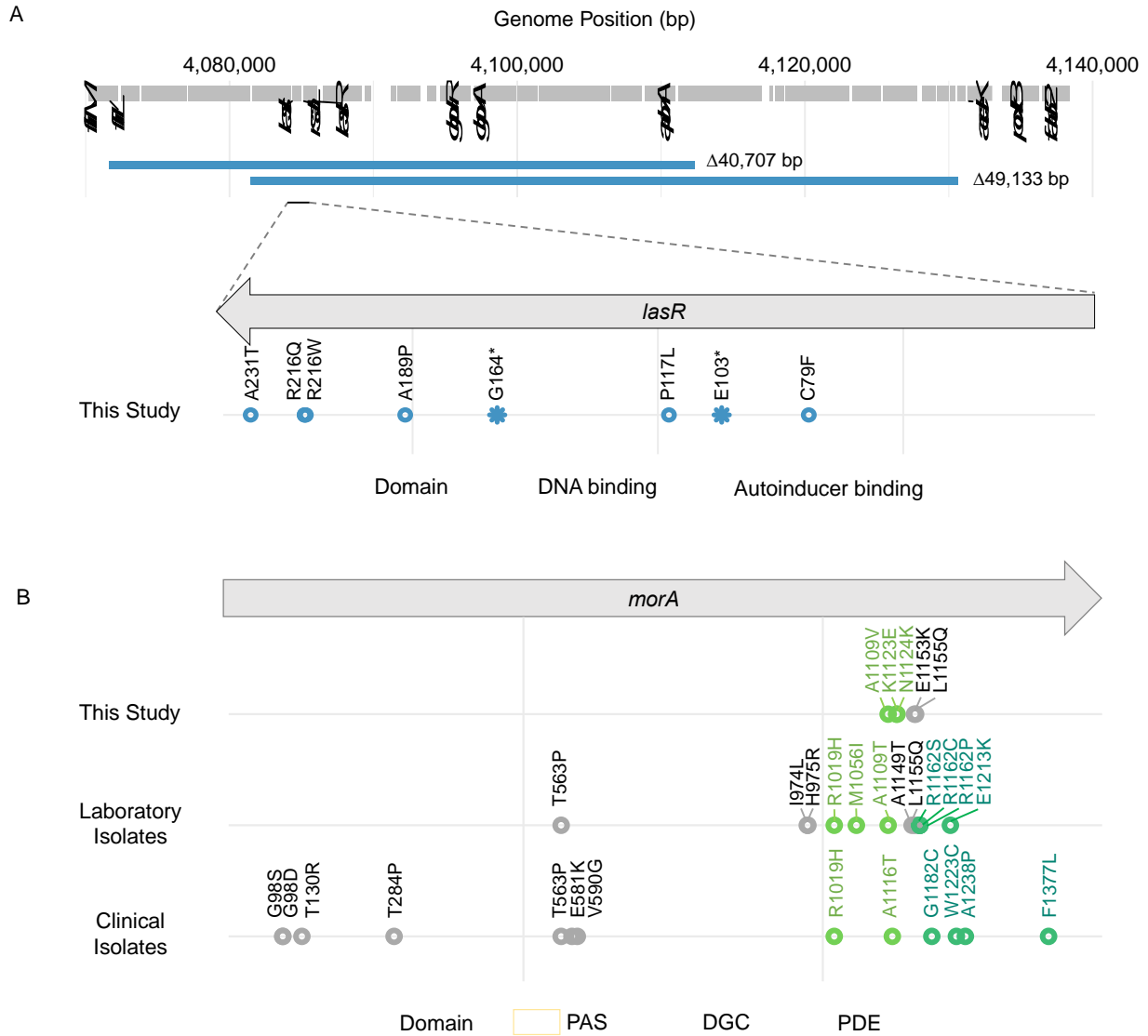


**Figure 10. Parallel evolution of mutations in *lasR* and *morA* reveal sites under strong selection.**

A) Two large deletions that include the *lasI* and *lasR* genes were detected as well as many nonsynonymous SNPs and missense mutations. Top: the extent and overlapping region of these deletions; bottom: evolved *lasR* mutations by relative position. B) Mutations in *morA* were also frequently selected, primarily within the diguanylate cyclase (DGC) domain and linker region between the DGC and phosphodiesterase (PDE) domains (This Study). We also identified nonsynonymous *morA* mutations in other evolution experiments in our laboratory and other studies (Laboratory Isolates) (Sanz-García et al., 2018; Wong et al., 2012). Identical mutated sites have been identified in clinical isolates from people with cystic fibrosis (Clinical Isolates) (Marvig et al., 2015; Smith et al., 2006).

Mutations are shaded by domain in which they occur.

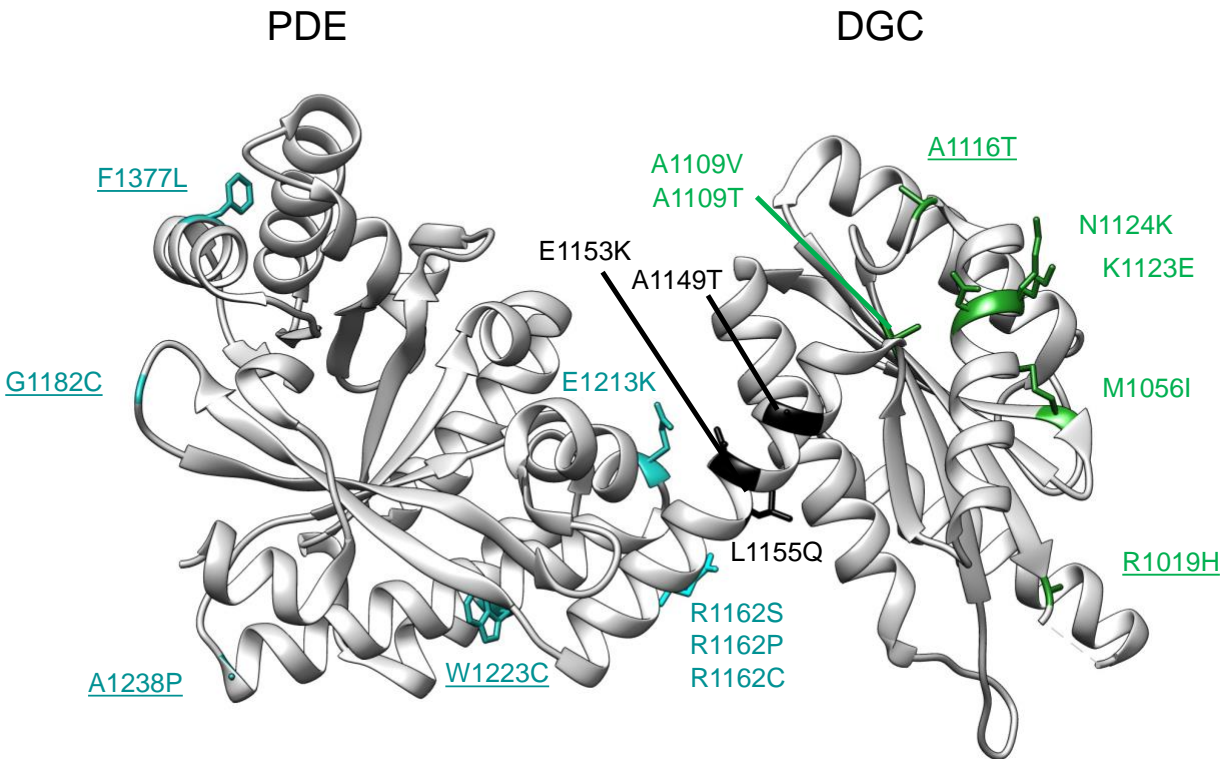


**Figure 11. Mutated residues within MorA detected in this experiment, other laboratory experiments and clinical isolates are illustrated on the structure of the PAO1 MorA DGC and PDE domains (PDB 4RNF).**

Mutated residues in the DGC domain are indicated in green, and mutated residues in the PDE domain are indicated in blue. Mutations are labeled by amino acid change and those detected in clinical isolates are underlined. Mutations identified in this study: A1109V, K1123E, N1124K, E1153K, L1155Q. Mutations identified in other laboratory isolates: R1019H, M1056I, A1109T, A1149T, L1155Q, R1162S, R1162C, R1162P, E1213K (Sanz-García et al., 2018; Wong et al., 2012). Mutations identified clinical isolates: R1019H, A1116T, G1182C, W1223C, A1238P, F1377L (Marvig et al., 2015).

Biofilm-adapted populations also nearly exclusively selected mutations associated with cystic fibrosis infection including genes regulating cyclic-di-GMP, quorum sensing, and type IV pili (Marvig et al., 2015; Winstanley et al., 2016). All biofilm populations acquired at least two mutations in regulators of cyclic-di-GMP (*wspAF*, *roeA*, and PA14\_64050), often on different

sublineages at high frequencies (Figure 9). These findings add to evidence that modulating levels of cyclic-di-GMP is advantageous in a biofilm environment (Gloag et al., 2019; McDonald et al., 2009). Yet, the PA14 genome harbors ~40 genes containing DGC domains, PDE domains, or both that could alter cyclic-di-GMP levels (Kulesekara et al., 2006), so the repeated selection of mutations in only these three genes suggests that these regulators of cyclic-di-GMP are not redundant but rather are environment-specific, as shown elsewhere (Ha et al., 2014a). Biofilm lineages 1 and 2 also acquired mutations in *lasR*, suggesting that altered quorum sensing was beneficial in both planktonic and biofilm environments. However, these regulators of quorum sensing and cyclic-di-GMP were not among the most frequently mutated genes in identical evolution experiments from our laboratory using growth medium containing arginine as sole carbon source, indicating that their benefit is linked to available nutrients and concentrations (Harris et al., 2021). Most importantly, the almost exclusive selection of mutations known to arise during chronic infection in CF suggests that our simple nutritional model closely recapitulates several major selective forces acting in the CF airway.

### **3.3.2 Mutations in *lasR*, *morA*, and *wspF* underlie rapid morphological and phenotypic diversification**

Colony morphologies became conspicuously diverse in both biofilm and planktonic treatments after twelve days of selection, so we picked clones with representative phenotypes and sequenced their genomes to identify the causative mutations (Figure 12). These genotypes demonstrated that *lasR*, *morA*, and *wspF* lineages arose independently and identified additional *lasR* and *wspF* mutations that were undetected by population WGS. Mutations in *wspF* or between the DGC and PDE domains of *morA* produced wrinkly or rugose small colony variants (RSCVs).

We measured the motility and biofilm production of isolated mutants and found that *lasR* and *morA* mutants from the same population were functionally distinct (Figure 13). All *morA* mutations decreased swimming motility and increased biofilm, whereas *lasR* mutants showed no change in biofilm or swimming motility, except for one that also had disrupted flagellar genes (PA14\_45800 to PA14\_46240  $\Delta$ 40,707), which lost swimming motility. Unsurprisingly, most mutants isolated from biofilm-evolved populations produced more biofilm and showed decreased swimming motility (Figure 13) and swarming motility (Figure 14) than the ancestral strain. Therefore, similar phenotypes evolved in replicate populations associated with parallel genotypes.

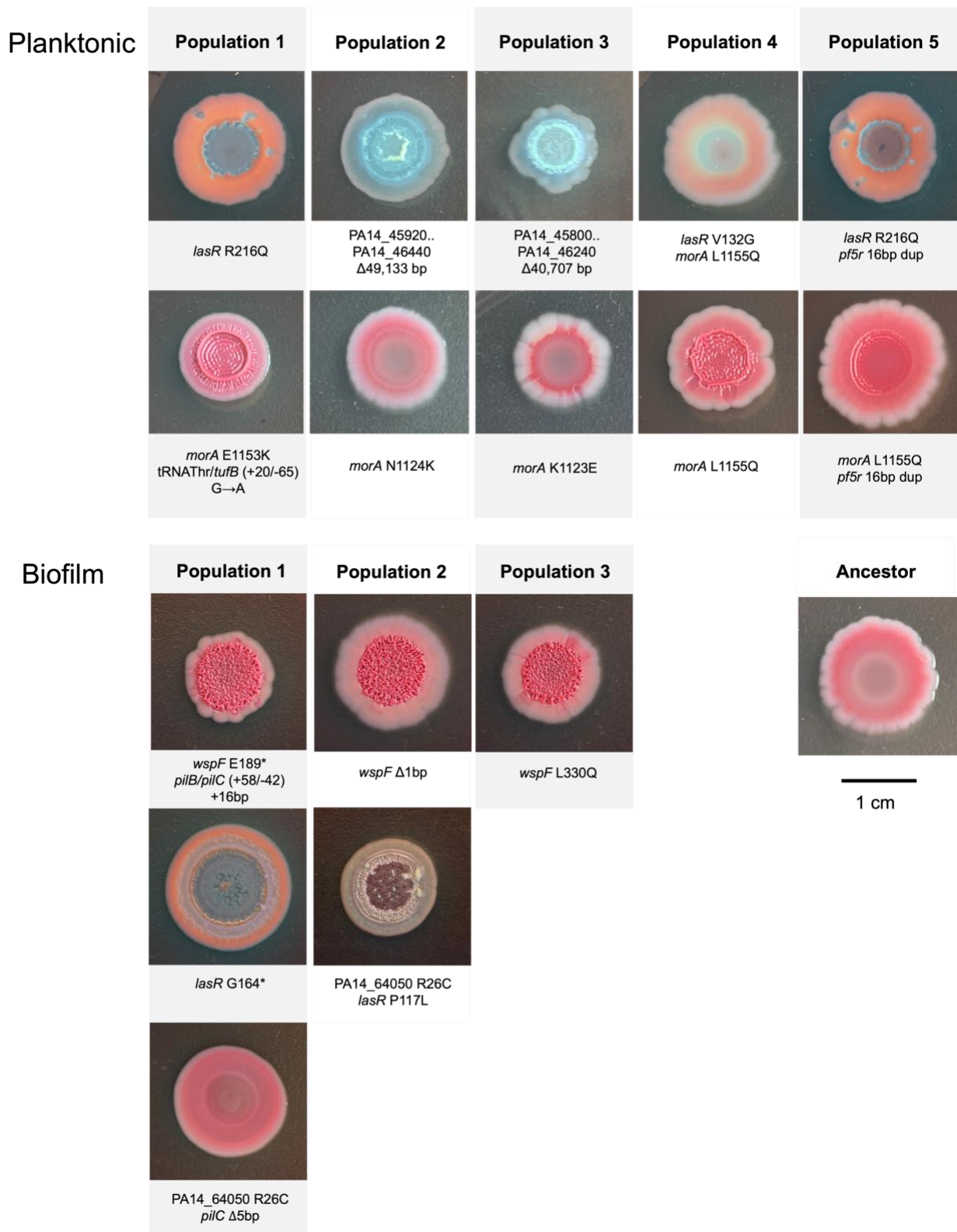


**Figure 12. Mutations in the *lasR*, *morA*, and *wspF* genes produce rapid morphological diversity over short timescales.**

Images show representative morphologies of evolved mutants following incubation on agar supplemented with Coomassie Blue and Congo Red dyes. Mutations listed are the only variants detected between the isolated clone and the ancestor. Certain mutations identified in clones were not detected by population sequencing, thus likely represent rare haplotypes within the evolved lineages.

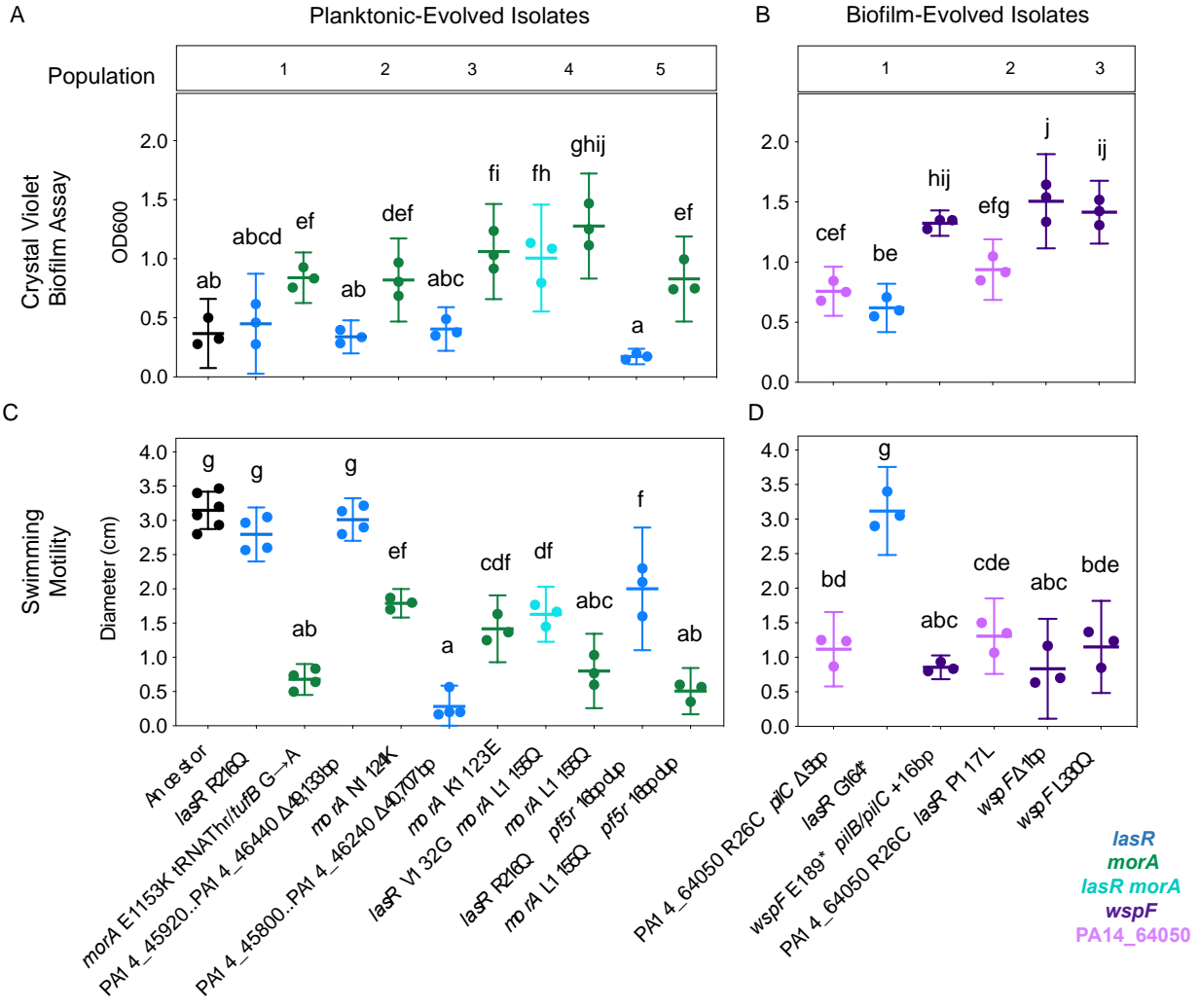


**Figure 13. Mutations in *lasR* and in multiple cyclic-di-GMP regulators produce coexisting subpopulations with distinct biofilm and motility phenotypes.**

Biofilm production by isolates from A) planktonic lineages and B) biofilm lineages. Swimming motility by isolates from C) planktonic lineages and D) biofilm lineages. Strains are labeled by genotype. Datapoints represent the average of technical replicates from at least three independent experiments and are shown with mean and 95% CI. Data were analyzed by one-way ANOVA (Biofilm:  $F(16,34) = 32.76$ ,  $p < 0.0001$ , Swimming Motility:  $F(16,41) = 72.67$ ,  $p < 0.0001$ ) with Tukey's multiple comparisons test. Groups labeled with the same letter are not statistically different ( $p < 0.05$ ).

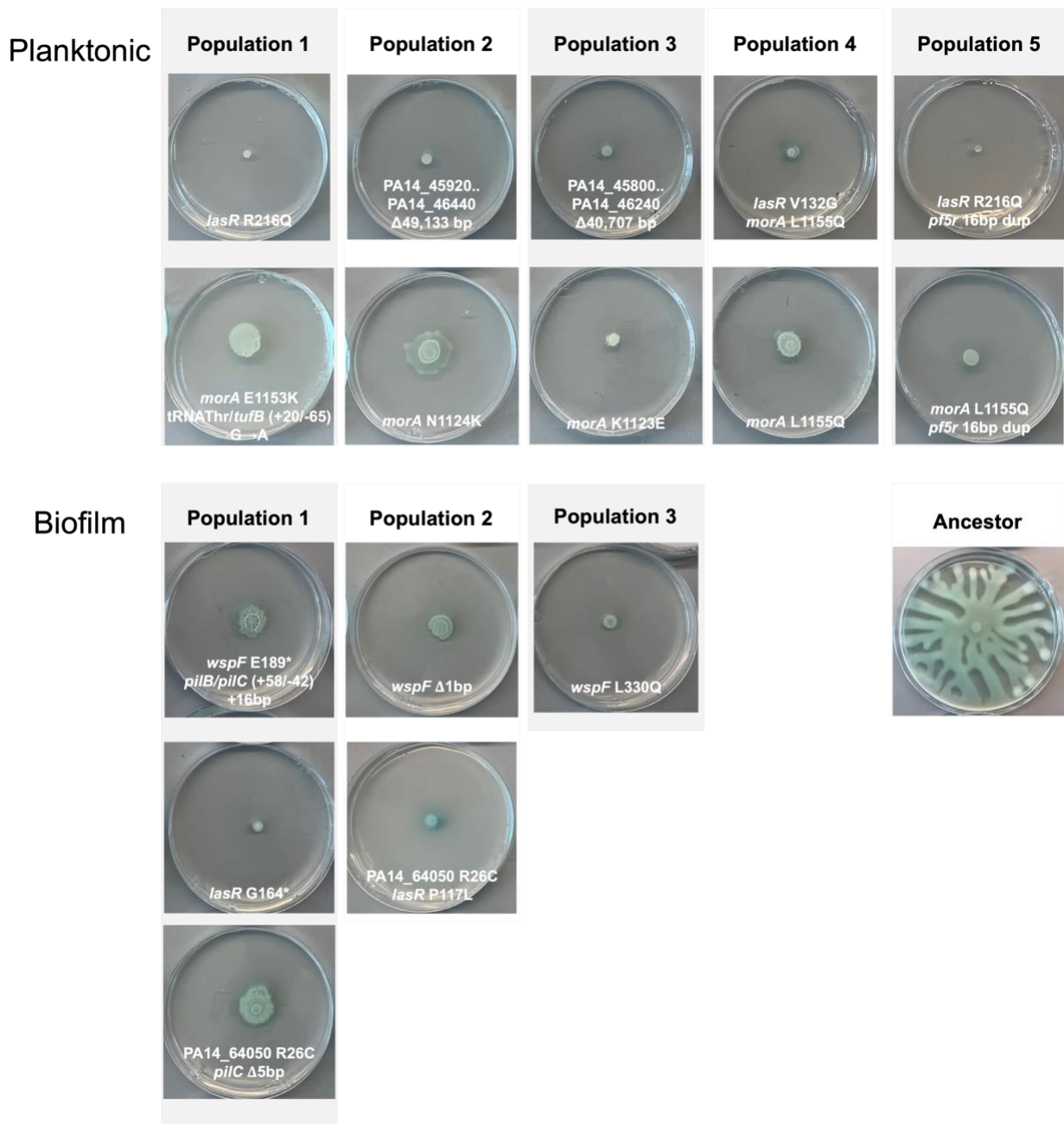


**Figure 14. Decreased swarming motility of all clones isolated from evolved populations.**

Isolated clones from planktonic populations and biofilm populations were used to inoculate 0.5% agar plates. Plates were photographed after 24 hours of incubation.

### 3.3.3 *morA* mutations produce adaptations specific to high nutrient concentration

The repeated selection of *morA* and *lasR* mutations in planktonic populations indicates that independently of any advantages of increased biofilm or altered virulence factor production in a host, they produce growth advantages. Prior studies have shown that *morA* mutant phenotypes depend on carbon sources (Ha et al., 2014a) and that *lasR* mutants enhance growth in amino acids (D'Argenio et al., 2007). To build upon these findings and to explore possible mechanisms explaining their coexistence, we measured mutant fitness in each of the carbon sources in the evolution medium: glucose, amino acids, and lactate (Figure 15). A mutant with a nonsynonymous SNP in the linker domain of *morA* outcompeted the ancestor in medium containing all carbon sources but was less fit in media containing only a subset of the carbon sources (Figure 15B). Other isolates with SNPs in *morA* also grew worse than the ancestor when cultured in only amino acids or only lactate (Figure 16). These findings suggest that fitness of *morA* mutants may be influenced by nutrient identity, nutrient level, or both. To distinguish between these possibilities, we performed competition assays in various nutrient levels and found that *morA* mutant fitness was indeed dependent on nutrient concentration (Figure 15B). For instance, halving the concentration of each of the carbon sources from net 25mM to 12.5mM in the evolution medium decreased *morA* mutant fitness. Therefore, nutrient abundance alone is sufficient for the selection of *morA* mutants, though nutrient composition may modulate the strength of this selection.

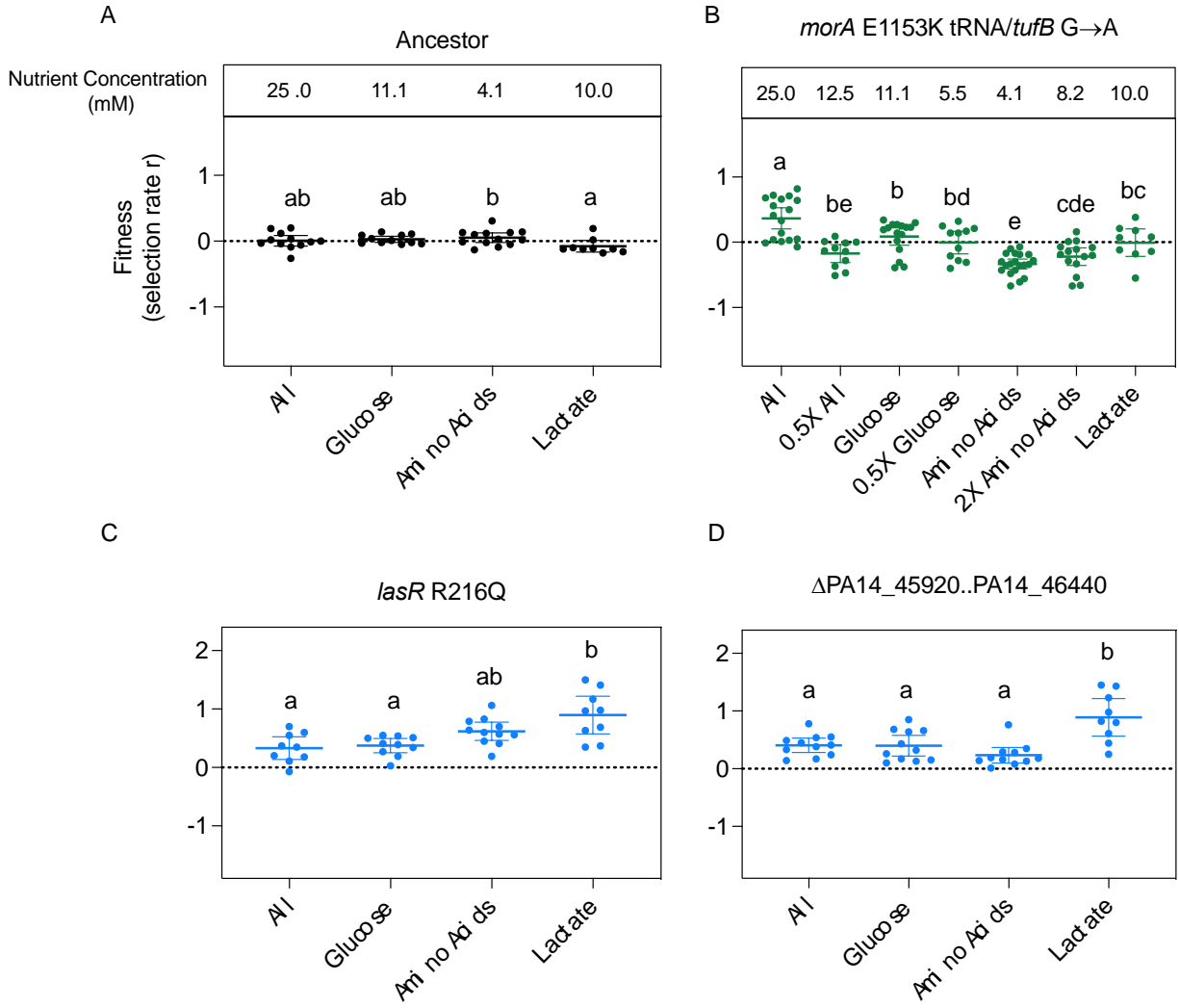


**Figure 15. Environment-specific fitness advantages of *lasR* and *morA* mutants.**

A marked ancestral strain was competed against A) the ancestral strain, B) an isolate with a *morA* SNP (E1153K) and an intergenic SNP between a tRNA and the *tufB* gene, C) an isolate with a SNP in *lasR* (R216Q), and D) an isolate with a large deletion encompassing *lasR* and *lasI*. Competitions were performed in the medium used for the evolution experiment (All) as well as medium containing only a subset of the carbon sources (Glucose, Amino Acids, Lactate). The *morA* mutant was also competed in media in which the concentration of nutrients was doubled or halved to determine the effect of nutrient concentration on fitness (0.5X All, 0.5X Glucose, 2X Amino Acids). Datapoints represent fitness measurements from independent competitions spread across at least three batches of assays. Mean and 95% CI are shown. Within each genotype, statistical differences in fitness in each media were determined using ANOVA (Ancestor:  $F(3, 41) = 2.680$ ,  $P = 0.0594$ , *morA* tRNA/*tufB*:  $F(6, 92) = 15.20$ ,  $P < 0.0001$ ,

*lasR* R216Q:  $F(3, 35) = 8.064, P=0.0003, \Delta PA14\_45920..PA14\_46440: F(3, 38) = 10.07, P<0.0001$ ) with Tukey's multiple comparisons test. Groups labeled with the same letter are not statistically different ( $P < 0.05$ ).

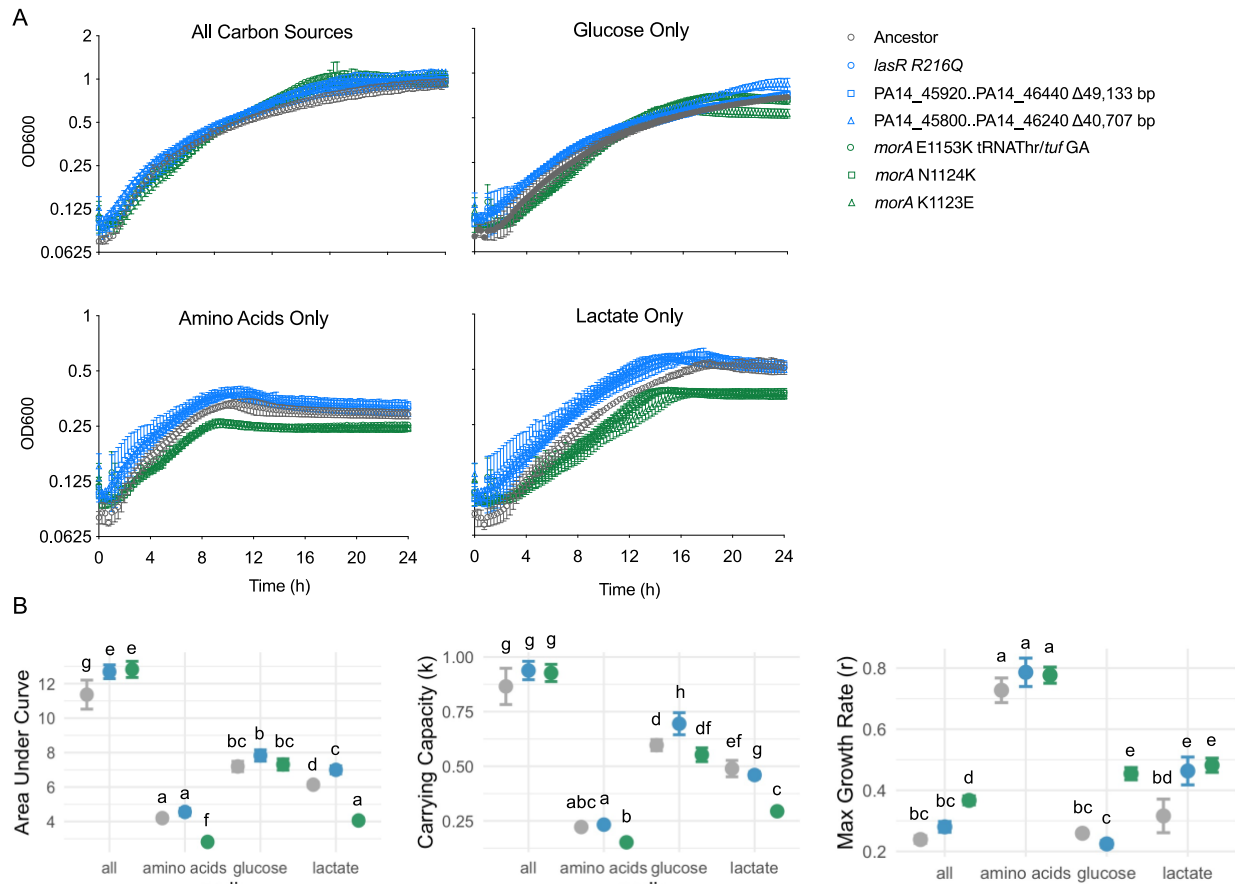


**Figure 16. Growth curves of evolved clones in different carbon sources reveal distinct growth advantages for mutants with *morA* and *lasR* alterations.**

A) Growth curves were performed in the media used for the evolution experiment (All Carbon) as well as media containing only a subset of the carbon sources (Glucose Only, Amino Acids Only, Lactate Only). Datapoints represent the mean of three independent experiments and error bars represent 95% CI. Three distinct *lasR* mutants and *morA* mutants were utilized for each growth curve assay. B) Area under curve, carrying capacity ( $k$ ), and maximum growth rate ( $r$ ) were determined for the growth curves visualized in A. Mean and 95% CI for the ancestor (gray), *lasR* mutants (blue), and *morA* mutants (green) are shown. Data were analyzed by two-way ANOVA with Tukey's multiple comparisons, groups labeled with the same letter are not statistically different ( $p < 0.05$ ).

### 3.3.4 *lasR* mutations are beneficial in the absence of a competitor

The fitness advantage of *lasR* mutants in chronic infections has been proposed to derive from multiple features, including social cheating, growth advantages in amino acids or in microoxic environments, and increased growth at high cell densities (Barth and Pitt, 1996; Clay et al., 2020; Dandekar et al., 2012; D'Argenio et al., 2007; Heurlier et al., 2005; Hoffman et al., 2010; Passador et al., 1993; Sandoz et al., 2007). Social cheating refers to the ability of a *lasR* mutant to reap the benefits of public goods secreted by LasR+ cells within the population, including proteases, pyocyanin, and hydrogen cyanide, without undergoing the cost of producing those factors themselves (Popat et al., 2012; Sandoz et al., 2007; Wilder et al., 2011). However, we observed that in the absence of a competitor, *lasR* mutants demonstrated greater area under growth curves than the ancestor (AUC, Figure 16) and similar or greater growth yields (Figure 17). This result shows that exploitation of a competitor is unnecessary for increased *lasR* mutant fitness.

Prior studies of *lasR* mutants have implicated altered carbon catabolite repression as the source of their growth advantages in aromatic amino acids (D'Argenio et al., 2007). Yet we found that *lasR* mutants attained similar fitness advantages in media containing only glucose or only lactate as in only amino acids (Figure 15C and 15D). Nonetheless, we tested whether *lasR* mutations altered carbon catabolite repression by analyzing the nutrient levels in the spent medium of a *lasR* mutant compared to spent medium of the ancestor. We cultured strains separately in the evolution medium and used HPLC to quantify nutrient levels every hour for the first eight hours of growth. We hypothesized that *lasR* mutations may alter the rate or order of nutrient consumption when growing in medium containing multiple carbon sources. We noticed *lasR* mutants produced a spike in OD-normalized amino acid levels at one hour post inoculation that we cannot explain, but no subsequent significant differences in nutrient consumption rate or order were found (Figure

18). Therefore, we cannot attribute the selective advantage of *lasR* mutants in this medium to altered carbon catabolite repression, but it is possible that some relevant metabolic changes were too subtle to be detected using this approach. The specific metabolic source of the growth advantage of *lasR* mutations therefore remains unclear in this environment and merits further study.

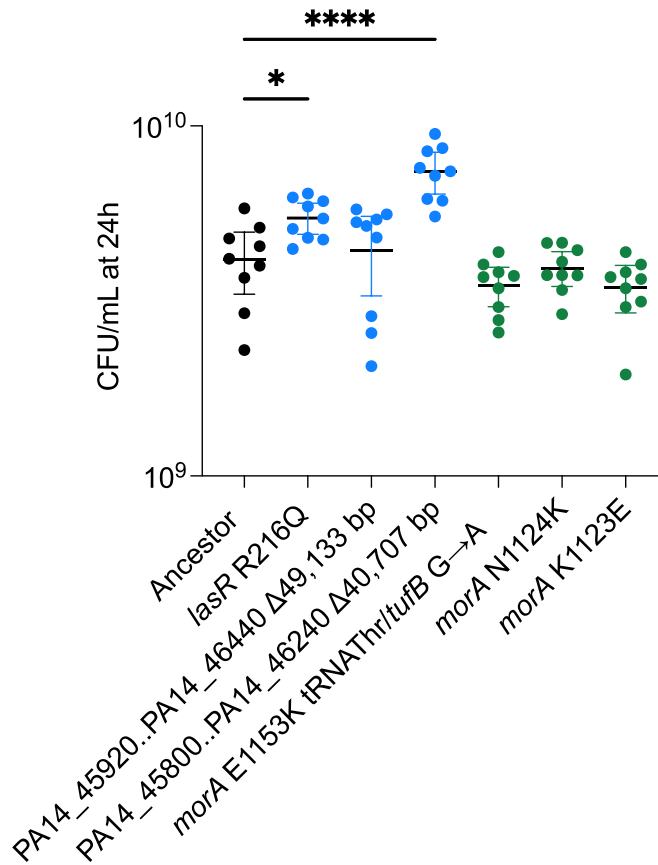


**Figure 17. *lasR* mutations increase growth yield in independent culture.**

Clones isolated from planktonic cultures were incubated in the conditions of the evolution experiment for 24 hours then plated for CFU. Mean and 95% CI are shown for data collected from three experiments with three cultures each. Data were analyzed by one-way ANOVA ( $F(6,56) = 18.36, p < 0.0001$ ) with post hoc comparisons between mutants and the ancestor using Dunnett's multiple comparisons test ( $p < 0.05$ ).

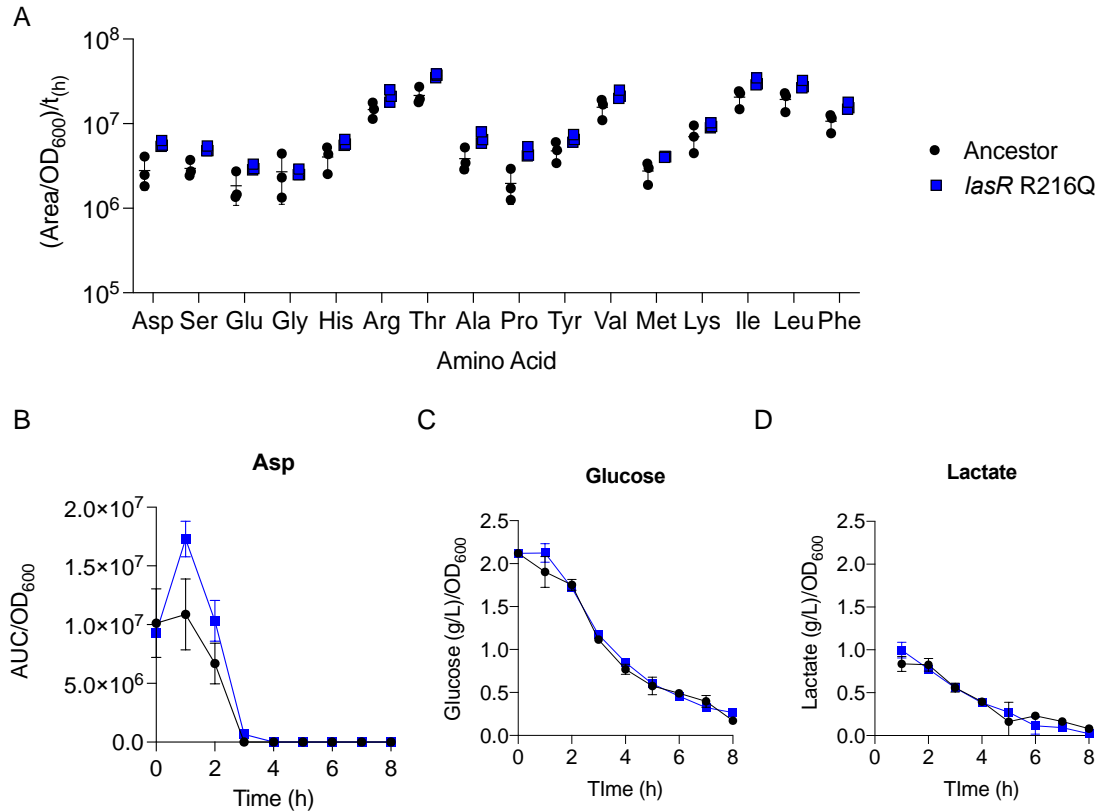


**Figure 18. HPLC analysis of supernatants from a *lasR* R216Q mutant and the ancestral strain reveal that nutrients are consumed at similar rates between the two genotypes.**

Despite a spike in amino acid level at early timepoints for the *lasR* mutant, amino acids are consumed at similar rates as in the ancestral strain. Data represents the consumption of nutrients from media containing all carbon sources (amino acids, glucose, and lactate). Dynamics of amino acid levels for A) all amino acids and B) a representative amino acid (Aspartic acid) are shown. Consumption of C) glucose and D) lactate also occurs at similar rates between genotypes. Mean and SD are shown for at least two biological replicates. The slopes of nutrient consumption for the ancestral strain and *lasR* mutant were compared by t-tests controlled for false discovery rate (Benjamini-Hochberg,  $q = 5\%$ ), and no statistically significant differences were found.

### **3.3.5 Ecological interactions between *morA* and *lasR* mutants facilitate the maintenance of diversity**

We found that *morA* and *lasR* genotypes defined coexisting subpopulations in four out of five planktonic lineages, prompting us to ask if their relative fitness advantages derived from ecological interactions between them. We tested their ability to facilitate each other's coexistence by mixing genotypes at different starting concentrations (Figure 19). Each mutant was more fit when introduced at a lower proportion, consistent with a negative frequency-dependent interaction, or a relationship in which the fitness of a competitor increases as it becomes rarer (Antonovics and Kareiva, 1988; Turner et al., 2020). We repeated this experiment using different *morA* and *lasR* mutants and found this frequency-dependent interaction was consistent (Figure 20). Therefore, nutrients present in the cystic fibrosis lung environment are sufficient to rapidly drive stable, functional diversification, even in the absence of spatial heterogeneity. This finding is relevant to clinical settings as diversity within infections may increase recalcitrance to treatment (Clark et al., 2018).

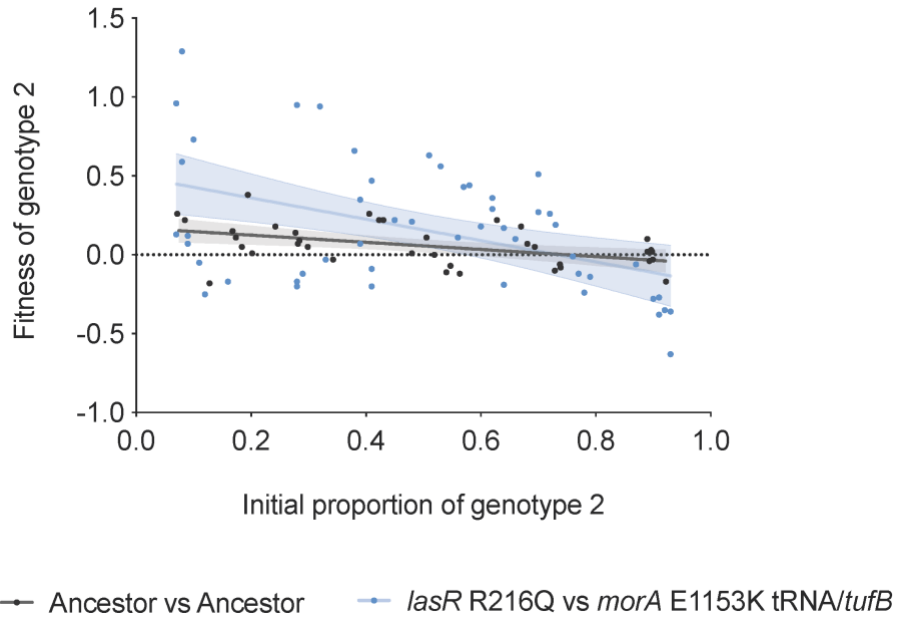


**Figure 19. Relative fitness of *lasR* and *morA* mutants is greater when in the minority.**

We performed direct competitions at the starting concentrations indicated and measured relative fitness at 48 hours.

Genotypes were differentiated using a lac-marked ancestral strain for the ancestral competitions and by colony morphology for the *lasR* mutant versus *morA* mutant competitions. The first competitor listed is genotype 1, the second is genotype 2. Data was analyzed by linear regression, shaded area represents 95% CI of the regression.

Ancestor versus ancestor: slope = -0.2060, *lasR* mutant versus *morA* mutant: slope = -0.6760, difference between the slopes was statistically significant  $F = 4.195$ ,  $DFn = 1$ ,  $DFd = 83$ ,  $p=0.0437$ .

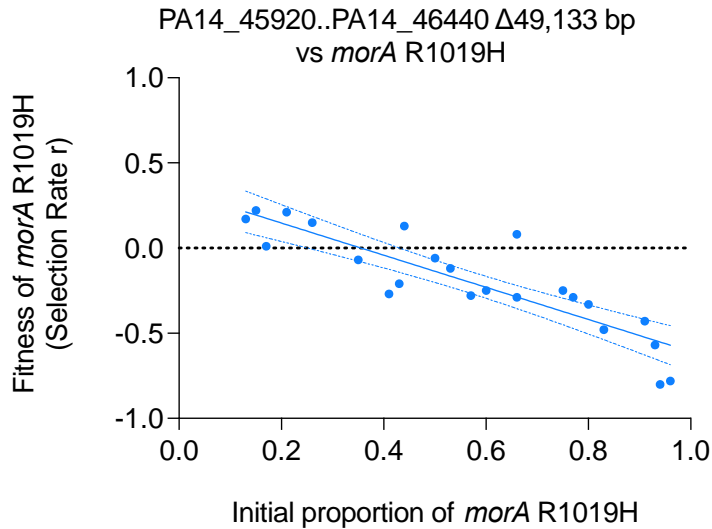


**Figure 20. The negative frequency dependence relationship between *lasR* and *morA* mutants persists across similar genotypes.**

We performed direct competitions at the starting concentrations indicated and measured relative fitness at 48 hours for a large deletion mutant including *lasR* and a *morA* mutant. Genotypes were differentiated by colony morphology. Data was analyzed by linear regression as shown, shaded area represents 95% CI of the regression. Slope = -0.9433, slope was statistically different from zero,  $F = 66.50$ ,  $DFn = 1$ ,  $DFd = 21$ ,  $P < 0.0001$ .

### 3.4 Discussion

The realization that chronic infections of the CF airway by *P. aeruginosa* not only involve adaptive evolution, but also a process of diversification, has motivated numerous explanations (Markussen et al., 2014). Most of these understandably focus on aspects of ourselves as hosts. However, one of the most basic and essential components of host-microbe interactions is nutrition. Here we show that both adaptation and diversification of *P. aeruginosa* occur during propagation in the nutrients found in the cystic fibrosis respiratory environment. Moreover, selected genotypes acquire mutations identical to those recovered from infections, including mutations in cyclic-di-

GMP regulators (*morA*, *wspF*, *roeA*) and quorum sensing regulators (*lasR*). Further, the phenotypes caused by these mutations are of potential clinical importance. Loss-of-function *lasR* mutations have been shown to alter the production of virulence factors and increase resistance to beta-lactam antibiotics (Azimi et al., 2020; D'Argenio et al., 2007), and are associated with lung disease progression (Hoffman et al., 2009). Similarly, high biofilm phenotypes such as those produced by *morA* mutants (RSCVs) have been shown to increase persistence under stresses like the immune system and antibiotics, making these infections more difficult to treat (Harrison et al., 2020; Høiby et al., 2010; Pestrak et al., 2018; Starkey et al., 2009). Selection for either of these phenotypes alone merits concern, but here we show that *morA* and *lasR* mutants frequently are co-selected *in vitro* and facilitate one another's coexistence. Though the mechanism underlying this ecological relationship is yet to be identified, the maintenance of this diversity poses its own risk for population persistence in the face of treatment.

One defining phenotype of many *P. aeruginosa* infections is increased secreted polysaccharides such as those produced by *morA* mutant genotypes. Their selection during planktonic serial transfer was surprising because biofilm matrix components ought to be costly to produce. While the mechanism underlying this paradox is unclear, our results suggest that evolved *morA* mutations were likely selected due to their strong fitness advantage when nutrients are abundant. In recent work, Katharios et al. present a model by which the phosphodiesterase activity of *morA* that degrades cyclic-di-GMP is induced during nutrient limitation to repress costly biofilm production and thus prevent cell death (Katharios-Lanwermyer et al., 2021). Consequently, disrupted *morA* signaling results in increased biofilm when nutrients are abundant, but cell death during nutrient limitation. Our findings are consistent with this report: nonsynonymous substitutions in *morA* increased biofilm and relative fitness but were costly when nutrient levels

were reduced. Abundant nutrients within the cystic fibrosis airway may therefore play an important role in selecting high biofilm mutants.

The specific types and locations of evolved mutations in *morA* and other genes can improve understanding of the selected phenotypes and even how the gene functions. In clinical isolates, both non-synonymous SNPs and deletion mutations in *morA* are prevalent (Marvig et al., 2015), but MorA harbors catalytically active DGC and PDE domains, as well as multiple sensor (PAS) domains, rendering the effect of different types and locations of mutations within the gene unclear. Further, most prior studies of effects of MorA on motility (Choy et al., 2004; Ha et al., 2014a), biofilm (Ha et al., 2014a; Katharios-Lanwermyer et al., 2021), and colony morphology (Harrison et al., 2020) in *Pseudomonas* species used deletion or nonsense mutants. We found that phenotypes of missense mutations in *morA* largely coincide with these deletion mutants, but with some nuance. For instance, missense mutations in *morA* decrease swimming and swarming motility, like *morA* deletions (Ha et al., 2014a), and this is sensible given that *morA* modulates timing of flagellar biosynthesis and both forms of motility are flagella-dependent (Choy et al., 2004; Ha et al., 2014b). But we identified varied levels of swimming motility among missense *morA* mutants, suggesting that the location of mutations within this protein alters mutant phenotype. This subtlety mirrors prior findings from our laboratory focused on a distant homolog in *Burkholderia cenocepacia* (Mhatre et al., 2020). Likewise, we saw that missense *morA* mutations increased biofilm formation in agreement with increased biofilm formation during early growth of *morA* deletions (Katharios-Lanwermyer et al., 2021). Certain missense mutations in *morA* also produced wrinkled colony morphologies, which is consistent with the RCSV phenotype reported for a nonsense mutation in *morA* (Harrison et al., 2020). Altogether, we find that missense mutations in *morA* produce similar

increases in biofilm and decreases in motility as caused by gene deletions, both consistent with disrupted PDE function, but to varying degrees.

A similar analysis can be applied to the wide spectrum of *lasR* mutants we observed during propagation in CF nutrients, including large deletions, nonsense mutations, and missense mutations, which is consistent with the range of mutations observed in clinical isolates (Feltner et al., 2016; Smith et al., 2006). In fact, we identified several missense mutations at identical residues (P117L, A231) or adjacent residues (C79, A189, R216) to those detected in clinical samples. Several of these missense variants reduce, but do not eliminate, LasR activity in PAO1 (Feltner et al., 2016). If these mutations confer similar phenotypes in PA14, the selection of *lasR* mutants in this experiment suggests that both complete loss and reduction of LasR signaling are advantageous in this environment; however, the effect of *lasR* mutation is known to vary based on genetic background (Feltner et al., 2016). In addition, previous studies indicate that *P. aeruginosa* may induce the RhlR-RhlI quorum sensing system to overcome defective LasR (Feltner et al., 2016), therefore *lasR* deletion mutants identified in our experiment are not necessarily completely defective in quorum sensing. However, the substantial overlap between genotypes and phenotypes from this study and from prior work on laboratory and clinical mutants indicates shared selective forces. Specifically, altered LasR signaling is advantageous during growth on CF nutrients either with or without biofilm selection, but some mutants may maintain some level of LasR activity or quorum sensing through RhlR.

We investigated the contributions of social cheating and improved growth on amino acids to the fitness of *lasR* mutants in CF nutrients but were unable to completely attribute *lasR* mutant fitness to either variable. In the absence of a clear explanation for selection of *lasR* mutants in this environment, we suggest a few plausible ones. First, *lasR* mutations de-repress growth and provide

resistance to autolysis at high cell densities (Heurlier et al., 2005; Hoffman et al., 2010), which is consistent with our finding that *lasR* mutants produce greater net growth than LasR+ strains. Second, altered LasR signaling could reduce expression of metabolically costly products and select *lasR* mutants even in the absence of cooperators. Third, *lasR* mutants exhibit advantages in microoxia, which likely occurs during late-phase growth in our cultures (Clay et al., 2020). These explanations are all consistent with our observations that *lasR* mutants are advantageous in the absence of competitors or cooperators as well as conditions lacking amino acids. We might reconcile these explanations by noting that growth in CF nutrients is sufficient to select *lasR* mutants, but their advantages may not be specific to these conditions. Rather, *lasR* mutants are frequently selected in a broad range of environments including CF (Marvig et al., 2015; Smith et al., 2006), SCFM (Azimi et al., 2020; Schick and Kassen, 2020), and other laboratory media (Hernando-Amado et al., 2019). Still, the physiological and regulatory mechanisms underlying the fitness advantages of *lasR* mutants demand further study.

This evolution experiment also reveals at least two curious findings regarding the genetics of adaptation by *P. aeruginosa*. First, adaptation to CF nutrients is produced by mutated global regulators of multicellular behavior (quorum sensing, biofilm formation) with remarkable consistency. Although many other ways of increasing fitness in these nutrients and propagation methods surely exist, it is notable that the most beneficial mutants in this environment were those which alter massive and complex regulons, rather than downstream effectors of cell behavior (Jenal et al., 2017; Whiteley et al., 1999). Second, we detected several large deletions and structural variants in prevalent genotypes, including those that result in the loss of both *lasI* and *lasR*. In clinical isolates, SNPs within *lasR* are frequently detected, however we hypothesize that large deletions may be underreported due to the computational challenge of identifying them in draft

genomes produced by short-read sequencing. One-fourth of mutations in this evolution experiment were indels or structural variants, so sequencing efforts of clinical isolates ought to analyze these possible alterations whenever feasible.

In summary, extensive genetic adaptation and diversification is a well-known feature of *P. aeruginosa* populations growing in the cystic fibrosis respiratory tract (Jorth et al., 2015) and experimental models of infection (Azimi et al., 2020; Davies et al., 2017; Palmer et al., 2007; Schick and Kassen, 2018) but the specific selective causes have been elusive. Studying adaptation *in vivo* is challenging because obtaining an early infecting strain that serves as an appropriate internal reference for subsequent isolates is often not possible. Further, in more established infections, evolved mutations may be too numerous to infer the phenotypic impact any single change. Thus, linking mutations known to occur *in vivo* with the conditions that selected them and the phenotypes they confer is critical to understand how *P. aeruginosa* adapts to the CF respiratory environment. Remarkably, the evolution of genotypes producing more biofilm and altered quorum sensing can be selected by a subset of nutrients found in the cystic fibrosis airway and coexist by reciprocal ecological facilitation. Although the presence of other microbes, host factors, or antibiotic pressure may only add to the potential diversification of opportunists like *P. aeruginosa*, they may not be required to promote increased persistence *in vivo*.

## 3.5 Methods

### 3.5.1 Evolution experiment

*Pseudomonas aeruginosa* strain UCBPP-PA14 (Rahme et al., 1995) was propagated for twelve days in minimal medium supplemented with the nutrients shown to be abundant in the cystic fibrosis respiratory environment (Palmer et al., 2007). The evolution experiment was described previously in Chapter 2, in which these lineages were used to test whether mutations in lineages exposed to tobramycin occurred in the absence of antibiotic selection but were not analyzed further. Briefly, the minimal medium consisted of 11.1mM glucose, 10mM DL-lactate (Sigma-Aldrich 72-17-3), 20 mL/L MEM essential amino acids, 10 mL/L MEM nonessential amino acids (Thermofisher 11130051, 11140050), an M9 salt base (0.1 mM CaCl<sub>2</sub>, 1.0 mM MgSO<sub>4</sub>, 42.2 mM Na<sub>2</sub>HPO<sub>4</sub>, 22 mM KH<sub>2</sub>PO<sub>4</sub>, 21.7mM NaCl, 18.7 mM NH<sub>4</sub>Cl), and 1 mL/L each of Trace Elements A, B, and C (Corning 99182CL, 99175CL, 99176CL). We propagated cultures in 18x150mm glass tubes containing 5mL of medium and incubated in a roller drum at 150rpm at 37°C. Lineages were initiated by resuspending a single ancestral clone in PBS and using this suspension to inoculate each population. Five lineages each were propagated with either planktonic or biofilm selection: planktonic through a dilution of 50uL into 5mL of fresh medium every 24 hours, and biofilm through transfer of a colonized bead to a tube with fresh medium and 3 new beads. The evolution experiment continued for twelve days with sampling for freezing in 25% glycerol at -80 °C on days six and twelve. Planktonic populations were sampled by freezing 1mL aliquots and biofilm populations were sampled by sonicating a bead in PBS and freezing a 1mL aliquot. We performed population WGS by inoculating frozen populations into the evolution media and incubating for 24 hours, then removing an aliquot for DNA extraction for planktonic

populations and sonicating a colonized bead and removing an aliquot for biofilm populations. We performed population WGS at day twelve for each lineage. We also isolated clones with colony morphologies and phenotypes distinct from the ancestor and sequenced these clones by WGS. Genotypes of evolved clones are shown in Table 4.

**Table 4. Genotypes isolated from evolved populations in Chapter 3.**

<b>Sample Name</b>	<b>Population of Origin</b>	<b>Variants</b>
Ancestral Strain		
MRS 1301	Planktonic, Population 1	<i>lasR</i> R216Q
MRS 1302	Planktonic, Population 2	<i>morA</i> N1124K
MRS 1303	Planktonic, Population 3	<i>morA</i> K1123E
MRS 1304	Planktonic, Population 4	<i>morA</i> L1155Q
MRS 1305	Planktonic, Population 4	<i>lasR</i> V132G <i>morA</i> L1155Q
MRS 1306	Planktonic, Population 5	<i>lasR</i> R216Q <i>pf5r</i> 16bp DUP
MRS 1307	Planktonic, Population 5	<i>morA</i> L1155Q <i>pf5r</i> 16bp DUP
MRS 1308	Biofilm, Population 2	PA14_64050 R26C <i>lasR</i> P117L
MRS 1309	Biofilm, Population 2	<i>wspF</i> Δ1bp
MRS 1310	Biofilm, Population 3	<i>wspF</i> L330Q
MRS 1202	Planktonic, Population 2	PA14_45920..PA14_46440 Δ49,133 bp
MRS 1203	Planktonic, Population 3	PA14_45800..PA14_46240 Δ40,707 bp
MRS 1219	Biofilm, Population 1	PA14_64050 R26C <i>pilC</i> Δ5bp
MRS 1220	Biofilm, Population 1	<i>lasR</i> G164*
MRS 1221	Biofilm, Population 1	<i>wspF</i> E189* <i>pilB/pilC</i> (+58/-42) +16bp
MRS 1266	Planktonic, Population 1	<i>morA</i> E1153K <i>tRNA<sup>Thr</sup>/tufB</i> (+20/65) G->A

### 3.5.2 Whole genome sequencing and analysis

We extracted DNA using the DNeasy Blood and Tissue Kit (Qiagen, Hilden, Germany) and prepared the sequencing library as previously described (Baym et al., 2015; Turner et al., 2018) using the Illumina Nextera kit (Illumina Inc., San Diego, CA). We sequenced populations to an average read depth of 86-254x and clones to an average read depth of 10-58x using an Illumina NextSeq500. Sequences were trimmed using the trimmomatic software v0.36 with the following criteria: LEADING:20 TRAILING:20 SLIDINGWINDOW:4:20 MINLEN:70 (Bolger et al., 2014). The breseq software v0.35.0 was used to call variants using the -p polymorphism flag when analyzing population sequences (Deatherage and Barrick, 2014). These parameters detect variants at >5% frequency within a population. To minimize false positive variant calls, we implemented breseq parameters requiring that variants be supported by at least three reads on each strand. For our reference genome, we used the *P. aeruginosa* UCBPP-PA14 109 genome (NC\_008463) with annotations from the *Pseudomonas* Genome DB (Winsor et al., 2016). Mutations that were detected between our ancestral strain and reference genome were removed from subsequent analysis as they were not selected by the experimental conditions. Variant calls indicative of poor read mapping were also removed, including variants that occurred at only the ends of reads, only within reads with many other mutations, or only at low total read depth. The breseq software also reports new junctions within the genome which may occur due to mobile element insertions, large deletions, structural rearrangements, and prophage excision and circularization, which we included in our analysis. Unfiltered breseq output and code documenting all analysis steps can be accessed at [https://github.com/michellescribner/pa\\_nutrient](https://github.com/michellescribner/pa_nutrient). Filtering and plotting was performed in R v4.0.5 using packages tidyverse and ggrepel (R Core Team, 2021; Slowikowski et al., 2021; Wickham et al., 2019).

### 3.5.3 Analysis of *morA* mutations detected in laboratory and clinical environments

To identify instances of residue and domain-level parallelism, we analyzed nonsynonymous mutations in *morA* detected in this experiment, other laboratory experiments (Sanz-García et al., 2018; Wong et al., 2012), and clinical isolates (Marvig et al., 2015). We determined the locations of *morA* mutations using the supplementary data of two studies (Marvig et al., 2015; Wong et al., 2012) and by analyzing sequences of populations propagated in the absence of antibiotic using breseq for Sanz-García et al. (Sanz-García et al., 2018).

We also visualized *morA* mutations detected in other evolution experiments from our laboratory. These mutations were detected in an evolution experiment identical to this study but with the following alterations: populations were cultured in deep well plates with daily transfer through either 1:100 dilution or transfer of a colonized pipette tip into a well containing 5mL fresh media. Deep well plates were incubated with shaking at 100rpm. Three evolved lineages from each treatment were sequenced following twelve days of transfer. Whole population genome sequence data for these evolved populations are available in NCBI BioProject PRJNA692838.

The domain positions within the MorA protein were determined from the Pfam database (Mistry et al., 2021). All nonsynonymous mutations detected in clinical and laboratory studies were visualized on the protein structure of PAO1 MorA published by Phippen et al. in Figure 11 (Berman et al., 2000; Phippen et al., 2014). Mutations were visualized based on their relative position within the PAO1 MorA protein using UCSF Chimera with color corresponding to domain (Pettersen et al., 2004).

### **3.5.4 Morphology**

Morphologies of evolved mutants were visualized on agar plates containing 1% tryptone, 20ug/L Coomassie brilliant blue, and 40ug/mL Congo Red. Strains were grown overnight in the evolution media and 5uL was spotted onto plates. Plates were then incubated for 24 hours at 37°C followed by 72 hours at room temperature before photographing.

### **3.5.5 Motility and biofilm assays**

Motility and biofilm assays were performed similarly to as previously described with the alterations noted below (Ha et al., 2014c, 2014b; O'Toole, 2011). For swimming motility assays, evolved mutants were inoculated in the evolution medium and incubated overnight. A sterile pipette tip was dipped into cultures and used to stab 0.3% agar supplemented with an M8 base, glucose, casamino acids, and MgSO<sub>4</sub>. Plates were incubated for 24 hours at 37 °C and diameter of the resulting growth was measured. Swarming motility assays were performed analogously to swimming assays, except plates contained 0.5% agar and 2.5uL of culture was spotted onto each plate. Plates were incubated for 24 hours at 37 °C then photographed. We estimated biofilm production of evolved mutants by crystal violet assay (O'Toole, 2011). We diluted overnight cultures of evolved mutants 1:100 in fresh minimal medium to a volume of 200uL in a 96 well plate. After incubation for 24 hours at 37°C with shaking for 30 seconds every 15 minutes, we gently rinsed plates twice with water. We stained wells with 250uL of 0.1% crystal violet, incubated for 15 minutes, rinsed three times with water, then allowed them to dry overnight. Crystal violet was solubilized by adding 250 µl 95% EtOH solution (95% EtOH, 4.95% dH<sub>2</sub>O, 0.05% Triton X-100) to each well for 15 minutes. Biofilm formation was then visualized by

measuring Abs OD<sub>600</sub>. Datapoints are the average of technical replicates from at least three independent experiments.

### 3.5.6 Fitness assays

Evolved mutants were incubated for 24 hours in the evolution medium, then inoculated into fresh tubes at the indicated starting proportions with a competitor (25uL of competitor A and 25uL of competitor B in 5mL fresh evolution medium to generate a starting proportion of approximately 0.5). Cultures were serially diluted in PBS and plated onto ½ concentration tryptic soy agar at the starting timepoint to estimate precise initial proportions. Cultures were then incubated for 24 hours, diluted 1:100 into fresh medium, and incubated for another 24 hours. At the 48-hour timepoint, cultures were again plated. Fitness was calculated as selection rate as described by Turner et al (Turner et al., 2020) where A and B represent competitors A and B and t=0 and t=2 denote CFU/mL at timepoints 0 and 48 hours. Strains were differentiated by competing against a Lac<sup>+</sup> marked ancestor that appears blue on agar containing X-Gal or differentiated by colony morphology in competitions of *morA* versus *lasR* mutants.

$$r = \frac{\ln \frac{A_{t=2}}{A_{t=0}} - \ln \frac{B_{t=2}}{B_{t=0}}}{2}$$

### 3.5.7 Growth curves

We measured growth curves of evolved mutants by growing cultures overnight in the evolution medium, then diluting 1:100 into 200uL of fresh medium in a 96 well plate. Cultures were incubated for 24 hours at 37 °C with shaking for 30 seconds every 15 minutes, and OD<sub>600</sub>

was measured at 15-minute intervals. We analyzed growth curves from at least three independent experiments with three replicates each. Growth curves were subsequently analyzed in R using the Growthcurver package (Sprouffske and Wagner, 2016).

### **3.5.8 Nutrient analysis**

The ancestral strain and *lasR* R216Q mutant were grown from freezer stocks in the evolution medium for 24 hours at 37°C. Cultures were diluted 1:100 into fresh medium supplemented with all carbon sources (glucose, lactate, amino acids) and incubated at 37°C. We removed 1mL aliquots from these cultures every hour for 8 hours and collected supernatants by centrifugation at 13,000g for 1 minute, then filtered using a 0.2 mm filter. Two biological replicates for the ancestor and three for the *lasR* mutant were analyzed for nutrient content. We measured cell density by Abs OD<sub>600</sub> for each aliquot prior to centrifugation.

Amino acid levels in the supernatants were analyzed using the Waters AccQ-Tag chemistry package. Samples were hydrolyzed using trichloroacetic acid precipitation. A 1:4 ratio of TCA was added to the samples, which were chilled on ice for 10 minutes and then centrifuged at 13,000 g for 10 minutes. The supernatant from the TCA precipitation was removed and pH balanced to pH 8.2-10 using KOH. The sample was derivatized using the AccQ-Tag methodology (Waters) and analyzed on a Waters HPLC system consisting of an e2985 Separations Module and a 2475 FLR Detector as per manufacturer's instructions. For glucose and lactate consumption, samples were enzymatically analyzed using a D-Lactic Acid/L-Lactic Acid Enzymatic Bioanalysis UV-Test kit and a D-Glucose Enzymatic Bioanalysis UV-Test kit (Roche Diagnostics) with a modified manufacturer's protocol to reduce total sample size to 300 uL. Results were read at 340 nm on a BioTek Synergy HTX plate reader.

### **3.5.9 Statistical analysis**

Data was analyzed using GraphPad Prism 9 and using R where noted.

### **3.5.10 Data availability**

Data and code used for data analysis can be accessed at [https://github.com/michellescribner/pa\\_nutrient](https://github.com/michellescribner/pa_nutrient). All sequencing reads were deposited in NCBI under BioProject accession numbers PRJNA595915 and PRJNA692838.

**4.0 Prophage induction and rapid coevolution during laboratory propagation of *P. aeruginosa***

This chapter is adapted from the following manuscript in preparation:

**Michelle R. Scribner<sup>a,b,#</sup>, Nanami Kubota<sup>a,b,#</sup>, Vaughn S. Cooper<sup>a,b</sup>**

**Prophage induction and rapid coevolution during laboratory propagation of *P. aeruginosa***

<sup>a</sup>Department of Microbiology and Molecular Genetics, University of Pittsburgh, Pittsburgh, Pennsylvania, USA

<sup>b</sup>Center for Evolutionary Biology and Medicine, University of Pittsburgh, Pittsburgh, Pennsylvania, USA

<sup>#</sup>The following authors contributed equally to this work.

## 4.1 Project summary

Lysogenized bacteriophages are prevalent in bacterial genomes, and while they are frequently dormant, phage excision and replication may be spontaneously induced in certain environmental conditions. Although lysogeny is inherently costly, filamentous phages in the Inoviridae family can extrude virions from the host cell without lysis, thus produce a relatively minor burden. However, the stability of this relationship and impact on population fitness is underexplored. Here, we detected low basal levels of Pf5 prophage induction in populations of *P. aeruginosa* strain PA14 propagated in either planktonic or biofilm environments using deep whole genome sequencing. In addition, we discovered that clonal lineages of *P. aeruginosa* acquired mutations which increased Pf5 prophage induction and dramatically altered subsequent evolution after merely 80 generations of propagation. These mutations occurred within the gene encoding the repressor of prophage excision, *pf5r*. Strains with *pf5r* mutations exhibited strong fitness advantages in competition with an ancestral strain but decreased the productivity of the bacterial population. We also found that when we cultured the ancestral strain with *pf5r* mutants, the ancestral strain acquired identical *pf5r* mutations, suggesting that Pf5 with *pf5r* mutations can superinfect neighboring cells. Shortly thereafter, we detected rapid coevolution of phage and host through mutations which deleted genes encoding capsid proteins from the Pf5 genome and disrupted genes encoding type IV pili in *P. aeruginosa*. These findings reflect the fragile nature of lysogeny and the potential for rapid coevolution of phage and host following prophage induction, even in relatively simple environmental conditions.

## 4.2 Introduction

Bacteriophage are estimated to represent the most abundant biological entities on the planet, with an estimated  $10^{31}$  particles producing  $10^{23}$  infections per second (Hendrix, 2002; Suttle, 2007). However, we currently understand only a small fraction of their impact on microbial evolution. Phage can be broadly divided into two different types: lytic phage, which release progeny by lysis of their bacterial host, and temperate phage, which can either induce lysis upon infection or integrate their genomes into the bacterial chromosome (lysogeny) to await subsequent phage induction. Of 2110 complete bacterial genomes on Genbank, 46% are lysogenized (Touchon et al., 2016). Phage are also abundant in host microbiomes, including that of humans, demanding further study of the roles that phage play in microbial pathogenesis and evolution (James et al., 2015; Letarov and Kulikov, 2009).

Lytic and temperate phage can impose massive costs to host cells through replicative burden and cell lysis; however, lysogeny can facilitate fragile commensal and even mutualistic relationships when the cost of phage replication is offset by encoding traits beneficial to the bacterial host (Hay and Lithgow, 2019). Lysogenized phage, or prophage, may be advantageous to their hosts when they are weaponized to lyse competing microbes or by providing immunity from subsequent infection (Bondy-Denomy et al., 2016). In addition, prophage can facilitate the acquisition of virulence factors or other beneficial genetic material, such as antibiotic resistance genes (Busby et al., 2013; Figueroa-Bossi et al., 2001; Modi et al., 2013). For example, the CTX bacteriophage in *Vibrio cholerae* contains the machinery to produce cholera toxin, which, though costly in many environments, is highly beneficial during infection (Hay and Lithgow, 2019). Furthermore, phage can integrate into new sites within the bacterial genome and disrupt genes, effectively serving as a genetic regulator in a process known as active lysogeny. Integration into

new sites can also reconstitute dysfunctional tRNAs (Ventura et al., 2003). As with *de novo* mutations, most phage insertions are neutral or costly, but some can produce fitness advantages. A recent study demonstrated benefits of active lysogeny during competition between *P. aeruginosa* strains in a wound infection (Marshall et al., 2021). As a result of advantages like these, deleting prophage from their hosts can be detrimental to host fitness in certain environments (Shapiro et al., 2016).

Pf phage are single-stranded filamentous phage found in ~36-52% of *P. aeruginosa* strains and detected in the sputum of many people with cystic fibrosis (CF) (Burgener et al., 2019). Pf phage are members of the Inoviridae family, which can replicate and extrude virions without lysis of the host cell (Mai-Prochnow et al., 2015; Rice et al., 2009). These phage may be induced by host factors in a variety of conditions including bacterial stress, particularly oxidative stress, anaerobic environments, and biofilms (Platt et al., 2008; Wei et al., 2012). The commonly used PA14 strain is lysogenized by a Pf bacteriophage, Pf5 (Figure 21). Pf5 is ~10kbp and contains its own excisionase, which promotes excision and replication of the prophage genome (Li et al., 2019). In the closely related Pf4 prophage in PAO1, the action of the excisionase is repressed at the transcriptional level by the prophage repressor (Pf4r), thus the repressor maintains lysogeny (Li et al., 2019). Phage-encoded repressors are thought to confer immunity to superinfection by inhibiting replication of exogenous phage with similar repressors (Waldor and Friedman, 2005).

Pf phage are associated with several phenotypes for *P. aeruginosa*, including enhanced biofilm formation, but the impact of lysogeny on the host is a subject of continued study. Pf phage genes are expressed at high levels in biofilms (Folsom et al., 2010; Whiteley et al., 2001) and virions are detected at high titers (McElroy et al., 2014; Rice et al., 2009; Webb et al., 2003). Pf phage released from host cells facilitate the assembly of the biofilm matrix and enable protection

from desiccation and specific antibiotics (Secor et al., 2015). Likewise, some small colony variants (SCVs) isolated from *P. aeruginosa* biofilms produce high levels of Pf phage (Webb et al., 2004) and *P. aeruginosa* strains lacking Pf4 bacteriophage exhibit deficient biofilm formation (Rice et al., 2009). However, the relationship between Pf and biofilm remains somewhat unclear, because inactivation of host factors which dramatically increase Pf5 expression also decrease biofilm formation (Lee et al., 2018).

Pf prophage can be advantageous to *P. aeruginosa* in certain environments, but the benefit of lysogeny is nonetheless precarious. For example, while prophage generally confer immunity to similar exogenous phage through the action of the prophage repressor, cells can be successfully infected and lysed by exogenous phage in a process called superinfection (Hui et al., 2014; McElroy et al., 2014). The mechanism by which superinfective phage lyse the host cell is unclear (Secor et al., 2020). However, mutations within the prophage repressor gene of Pf4 can induce superinfective phage in PAO1 biofilms and subsequently trigger rapid antagonistic coevolution between the phage and host (McElroy et al., 2014). For instance, phage often attach to and infect host cells using type IV pili, so mutations causing complete loss of pili, reduced numbers of pili, or inability of pili to retract are selected defenses against phage infection in *P. aeruginosa* (Davies et al., 2016; Lythgoe and Chao, 2003; McElroy et al., 2014).

In this study, we unexpectedly discovered that mutant Pf5 were selected during propagation of *P. aeruginosa* strain PA14 in nutrients abundant in the CF respiratory environment. Pf5 mutant genotypes coincided with increased replication of Pf5 and provided their hosts with strong relative fitness advantages over strains lacking mutant Pf5. However, strains infected by mutant Pf5 reached lower cell densities when cultured alone, suggesting that prophage induction is costly to the host. Subsequently, phage and host genotypes rapidly coevolved via mutations in viral capsid

genes and the host type IV pilus. These results reveal that superinfective phage can evolve in simple environmental conditions and rapidly trigger the development of complex phage-host dynamics indicative of simultaneous evolution of putative viral defectors and phage-resistance.

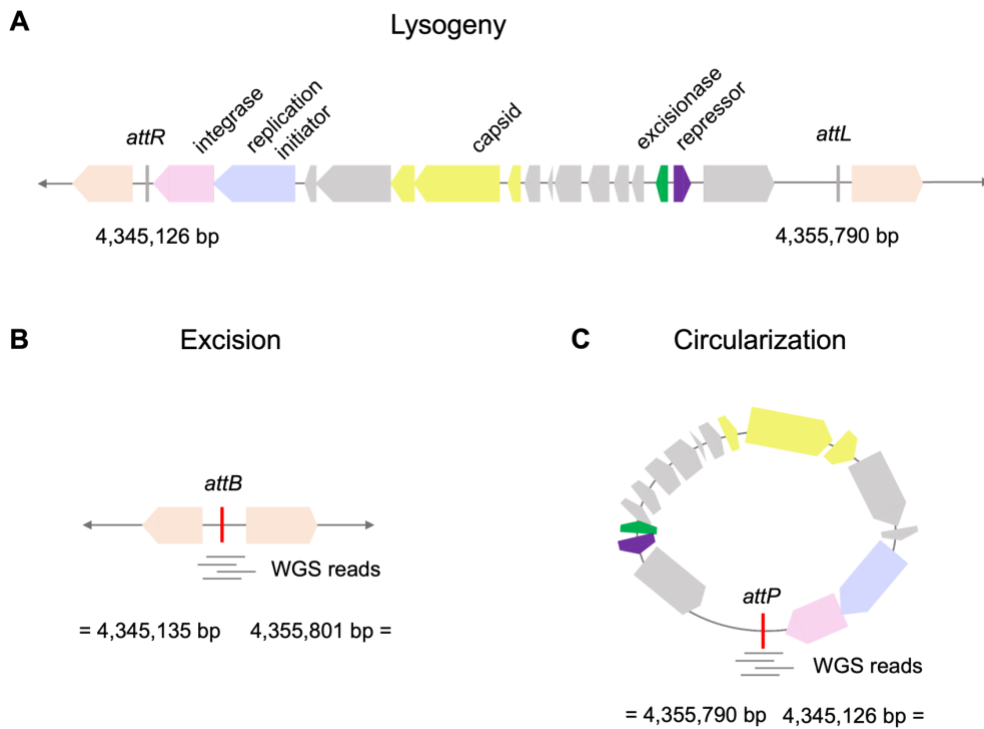


**Figure 21. Excision and circularization of Pf5, a prophage within *P. aeruginosa* strain PA14, can be detected by deep whole genome sequencing.**

A) Annotated Pf5 genome at its site of lysogeny within PA14. The Pf5 genome can B) excise and C) form a double-stranded, circular replicative form. Sequences mapping to the *attB* and *attP* sites detect excision and circularization, respectively, as new junctions within the genome. At either side of the predicted junction, “=” represents the location of the adjacent homologous sequence in the reference genome.

## 4.3 Results

### 4.3.1 Prophage Pf5 is induced at low levels during growth in CF nutrients

In a previous experiment, we propagated PA14 for twelve days in medium mimicking the nutrients in the cystic fibrosis respiratory environment (Scribner et al., 2021). Deep sequencing of evolved populations revealed induction of the Pf5 prophage in every population and in populations of the ancestral strain (Table 5). When induced, the Pf5 genome is excised from the host chromosome and forms a double-stranded, circular replicative form (Martínez and Campos-Gómez, 2016). We can detect Pf5 induction using WGS data because the joining of the two ends of the Pf5 genome in its replicative form is detected as a new junction variant that is not present in the reference genome. Likewise, the extent of excision versus lysogeny is revealed by the fraction of sequencing reads which align to the *attB* versus the *attL/attR* sites, respectively (Figure 21). However, when packaged into virions, the Pf5 genome is single-stranded and thus is not detected using our sequencing technology. Prophage induction has been shown to occur during routine laboratory culture for *P. aeruginosa* PA14 and PAO1 (Li et al., 2019; Rice et al., 2009), but the extent and conditions facilitating induction are under-explored. Here, we determined that growth in CF nutrients alone is sufficient to induce prophage excision in both planktonic and biofilm lifestyles. We also detected Pf5 induction for populations propagated in a different selective medium by our laboratory, but in a lower proportion of populations (7 out of 30 samples) (Harris et al., 2021).

**Table 5. Populations propagated in CF nutrients evolved mutations within Pf5.**

We performed WGS of evolved populations following twelve days of propagation. The number of sequencing reads aligned to each detected variant (read depth) and relative frequency of each variant within the population (allele frequency) are shown. Only variants detected within Pf5 are indicated, but other mutations detected in these populations can be viewed in Appendix Table 2. At either side of a predicted junction, “=” represents the location of the adjacent homologous sequence in the reference genome (See Figure 21). Evidence of circularization and excision of Pf5 are detected by new junction evidence and indicated, though they do not represent *de novo* mutations.

Variant	Junction Position 1	Junction Position 2	Read Depth (Allele Frequency)										
			Ancestral Strain	Planktonic Populations					Biofilm Populations				
				1	2	3	4	5	1	2	3	4	5
Pf5 circularization	4345126 =	= 4355790	4 (3%)	17 (7%)	12 (5%)	31 (12%)	3 (2%)	7936 (99%)	31 (21%)	41 (17%)	37 (12%)	13 (7%)	8 (4%)
Pf5 excision	= 4345135	4355801 =						9 (8%)	5 (4%)				
PA14_48800 to <i>xisF5</i> circularization	4338302 =	= 4353244							1990 (85%)				
<i>pf5r</i> 16bp duplication	4353517 =	= 4353532						4588 (51%)					
<i>pf5r</i> G93W								2643 (28%)					
<i>xisF5/pf5r</i> intergenic (-46/-82) A->G								1575 (10%)					
Δ PA14_48810 to PA14_48880	= 4338990	4346095 =							724 (72%)				
Δ PA14_48810 to PA14_48880	= 4339008	4346003 =							47 (13%)				
Δ PA14_48810 to PA14_48880	= 4339366	4345624 =							11 (6%)				
Δ PA14_48810 to PA14_48880	= 4339381	4345620 =							9 (5%)				
Δ PA14_48830 to PA14_48880	= 4339804	4345601 =							14 (9%)				

### 4.3.2 Mutant Pf5 genotypes invaded two evolved populations

Mutations in the Pf5 genome were detected in two populations: planktonic population 5 and biofilm population 1 (Table 5). Three mutations were detected in planktonic population 5: i) duplication of 16 bp (231/267 nt) in the prophage repressor gene (*pf5r*), ii) a SNP downstream of this duplication that produces a nonsynonymous change due to the upstream frameshift (G93W), and iii) a SNP in the intergenic region upstream of *pf5r*. The *pf5r* mutations were accompanied by 61X higher read depth for Pf5 than the PA14 genome as a whole (Figure 22). In contrast, read

depth for Pf5 was only 1.4X higher than the rest of the genome in the ancestral strain. Genomes exhibit variation in depth of coverage due to genome architecture and bias during sequencing, but read depth of a region is generally correlated with copy number (Zhao et al., 2013), suggesting that replication Pf5 was increased in planktonic population 5. Deletion of *pf4r* increases Pf4 production in PAO1 because Pf4r normally transcriptionally represses the prophage excisionase (Li et al., 2019). Overexpression of either Pf4r or Pf5r on a PAO1 $\Delta$ Pf4 background confers increased immunity against infecting Pf4 (Li et al., 2019), suggesting that Pf5r also functions as a repressor of the excisionase. Therefore, we hypothesized that evolved *pf5r* mutations increased induction of Pf5 in this population.

Four distinct types of Pf5 variants were identified in biofilm population 1, including: *i*) Pf5 circularization, *ii*) Pf5 excision, *iii*) a new Pf5 circularization at shifted positions (PA14\_48800 to *xisF5* circularization), and *iv*) multiple distinct deletions of 6 genes upstream of Pf5 ( $\Delta$  PA14\_48810 to PA14\_48880) (Table 5). Again using sequencing coverage as a proxy for the relative copy number of these elements, the new Pf5 circular element (PA14\_48800 to *xisF5*) became more abundant. The region of the 6-gene deletions (PA14\_48810 to PA14\_48880) showed an average read depth consistent with the average read depth for the PA14 genome, implying that the 6-gene deletions arose within the new circularized element (Figure 23). These variants also coincided with the parallel evolution of mutations in pilus genes in this population, which we hypothesize were selected to evade Pf5 superinfection (Bondy-Denomy et al., 2016).

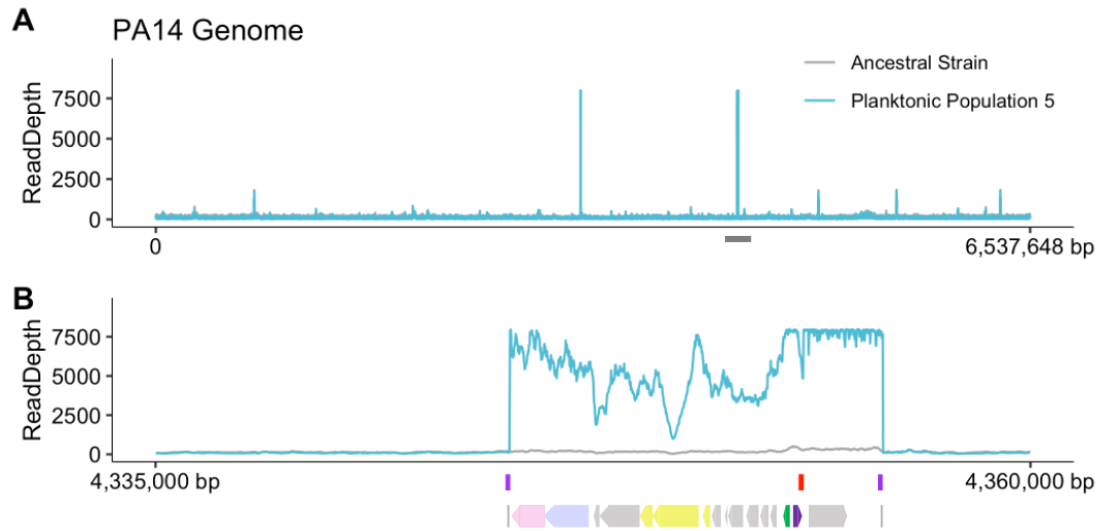


**Figure 22. Increased replication of Pf5 in planktonic population 5.**

Read depth at every position within the PA14 genome for A) the entire PA14 genome and B) the Pf5 genome is shown. Variants within the Pf5 genome are labelled by color: purple reflects Pf5 circularization and red reflects the location of *pf5r* mutations. A schematic of the Pf5 genome is indicated below its site of lysogeny, see Figure 21 for gene annotations.

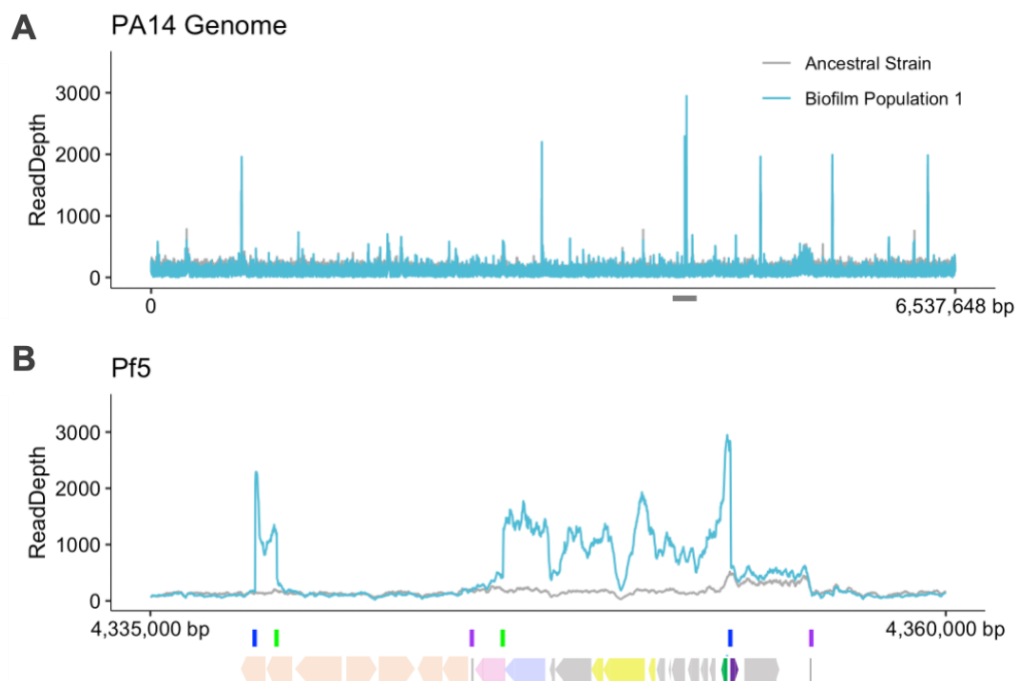


**Figure 23. Increased replication of a truncated Pf5 genome in biofilm population 1.**

Read depth at every position within the PA14 genome was visualized for A) the entire PA14 genome and B) the Pf5 genome. New junction variants within and surrounding the Pf5 genome are indicated by color: purple reflects Pf5 circularization, blue reflects putative circularization of a truncated Pf5 genome from PA14\_48800 to the excisionase *xisF5*, and green reflects the location of deletions upstream of Pf5. A schematic of the Pf5 genome is indicated below its site of lysogeny, see Figure 21 for gene annotations.

#### 4.3.3 *pf5r* mutations stimulate Pf5 induction and replication of an uncharacterized element

To determine if *pf5r* mutations increase Pf5 induction, we analyzed two *P. aeruginosa* clones with *pf5r* mutations isolated and sequenced in Chapter 3 (Table 6). Both strains possessed the 16bp duplication in *pf5r* and downstream SNP (G93W). These strains also had nonsynonymous mutations in another gene (*lasR* R216Q or *morA* L1155Q), therefore these strains are subsequently referred to as *lasR pf5r* and *morA pf5r*, respectively. The sequencing coverage of both strains

showed increased Pf5 induction compared to strains with only *lasR* and *morA* mutations, suggesting that induction was triggered by one or both *pf5r* mutations (Table 6, Figure 24). Surprisingly, despite sequencing the genomes of clones (or clonal populations grown only to amplify genomic DNA sufficiently) that should have extremely limited diversity, the *pf5r* mutations were found at intermediate frequencies, suggesting that a heterogeneous population of phage genomes persisted in otherwise clonal *P. aeruginosa*. In fact, thousands of sequencing reads mapped to the ancestral sequence of the *pf5r* gene in these strains, indicating that *pf5r* mutations increase the replication of both mutant and ancestral Pf5 genomes.

In addition, we detected circularization and increased copy number of an uncharacterized circularized element in *lasR pf5r* and *morA pf5r* mutants (Figure 24C and F, Table 6). We also detected this circularization in all other evolved clones and the ancestral strain, but with much lower copy number (Table 6, Appendix Table 3). This region harbors three genes encoding hypothetical proteins (PA14\_35710-PA14\_35730) and is directly adjacent to a Tn3 family transposase (PA14\_35740). The three genes within the circularized region are all uncharacterized to the best of our knowledge, therefore the effect of increased replication of this region is unclear. However, we found that an 87bp region within this circularization is 97% identical to a region upstream of the replication initiation factor in Pf5, suggesting that this homology may be targeted by the replication initiator or other Pf5 element (Figure 24G).

**Table 6. *pf5r* mutations induce Pf5 excision and circularization.**

The number of aligned sequencing reads (read depth) and allele frequency of variants detected in evolved clones are shown. Strains are named according to their mutated genes (*lasR*, *lasR pf5r*, *morA*, and *morA pf5r*). At either side of a predicted junction, “=” represents the location of the adjacent homologous sequence in the reference genome. Evidence of circularization and excision of Pf5 are detected by new junction evidence and indicated, though they do not represent *de novo* mutations.

Variant	Junction Position 1	Junction Position 2	Read Depth (Allele Frequency)			
			<i>lasR</i>	<i>lasR pf5r</i>	<i>morA</i>	<i>morA pf5r</i>
Pf5 circularization	4345126 =	= 4355790		3285 (99%)	5 (6%)	1590 (98%)
Pf5 excision	= 4345135	4355801 =		10 (18%)		10 (23%)
New circularization	3175697 =	= 3177289	183 (57%)	6606 (99%)	191 (56%)	22398 (99%)
<i>pf5r</i> 16bp duplication	4353517 =	= 4353532		1081 (30%)		724 (42%)
<i>pf5r</i> G93W				3757 (30%)		1741 (43%)
<i>lasR</i> R216Q			146 (100%)	114 (100%)		
<i>morA</i> L1155Q					69 (100%)	39 (100%)

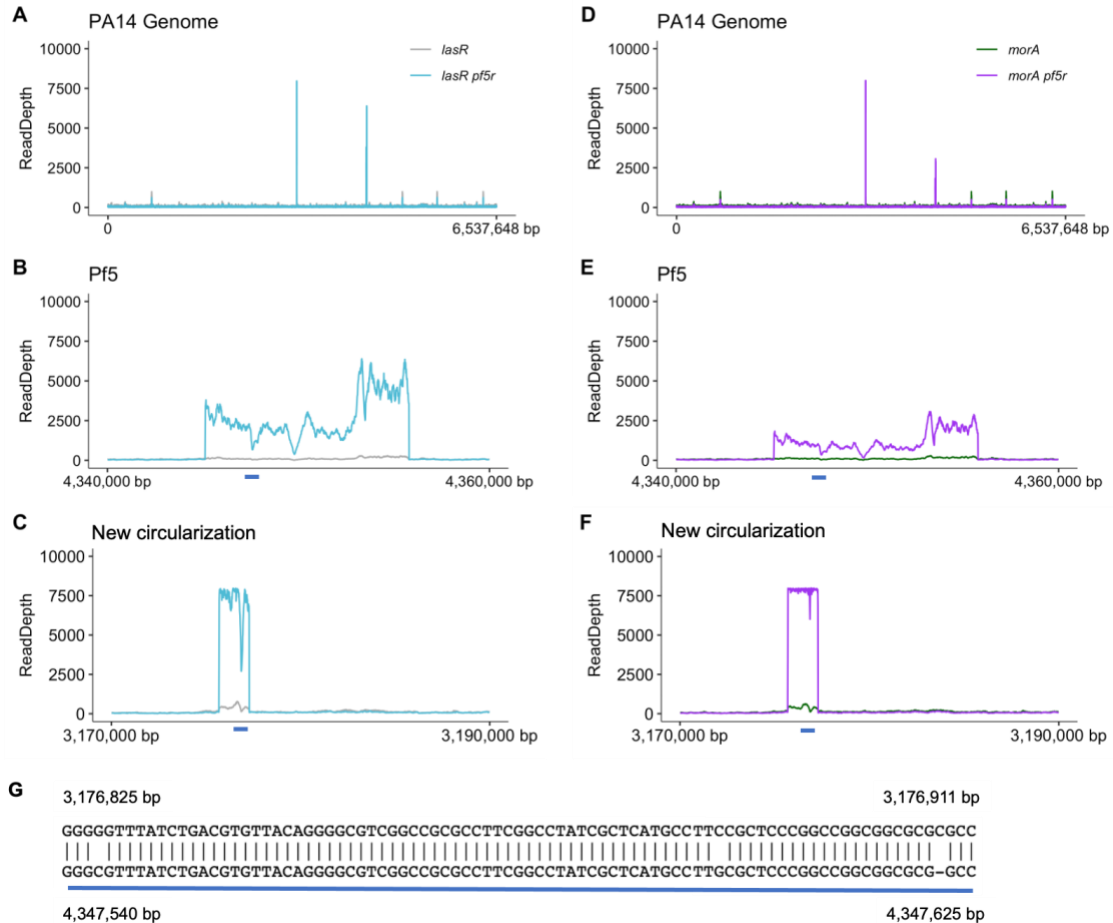


**Figure 24. *pf5r* mutations increase replication of Pf5 and an uncharacterized circular element.**

Sequencing read depth at every position within the PA14 genome for A) the entire PA14 genome, B) the Pf5 genome, and C) the novel 1592 bp circularization for *lasR* mutants with and without *pf5r* mutations. The same data are visualized for *morA* mutants with and without *pf5r* mutations (D-F). G) The Pf5 prophage and an uncharacterized 1592 bp circularization share a 87bp region of sequence identity. The 87bp region of homology is shown and is indicated in previous panels with a blue line. Identity = 84/87 (97%), gaps = 1/87 (1%).

To test whether the new junctions predicted by WGS data reflect excision and circularization of the prophage genome, we measured levels of *attB* and *attP* in the *lasR pf5r* and *morA pf5r* strains by qPCR (Table 7, Figure 25). One amplicon (*attB*) is detected only when Pf5 is excised, whereas the other (*attP*) is only produced when Pf5 is its circular form. Increased levels of both

amplicons were detected in both mutants, as predicted. In future work, we aim to quantify levels of prophage induction for *pf5r* mutants in the ancestral strain because changes to quorum sensing and biofilm due to *lasR* and *morA* mutations could alter levels of prophage induction in *pf5r* mutants. However, WGS data for *lasR* and *morA* mutants without *pf5r* mutations indicate that *lasR* and *morA* mutations alone do not produce high levels of Pf5 induction (Figure 24, Table 8).

**Table 7. Primers used for quantification of Pf5 excision and circularization by qPCR.**

Primer ID	Pair #	Direction	Sequence (5' to 3')
PA14 <i>gyrB</i> -f	1	forward	CACAGCATCCAGCGATAACAAG
PA14 <i>gyrB</i> -r	1	reverse	CGCGTTGCTTTCGATGAAGT
Pf5-Cf	2	forward	TTATGACCAACACCCCAAACG
Pf5-Cr	2	reverse	CATTGTGCGCCGGAGTACCT
Pf5-f	3	forward	GTGCTCTGGAATCCGGGTGT
Pf5-r	3	reverse	CGTTGAACAGGAGGAAATGGGT

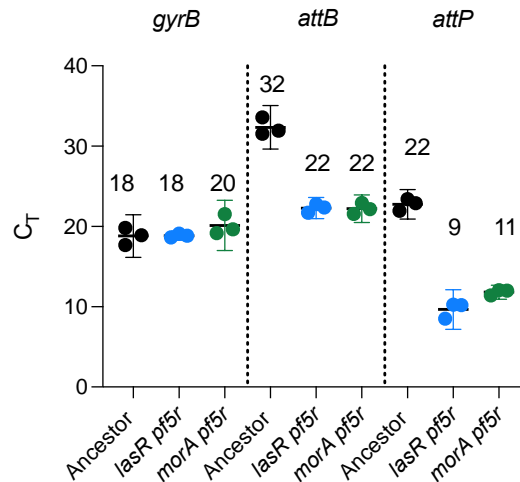


**Figure 25. Increased Pf5 excision and circularization was confirmed for *pf5r* mutants by qPCR.**

We verified the prophage excision determined by WGS using primers flanking the *attB* and *attP* sites, which only produce a product in the event of prophage excision and circularization, respectively. Ct values for the ancestral strain, a mutant with *lasR* and *pf5r* mutations, and a mutant with *morA* and *pf5r* mutations are shown.

**Table 8. Average read depth of PA14 and Pf5 genomes for isolated clones.**

Average read depth was calculated for the Pf5 genome and entire PA14 genome, including Pf5, for every isolated clone. The ratio of read depth for Pf5 versus PA14 is shown. See Tables 6 and 9 for mutations detected in each strain.

Average Read Depth			
Strain Name	PA14	Pf5	Ratio
PA14 Ancestral Strain	146.6	212.5	1.4
<i>lasR</i>	64.5	121.2	1.9
<i>morA</i>	69.2	116.7	1.7
<i>lasR pf5r</i>	56.0	2729.9	48.7
<i>morA pf5r</i>	54.1	1361.3	25.1
<i>pf5r.1</i>	123.3	9065.5	73.5
<i>pf5r.2</i>	111.9	2180.2	19.5
<i>lasR pf5r resequenced</i>	144.4	12477.7	86.4
<i>morA pf5r resequenced</i>	107.5	2315.4	21.5

#### 4.3.4 Prophage induction is costly for fitness, but costs vary with genetic background

Phage are inherently parasitic but can increase fitness of the host cell in certain environments (Secor et al., 2015). We discovered that mutations in *pf5r* reduced overall growth, as measured either by area under a growth curve (AUC) or cell density (OD<sub>600</sub> and CFU/mL) of a *lasR* mutant, suggesting that increased Pf5 induction is costly to the host (Figure 26). However, *pf5r* mutations only altered cell density (CFU/mL) in a *morA* mutant, suggesting that the effect of *pf5r* mutations depends on the genetic background. We suspect that OD<sub>600</sub> measurements of *morA*

may have been inflated by biofilm or dead cells, rendering this measurement unclear (Figure 26D). Regardless, *pf5r* mutations appear to confer distinct phenotypes depending on the presence of *morA* or *lasR* mutations. Surprisingly, we also note that *pf5r* mutations did not increase biofilm formation on a *lasR* or *morA* background (Figure 12).

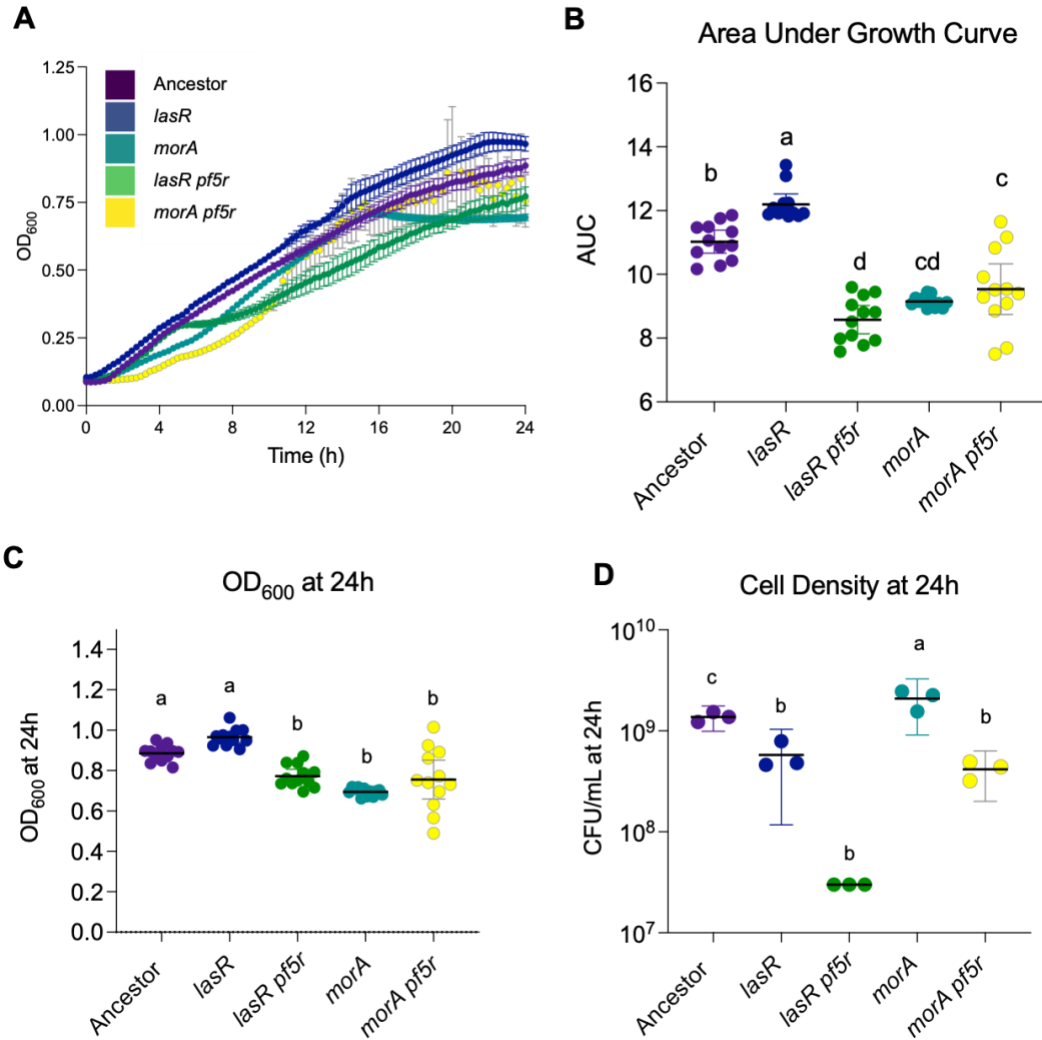


**Figure 26. *pf5r* mutations are costly to the host cell.**

A) Strains with and without *pf5r* mutations were cultured in the evolution media for 24 hours with  $OD_{600}$  measurements at 15-minute intervals. B) Area under the growth curves shown in A. C)  $OD_{600}$  at the final timepoint (24 hours) for the growth curves shown in A. D) Cultures were plated at the final timepoint to determine cell density. Mean with 95% CI are shown, means were compared by one way ANOVA with Tukey's multiple comparisons. Letters indicate means which are statistically different ( $p < 0.05$ ).

#### 4.3.5 Mutant Pf5 rapidly evolves and infects neighboring cells

The fact that identical *pf5r* mutations were detected in multiple clades in evolved populations suggested that mutant Pf5 phage may superinfect other genotypes. To test whether strains with wild-type Pf5 are susceptible to infection by mutant Pf5, we co-cultured a *lacZ*-marked ancestral strain with unmarked *pf5r* mutants for 24 hours, then isolated and sequenced two clones with the *lacZ* phenotype (Table 9). We also re-sequenced the genomes of the *lasR pf5r* and *morA pf5r* strains. We detected identical *pf5r* mutations in the *lacZ*-marked strains as found in *lasR pf5r* and *morA pf5r*, suggesting that the *lacZ*-marked strains were superinfected with mutant Pf5 (Table 9). We subsequently refer to these strains as *pf5r.1* and *pf5r.2*. Increased replication of Pf5 was also detected, suggesting that when *pf5r* mutations arise within *P. aeruginosa* cells, mutant phage genomes can quickly spread to other cells within the population and induce Pf5 replication (Figure 27). As in the *lasR pf5r* and *morA pf5r* strains, the *pf5r* mutations were present at intermediate frequencies, therefore the presence of Pf5 mutants in *P. aeruginosa* stimulates the replication of both ancestral and mutant phage.

Resequencing of *lasR pf5r* and *morA pf5r* genotypes revealed rapid coevolution of phage and host (Table 9). In *morA pf5r*, the Pf5 genome inserted into the *pilX* gene. The *pilX* gene is located within an operon that is essential for assembly of functional type IV pili (Belete et al., 2008), therefore insertion of the phage genome at this site would likely disrupt pili formation. We detected mutations in pilus genes in both this strain and biofilm population 1, indicating parallel evolution of mutations in pilus genes coinciding with Pf5 induction. Additionally, five different deletions of Pf5 capsid genes occurred at high frequencies in the resequenced *morA pf5r* and *lasR pf5r* strains, including one deletion that was also detected in *pf5r.1* and thus was likely acquired through a superinfecting phage. For strains with these deletions, the read depth for the capsid genes

was also greatly reduced, as expected (Figure 27B). However, some reads still mapped to the capsid genes, suggesting that a small proportion of Pf5 genomes retained this machinery to support production of complete phage. The rapid selection of capsid deletions in *pf5r.1* reflects that Pf5 genomes lacking capsid genes were packaged into virions using the capsid proteins encoded by intact Pf5 genomes. Thus, the mutant phage virions likely represent defective interfering particles, which are known to arise during propagation of filamentous phage at high multiplicity of infection (Horiuchi, 1983). The impacts of these defective phage on subsequent bacterial-phage coevolution deserve further study. Ultimately, these findings underscore the rapid eco-evolutionary impact of prophage induction on host population, phage population, and interactions between the two.

**Table 9. Mutant Pf5 rapidly superinfects ancestral *P. aeruginosa*, evolves, and integrates at new sites.**

The number of aligned sequencing reads (read depth) and allele frequency of variants detected by WGS are indicated. *Pf5r.1* and *pf5r.2* strains were isolated during coculture with *pf5r* mutants. At either side of a predicted junction, “=” represents the location of the adjacent homologous sequence in the reference genome.

Variant	Junction Position 1	Junction Position 2	Read Depth (Allele Frequency)			
			<i>pf5r.1</i>	<i>pf5r.2</i>	<i>lasR pf5r</i> <i>resequenced</i>	<i>morA pf5r</i> <i>resequenced</i>
Pf5 circularization	4345126 =	= 4355790	14812 (99%)	2325 (97%)	19658 (99%)	3276 (98%)
Pf5 excision	= 4345135	4355801 =	66 (73%)	21 (23%)	26 (27%)	35 (39%)
New circularization	3175697 =	= 3177289	13028 (99%)	20895 (99%)	25313 (99%)	20535 (99%)
New circularization 2	3176547 =	= 3177222				5312 (25%)
<i>pf5r</i> 16bp duplication	4353517 =	= 4353532	13723 (91%)	826 (38%)	16504 (88%)	2502 (78%)
<i>pf5r</i> G93W			14282 (98%)	2179 (41%)	18123 (92%)	3074 (84%)
PA14_24960 carbohydrate kinase V475V			87 (100%)			
Capsid Deletion	= 4348029	4352025 =	13096 (98%)		5575 (71%)	
Capsid Deletion	= 4347641	4352105 =			2054 (22%)	
Capsid Deletion	= 4348045	4352134 =			6358 (58%)	
Capsid Deletion	= 4347760	4352076 =				1492 (61%)
Capsid Deletion	= 4348212	4352077 =				831 (54%)
Pf5 insertion within <i>pilX</i>	4345126 =	= 5373053				41 (44%)
Pf5 insertion within <i>pilX</i>	= 4355793	5373057 =				40 (40%)
Pf5 insertion	= 3177385	4345126 =				221 (78%)

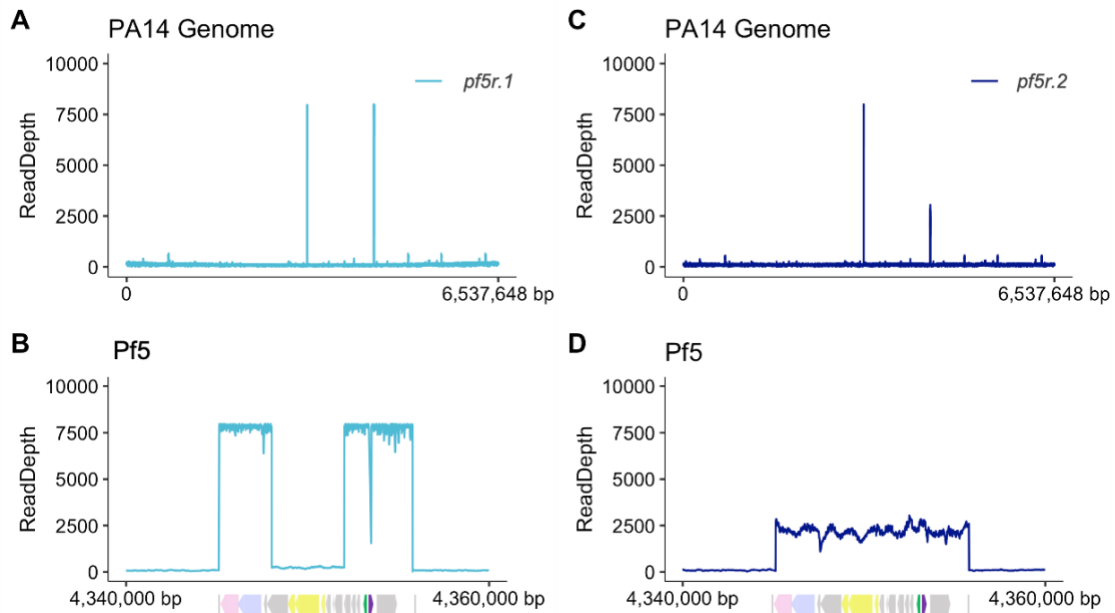


**Figure 27. Mutant Pf5 superinfects ancestral *P. aeruginosa* and increases Pf5 induction.**

Two mutants that arose during coculture with *pf5r* mutants, *pf5r.1* and *pf5r.2*, were sequenced. These strains demonstrate increased Pf5 read depth consistent with the increases observed in *morA pf5r* and *lasR pf5r* mutants. Read depth for the A) PA14 genome and B) Pf5 genome for the *pf5r.1* strain. Read depth for the C) PA14 genome and D) Pf5 genome for the *pf5r.2* strain.

#### **4.3.6 Pf5 induction increases the relative fitness of host cells even while decreasing absolute fitness**

Although *pf5r* mutations are costly to host cells, we found that Pf5 induction increases relative fitness of the host during competition with WT *P. aeruginosa* (Figure 28). These data illustrate an under-appreciated truth in evolutionary biology: adaptations that increase relative fitness for a competitor will be selected regardless of their impact on absolute fitness or growth. However, the mechanism underlying this fitness advantage is unclear, as strains without *pf5r*

mutations are vulnerable to becoming *pf5r* mutants themselves through transduction shortly after coculture. We also found that the *lasR pf5r* and *morA pf5r* strains outcompeted strains with only *pf5r* mutations (Figure 28). Other mutations beyond the *lasR* and *morA* mutations were also present in these strains, including the capsid deletions, so we are unable to determine if *lasR* or *morA* mutations were responsible for the fitness advantages (Table 9). However, in the competition of *lasR pf5r* versus *pf5r.I*, both strains had similar allele frequencies for their respective mutations, and *lasR pf5r* always outcompeted *pf5r.I*. Assuming that neither strain acquired additional mutations prior to this assay, these data suggest that *lasR* mutations increase fitness during superinfection with mutant Pf5. Characterizing the relationship between biofilm and quorum sensing mutations and prophage induction is therefore a major goal for future work.

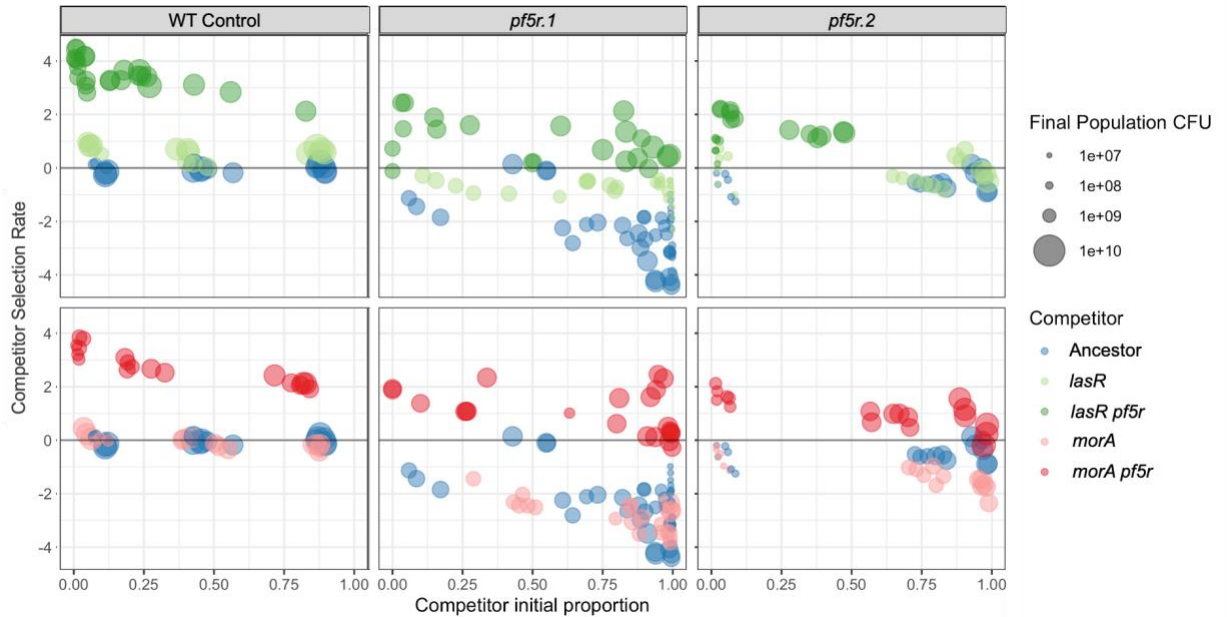


**Figure 28. Strains with mutant *pf5r* outcompete those with WT *pf5r*.**

Fitness was calculated as selection rate, or the difference in Malthusian parameters for each strain. Competitions were initiated at different starting proportions, as indicated. Strains with genotypes indicated in the top panel were competed against the competitor denoted by color: blue denotes the ancestral strain, green denotes *lasR* mutants with and without mutant Pf5, and red denotes *morA* mutants with and without mutant Pf5. The size of the circles denotes size of the population in CFU/mL after 24 hours of competition.

#### 4.4 Discussion

Filamentous phage can produce mutualistic relationships with their hosts due to their ability to transduce advantageous genes, integrate at beneficial positions, extrude from cells without lysis, and contribute to the integrity of biofilm matrix (Marshall et al., 2021; Secor et al., 2015). However, prophage replication and production of virions are costly processes, therefore the host remains at constant risk of prophage induction beyond the level which confers benefits. By performing deep whole genome sequencing of *P. aeruginosa* populations, we determined that Pf5

is induced during growth in CF nutrients in both planktonic and biofilm environments. Considering previous studies, we were surprised by this finding for two reasons. First, while prophage induction has been previously reported in *P. aeruginosa* biofilms (McElroy et al., 2014; Rice et al., 2009; Secor et al., 2015; Webb et al., 2003), and host conditions (Marshall et al., 2021), there are fewer references to prophage induction during planktonic culture (Li et al., 2019). However, we detected Pf5 circularization in both planktonic and biofilm environments, suggesting that prophage induction also occurs in planktonic conditions. Second, despite the consistency with which we detected Pf excision and circularization in evolved populations, these events were not referenced in other *P. aeruginosa* WGS studies with similar designs (Ahmed et al., 2018; Sanz-García et al., 2018; Schick and Kassen, 2020). We suspect that prophage induction may be underreported in WGS data due to computational challenges associated with detecting junction and low frequency variants. However, levels of prophage induction are dependent on environmental conditions and genetic background (Martínez and Campos-Gómez, 2016; Shapiro et al., 2016), so it is also possible that induction does not occur in every model system. Regardless, our findings suggest that the contribution of prophage induction to phenotypes and evolution in laboratory studies ought to be explored more thoroughly.

We also found that mutations in *pf5r* were rapidly selected in a planktonic *P. aeruginosa* population. Similar mutations were detected in McElroy et al., in which multiple variants in the analogous gene in PAO1 (*pf4r*) arose rapidly during biofilm growth (McElroy et al., 2014). We determined that mutations in *pf5r* increased Pf5 induction, suggesting that *de novo* *pf5r* mutations produce similar phenotypes as *de novo* mutations in *pf4r* (McElroy et al., 2014). Pf4r binds to its promoter sites as a homodimer, but the 16bp duplication and SNP detected in our work are not within the predicted DNA binding or dimerization regions, assuming that Pf5r adopts a similar

structure (Ismail et al., 2021). However, given the Pf5 induction phenotypes we detected, the *pf5r* mutations are still consistent with disrupted Pf5r function. The impact of the downstream SNP (*pf5r* G93W), which was selected on the genetic background of the duplication, is curious, as it is unclear whether it modulates the magnitude or specificity of Pf5r function. Nonetheless, the relative frequency of the SNP rose from less than 40% to ~85% in the *lasR pf5r* and *morA pf5r* mutants between WGS runs, suggesting that it confers a strong fitness advantage.

We discovered that *pf5r* mutations led to increased replication of a selfish genetic element with a region of high sequence identity to Pf5 (PA14\_35710 to PA14\_35730). We hypothesize that the replication initiation factor of Pf5, or another Pf5 protein, may bind to this region of homology and produce high levels of replication when Pf5 is induced. If this is the case, it suggests that Pf5 induction may inadvertently increase the replication of distant genomic regions which have homologous sequences. For strains superinfected with multiple phages, like MPAO1, which is lysogenized by both Pf4 and Pf6, this could produce increased replication of other prophage in addition to the one that acquired mutations. Recent studies have shown that Pf4r is able to bind a number of sites in the *P. aeruginosa* genome, and likely regulates gene expression by acting as a transcription factor (Ismail et al., 2021). Our data suggest that increased replication of distant regions of the genome is another mechanism by which Pf phage could alter *P. aeruginosa* biology.

We determined that *pf5r* mutations were detrimental to growth of the host strain but increase relative fitness in the presence of competitors. The advantage of *pf5r* mutants during competition is surprising, as non-*pf5r* mutants should quickly become infected with mutant phage and exhibit similar phenotypes following coculture. We hypothesize that changes to host cell physiology engender *pf5r* mutants with a transient protective advantage in the presence of WT competitors. However, the mechanism of this advantage is unclear. Regardless, the selection of hosts with *pf5r*

mutations illustrates an under-appreciated circumstance within of evolutionary biology: costly mutations may be selected within a population provided they produce relative fitness advantages during competition.

The fitness advantages of *lasR pf5r* and *morA pf5r* mutants relative to *pf5r* mutants is an intriguing avenue of future study. We know from the work in Chapter 3 that *morA* and *lasR* mutants both have growth advantages in CF nutrients, so it is possible that *morA* and *lasR* mutations do not produce a fitness advantage specific to Pf5 induction. Alternatively, mutations which alter transcriptional responses, including stress response, might alter the level of Pf5 induction within the host cell. Thus, *morA* or *lasR* mutations might compensate for the cost of *pf5r* mutations on the host, leading to the selection of *pf5r* mutations on a *morA* or *lasR* mutant background. Also, *morA* mutations, which produce increased Pel polysaccharide and biofilm formation (Katharios-Lanwermeier et al., 2021; Scribner et al., 2021), could feasibly produce a structural barrier which prevents phage from entering the cell. In addition, both *morA* and *lasR* mutations alter swarming motility of *P. aeruginosa* (Chapter 3), so it is possible that they might alter the function of type IV pilus in a manner that protects against Pf phage. Thus, an interaction between mutants with altered quorum sensing and biofilm phenotypes could have protective, compensatory, or nonexistent interactions with Pf5 induction. *LasR* and *morA* mutants, and more broadly altered quorum sensing and high biofilm variants, are often selected during chronic infection, and therefore the role of phage in their selection ought to be further elucidated.

We also found that mutations increasing prophage induction have critical impacts on subsequent evolution. Consistent with previous studies in PAO1, we identified rapid evolution of the Pf5 genome and multiple mutations in pilus genes (McElroy et al., 2014). Mutations in type IV pili likely represent antagonistic coevolution in which *P. aeruginosa* disrupts pilus biogenesis

to evade Pf5 superinfection. This is consistent with the cycle of defense and counter-defense expected from bacterial and viral coevolution (Koskella and Brockhurst, 2014). On the other hand, the deletions of structural genes within Pf5, likely produce viral cheaters which are packaged into the capsid produced by intact genomes. Cheaters are known to emerge rapidly in viral evolution experiments (Dennehy and Turner, 2004; Meir et al., 2020). Although the impact of capsid deletions on the host population is unclear, we speculate that a bacterial host with reduced copy number for capsid genes may gain a fitness advantage by transcribing and translating fewer structural genes. Yet, bacterial populations which maintain even a small portion of phage genomes with the structural genes could still produce virions and may maintain the fitness advantages of lysogeny. Regardless, these mutations reflect the speed at which adaptations are selected following phage superinfection. Altogether, this study demonstrates that propagation of a clonal lineage in CF nutrients was sufficient for the development of rapid and complex evolutionary changes.

## **4.5 Methods**

### **4.5.1 Bacterial strains and culture conditions**

All bacterial strains and populations described in this work were derived from *Pseudomonas aeruginosa* strain UCBPP-PA14 (Rahme et al., 1995). Evolved populations were propagated and sequenced as described in Chapter 2, and clones were isolated from evolved populations and sequenced as described in Chapter 3 unless otherwise indicated (Scribner et al., 2020, 2021). Briefly, planktonic lineages were propagated through a 1:100 dilution of the culture into fresh media every 24 hours, and biofilm lineages were propagated by transferring a colonized

polystyrene bead into fresh media containing new beads every 24 hours. Unless otherwise indicated, experiments were performed in the minimal medium used for the evolution experiment, which consisted of an M9 salt base (0.1 mM CaCl<sub>2</sub>, 1.0 mM MgSO<sub>4</sub>, 42.2 mM Na<sub>2</sub>HPO<sub>4</sub>, 22 mM KH<sub>2</sub>PO<sub>4</sub>, 21.7mM NaCl, 18.7 mM NH<sub>4</sub>Cl), and 1 mL/L each of Trace Elements A, B, and C (Corning 99182CL, 99175CL, 99176CL) supplemented with 11.1mM glucose, 10mM DL-lactate (Sigma-Aldrich 72-17-3), 20 mL/L MEM essential amino acids, 10 mL/L MEM nonessential amino acids (Thermofisher 11130051, 11140050). Cultures were incubated in 18x150mm glass tubes with 5mL of medium at 37°C in a roller drum at 150rpm.

Two new strains, *pf5r.1* and *pf5r.2*, were isolated and sequenced for this work. These strains were generating by coculturing a *lacZ*-marked ancestral PA14 strain with the *morA pf5r* and *lasR pf5r* mutants, then plating the population on ½ strength tryptic soy agar. Isolated clones with the *lacZ*-marked phenotype were chosen, cultured for 24 hours in the evolution medium, washed 3 times with PBS, then sequenced using the protocol referenced in Chapter 3. The *morA pf5r* and *lasR pf5r* strains were also cultured for 24 hours in the evolution medium, washed 3 times with PBS, then re-sequenced.

#### **4.5.2 Whole genome sequence analysis**

Variant calling analysis for the evolved populations was completed in Chapter 3. Briefly, sequencing reads were trimmed using trimmomatic v0.36 and variants were called using breseq v0.35.0 in polymorphism mode. To avoid false positive variant calls, we required that 3 reads from each strand to support variants and that variants reach at least 5% frequency within the population. However, in this chapter we reported the number of reads supporting Pf5 excision and

circularization in every population even if these criteria were not met. Variants in the Pf5 region are shown in Table 5 and all mutations may be viewed in the Supplemental Data.

Isolated clones were analyzed using a similar workflow, with distinctions noted below. Sequencing reads were trimmed using trimmomatic v0.36 and variants were called using breseqv0.35.0 in clonal mode, which assumes that variant alleles are present at 100% frequency in the sample. This mode also reports variants at intermediate frequencies but indicates that these reads have marginal read alignment evidence. Though we have previously excluded marginal read alignment evidence from analysis, in this chapter we reported variants with marginal read alignment evidence if they represented Pf5 excision, Pf5 circularization, or *pf5r* G93W.

To calculate genome coverage for evolved populations and clones, we used the BAM file generated in breseq output to calculate average read depth across 10bp windows using SAMtools (Li et al., 2009b). We then visualized coverage over regions of the genome using ggplot2 (Wickham et al., 2019). Though read depth of Pf5 is visualized at the site of its lysogeny within PA14, most Pf5 reads actually reflect the replicative form of Pf5.

### 4.5.3 qPCR

To validate the changes in Pf5 copy number detected by whole genome sequencing, we utilized primers which bind to regions flanking the *attB* and *attP* sites (Li et al., 2019). Strains were resurrected from freezer stocks in the experimental medium and cultured for 24 hours. Cultures were centrifuged at 13,000g for 1 minute, supernatant was removed, and genomic DNA was extracted from cell pellets using the QIAamp DNA mini protocol from QIAGEN using a QIAcube. DNA was diluted 1:100 then used as template for qPCR. Reactions were performed using the Sybr Green PowerUp Master Mix (Thermofisher Scientific A25741) according to the

manufacturer's protocol on Applied Biosystems StepOne Plus Real-Time PCR system. Three biological replicates were tested with three technical replicates each.

#### 4.5.4 Growth curves

Strains were revived from freezer stocks in the evolution media and cultured for 24 hours. They were then diluted 1:100 in 200uL fresh media in a 96 well plate. Plates were incubated for 24 hours at 37 °C with shaking for 30 seconds every 15 minutes and Abs OD<sub>600</sub> was measured at 15-minute intervals. Each well was plated for CFU following 24 hours of incubation.

#### 4.5.5 Fitness assays

Starting proportions of each competitor were measured by plating for CFU on ½ strength tryptic soy agar containing X-gal. Strains were differentiated by the presence of a blue colony phenotype caused by the presence of a *lacZ*-marker in one of the competitors. Competitions were incubated for 24 hours in the evolution media then again plated for CFU. The fitness of each competition is shown as selection rate  $r$ , the difference in Malthusian parameters for each strain. Selection rate was calculated as in (Turner et al., 2020) where A and B represent competitors and  $d=0$  and  $d=1$  reflect CFU/mL at timepoints 0 and 24 hours.

$$r = \frac{\ln \frac{A_{t=2}}{A_{t=0}} - \ln \frac{B_{t=2}}{B_{t=0}}}{2}$$

#### **4.5.6 Statistical analysis**

Data was analyzed using GraphPad Prism 9 and using R where noted.

#### **4.5.7 Data availability**

Data and code used for data analysis can be accessed at <https://github.com/michellescribner/prophage>. All sequencing reads were deposited in NCBI under BioProject accession numbers PRJNA595915 and PRJNA692838.

## 5.0 Conclusions

*Pseudomonas aeruginosa* is a versatile opportunistic pathogen with the ability to survive and grow under a variety of environmental stressors. The bacterium possesses regulatory genes which enable global transcriptional responses to its environment, including biofilm formation, and a genetic repertoire sufficient for metabolism of a wide range of carbon sources (Mathee et al., 2008). *P. aeruginosa* strains also frequently harbor filamentous prophages which may be weaponized against microbial competitors and contribute to biofilm integrity (Secor et al., 2015). In addition to intrinsic resistance to many antibiotics, the bacterium can also rapidly acquire resistance through horizontally acquired elements and spontaneous mutations, the latter of which is particularly relevant in infections of people with CF. Furthermore, during infection *P. aeruginosa* acquires mutations within regulatory genes, including those associated with biofilm and quorum sensing, which contribute to persistence (López-Causapé et al., 2017; Marvig et al., 2015). These factors culminate in a bacterium capable of producing dangerous and difficult to clear infections, but the mechanisms by which *P. aeruginosa* evolves further resistance to clearance during chronic infection require further study.

In this dissertation, we tested the effects of three selective pressures, tobramycin, biofilm lifestyle, and nutrients, on adaptation of *P. aeruginosa* using evolution experiments paired with whole genome sequencing. Due to the devastating impact of *P. aeruginosa* infections in people with immune deficiencies, several other research groups have also examined the evolution of *P. aeruginosa* in response to similar selective pressures in recent years (Abisado et al., 2021; Ahmed et al., 2018; Azimi et al., 2020; Feng et al., 2016; Hernando-Amado et al., 2019; McElroy et al., 2014; Sanz-García et al., 2018; Schick and Kassen, 2020; Wong et al., 2012). Our findings concur

in many aspects with those reported in these studies and provide several unique contributions. In Chapter 2, we performed the first study testing the impact of biofilm lifestyle on evolution of tobramycin resistance for *P. aeruginosa*. In addition, we provided a rare analysis of the repeatability of antimicrobial resistance across species by comparing the dynamics of resistance with an identical experiment in *A. baumannii*. In Chapters 3 and 4, we defined the mutations acquired during adaptation to aspects of the CF nutritional environment and biofilm growth, including parallel mutations in genes known to be mutated in clinical genomes. We applied our expertise in microbial population biology and genomics to provide a detailed analysis of evolved populations of *P. aeruginosa*, paying particular attention to polymorphic structural variants that were acquired in each selective pressure and in doing so, identified prophage induction in evolved populations. The overarching findings of this study and their implications are defined below.

### **5.1 Parallelism is predictable**

The most prominent and unifying finding of this dissertation is the extensive phenotypic and genotypic parallelism detected across clades and lineages. By this, we refer to the selection of multiple independent mutations in *fusA1* (7 mutations), *ptsP* (10 mutations), and *orfKHLN* (5 mutations), *lasR* (9 mutations), *morA* (5 mutations), and *wspF* (3 mutations). The finding that evolution proceeded by parallel adaptation is consistent with the findings of many other evolution experiments (McDonald, 2019) and with adaptation in CF (Clark et al., 2018; Marvig et al., 2015). However, we also found that many mutations were also selected in parallel across species and lifestyles, which defies some findings of previous studies.

In Chapter 2, we tested the impact of genetic background on evolution of tobramycin resistance by comparing experiments using *P. aeruginosa* with identical experiments from our laboratory using *A. baumannii*. In doing so, we found that mutations in *fusAI* and *ptsP* occurred with remarkable consistency between clades, lineages, lifestyles, and species. In addition, the evolutionary dynamics of resistance were similar across species. The impact of genetic background on evolution of drug resistance is a relevant consideration in combating drug resistance, as it indicates the extent to which evolution may be predicted for different strains and species treated with similar drugs. However, the impact of genetic background on evolution of drug resistance is most frequently examined between strains with only a few mutational differences (Card et al., 2021; Hernando-Amado et al., 2019; Santos-Lopez et al., 2021; Yen and Papin, 2017), or between strains of the same species (Vogwill et al., 2014). Instances of genetic parallelism across species can be discerned in some circumstances from clinical genomes or comparison across different studies, but we are not aware of any other studies which directly compare the evolution of resistance across species through parallel experimentation. Although certain mutations are known to confer resistance in diverse species, like mutations in gyrase, it has been appreciated by microbiologists and evolutionary biologists alike that strain background can influence phenotypes (Kasetty et al., 2021; Santos-Lopez et al., 2021; Vogwill et al., 2014, 2016). Recent studies, including from our laboratory, have shown that even relatively few genetic differences can alter subsequent evolutionary trajectories (Santos-Lopez et al., 2021; Yen and Papin, 2017), therefore it is remarkable that two distinct species would consistently select mutations in primarily two of the same genes. In this way, our findings reveal that selection of *fusAI* mutations in response to aminoglycoside treatment may be an exception to the general finding that genetic background influences evolution of drug resistance. We speculate that the strict conservation of this gene across

species may be related to this finding, thus we ought to consider the level of conservation for the target of an antibiotic when attempting to assess the predictability of its potential contributions to resistance.

The study described in Chapter 2 is also the first to characterize the impact of biofilm lifestyle on evolution of resistance to tobramycin, or any aminoglycoside, in either *P. aeruginosa* or *A. baumannii*. Similar studies have been published by our lab for *A. baumannii* in the presence of the fluoroquinolone antibiotic ciprofloxacin (Santos-Lopez et al., 2019) and by others for *P. aeruginosa* PAO1 in the presence of ciprofloxacin (Ahmed et al., 2018). For *A. baumannii* in the presence of ciprofloxacin, populations acquired distinct mechanisms of resistance depending on lifestyle. Specifically, both planktonic and biofilm populations evolved mutations in regulators of efflux pumps, but only planktonic populations evolved mutations in DNA gyrase (Santos-Lopez et al., 2019). Planktonic populations also acquired higher levels of resistance to ciprofloxacin. Similarly, Ahmed et al. found that mutations regulators of efflux pumps were present in both lifestyles but that DNA gyrase mutants were exclusively selected in planktonic populations (Ahmed et al., 2018). We speculate that in both studies, populations propagated in biofilm lifestyle may have experienced greater antibiotic tolerance, resulting in the selection of mutations that conferred lower MIC, but higher fitness, than in planktonic populations. However, in tobramycin, we found that the primary targets of resistance, *fusAI* and *ptsP*, were consistent between lifestyles for both species. Certain mutations were associated with biofilm lifestyle (LPS and cell membrane mutations), but ultimately the levels of resistance were similar across environments. Therefore, we detected a greater degree of similarity across lifestyles for populations propagated with tobramycin selection than has been shown previously for ciprofloxacin-evolved populations. We hypothesize that the distinct properties of tobramycin and ciprofloxacin, including charge and ability to

penetrate microbial biofilms (Tseng et al., 2013), may influence the evolution of resistance. However, tobramycin can be sequestered in *P. aeruginosa* biofilms due to its positive charge, whereas ciprofloxacin is not, therefore we would have predicted that tobramycin resistance would be more likely to differ across environments. Regardless, we have found that biofilm and planktonic populations acquire certain mutations that are associated with lifestyle, but that the evolution of tobramycin resistance is relatively predictable across environments compared to evolution of ciprofloxacin.

## 5.2 Simple is sufficient

In every environment examined within this dissertation, the most frequently mutated genes were those that are also known to be mutated in clinical genomes, from *fusA1* in the presence of tobramycin, to quorum sensing and biofilm regulators in the absence of drug. This finding highlights the importance of tobramycin, nutrient adaptation, and biofilm lifestyle in the evolution of *P. aeruginosa* during infections. In addition, the finding that many of the mutations detected in clinical genomes are selected *in vitro* implies that the advantages of the selected adaptations are not specific to infection. In fact, many of the mutations that we detected in response to tobramycin, nutrient adaptation, and biofilm selection have also been repeatedly detected within other *in vitro* evolution experiments (Abisado et al., 2021; Ahmed et al., 2018; Azimi et al., 2020; Feng et al., 2016; McElroy et al., 2014; Sanz-García et al., 2018; Schick and Kassen, 2018; Wong et al., 2012). Regarding this point, it is critical to emphasize that while propagation of *P. aeruginosa* in CF nutrients is sufficient to select for *lasR* mutants, the precise nutrient composition of the CF respiratory environment is not required for the selection of *lasR* mutants. Rather, these other

experiments show that *lasR* mutations have also been selected in other nutritional environments, including laboratory media and minimal media supplemented with only glucose (Abisado et al., 2021; Hernando-Amado et al., 2019; Schick and Kassen, 2020). However, experiments from our laboratory in different media but identical propagation methods did not select for frequent mutations in *lasR* (Harris et al., 2021), suggesting that the nutritional environment nonetheless plays a role in the fitness advantage of *lasR* mutants.

Several explanations for the fitness advantage of *lasR* mutants have been demonstrated in specific environments, including social cheating, reduced production of energetically costly virulence factors, altered carbon utilization, growth advantage at high cell densities, increased resistance to certain antibiotics, and growth advantage in microoxia (Clay et al., 2020; D'Argenio et al., 2007; Hoffman et al., 2010). We hypothesize that these factors may each contribute to selection of *lasR* mutants, but to varying degrees in different environments. In our evolution experiments, the fitness of *lasR* mutants could not be explained by social cheating or solely by altered carbon utilization. In contrast, our finding that *lasR* mutants possess a growth advantage in the absence of competitors is consistent with the idea that disrupted LasR decreases the production of many transcripts that are energetically costly to produce. Our findings are also consistent with the model that growth advantage in microoxia and at high cell densities could contribute to *lasR* mutant selection. The relative contributions of these proposed growth advantages for *lasR* mutants in different environments ought to be studied more extensively in future work.

Another relevant question in our work is why *lasR*, *morA*, and *wsp* mutations, which are frequently selected in the absence of drug in many studies, are not selected in the presence of tobramycin. Two other studies have reported nearly identical genetic targets of selection in PA14: *fusAI* and *ptsP* in the presence of tobramycin and *lasR* mutants only in the absence of drug

(Abisado et al., 2021; Sanz-García et al., 2018). Both research groups examined the relationship of *lasR* mutants to tobramycin treatment. Abisado et al. reported that tobramycin suppresses the selection of *lasR* mutants directly because *lasR* mutants are more susceptible than the ancestral strain. In addition, they reported indirect suppression of *lasR* mutants through selection of *ptsP* mutants, which secrete pyocyanin and suppress cheaters (Abisado et al., 2021). However, others detected no difference in susceptibility between a *lasR* mutant and the ancestral strain (Hernando-Amado et al., 2019). In fact, Hernando-Amado et al. propagated a *lasR* mutant in the presence of tobramycin and found that it evolved higher levels of resistance than the ancestral strain. As a result, it is unclear whether lack of selection for *lasR* mutants in the presence of drug is notable in our study. Rather, we point out that if *lasR* mutants do not increase resistance to tobramycin, it is logical that they would be outcompeted by resistant haplotypes in the presence of increasing concentrations of drug.

It is worth noting that the mutations detected in these evolution experiments do not encapsulate the diversity of mutations detected *in vivo*. For instance, we did not detect mutations associated with iron acquisition, increased mutation rate, or resistance to other antibiotics (Marvig et al., 2015; Smith et al., 2006; Winstanley et al., 2016). We also did not detect mutations or phenotypes related to mucoidy, which is consistent with similar evolution experiments (Azimi et al., 2020; Schick and Kassen, 2018, 2020). Curiously, in tobramycin-evolved populations, we did not detect mutations in regulators of efflux pumps that are predicted to confer aminoglycoside resistance *in vivo*, like *mexZ* (Winstanley et al., 2016). The spectrum of mutations detected within this study may have been limited to some extent by its short duration, but another likely explanation is that other selective pressures contribute to adaptation *in vivo* that were not represented within this experiment. Therefore, the absence of these mutations from our evolution

experiments and others suggests that mutations in these genes are not selected exclusively due to nutrient, biofilm, or tobramycin adaptation. Regardless, we conclude that simple environmental conditions are sufficient to select complex phenotypes, including altered quorum sensing and biofilm, via mutations commonly linked to adaptations during infections.

### 5.3 Prophage are precarious

We also observed that increased prophage induction was selected during laboratory propagation, highlighting the surprising genetic and ecological complexity of populations after less than 100 generations of propagation in a relatively simple environment. Mutations in the prophage repressor were previously reported to be selected in PAO1 biofilms (McElroy et al., 2014), but this is the first study to report this phenomenon in PA14. Ultimately, the finding that mutants that induce prophage replication can be rapidly selected within populations of PA14, which decrease the absolute fitness of the bacterial population, reflects that despite the advantage of lysogeny in certain environments, prophage are highly precarious to harbor.

We also discovered the consistent induction of Pf5 phage at low levels even in lineages without repressor mutations. While basal induction of Pf phage is known to occur for *P. aeruginosa* strains during laboratory culture (Li et al., 2019), it is not frequently reported using WGS data. Our detection of prophage induction was made possible by multiple genomic and bioinformatic innovations. First, we sequenced samples to sufficiently high depth and utilized computational tools that report polymorphic variants, which enabled the detection of low frequency variants supporting prophage circularization and excision. Second, we analyzed junction evidence detected in our sequencing reads. In addition, this study was enabled by the fact

that Pf5 forms a double-stranded replicative form detectable by WGS yet was not convoluted by genomes within virions because extruded genomes are single-stranded. We hypothesize that many other studies performing WGS analysis could benefit from attempting similar approaches given the consistency of prophage induction in our samples.

#### 5.4 Future directions

A number of outstanding questions remain with regard to the induction of Pf phage in *P. aeruginosa*. First, we propose conducting an analysis of published *P. aeruginosa* sequencing data to determine the prevalence and magnitude of prophage induction during laboratory culture. We have detected Pf5 induction in the medium used in this dissertation (M9 salts supplemented with glucose, lactate, and amino acids), in addition to medium supplemented with only galactose and arginine as carbon sources (Harris et al., 2021), therefore we predict that prophage induction may occur in a variety of conditions. However, we detected induction in a greater proportion of samples in the medium used in this dissertation, so it would be useful to test the effect of different environments on prophage induction. In addition, we propose sampling PA14 strains periodically throughout a 24-hour timespan to determine the timing of prophage induction during culture. It would also be advantageous to examine the level of prophage induction in biofilm versus planktonic conditions in a larger dataset and with more diverse strains than generated by this evolution experiment. We also did not have an opportunity to examine the impact of high biofilm (*morA*) or quorum sensing (*lasR*) mutations on levels of prophage induction quantitatively, but both would be useful given the impact of these mutations on growth of *P. aeruginosa*. We propose

quantifying prophage induction by both WGS and qPCR for *pf5r* mutants with and without *morA* and *lasR* mutations to determine the impact of biofilm and QS alterations on prophage induction.

We also propose investigating clinical genomes to determine whether mutations to prophage genomes are selected *in vivo*. In a study of 474 clinical genomes (Marvig et al., 2015), no mutations were detected in the prophage repressor gene during the sampling period, with the exception of one clone type which also showed numerous synonymous mutations within the prophage genome. While it is possible that these mutations are genuine, it is possible that these mutations derive from a computational artifact, so verification is needed. We also note a synonymous mutation that was selected in the prophage replication initiation gene (PA0727 H180H) in PA01-B11 during chronic infection in a porcine wound model (Marshall et al., 2021), which ought to be investigated further for impact on prophage induction. Additionally, mutations were detected in samples collected from the sinuses of two people with CF in PA0718, encoding a hypothetical protein within the Pf genome (Armbruster et al., 2021). However, it would be advantageous to repeat variant calling analysis for this and other studies using methods that report polymorphisms, as it is possible that clonal isolates of *P. aeruginosa* may have prophage repressor mutations at intermediate frequencies. In addition, prophage repressor mutations may occur as structural variants or indels, thus detection requires parameters which report such variants. Finally, prophage mutations may fix prior to isolation of a lineage from a chronic infection, preventing detection of new changes during subsequent sampling, therefore more thorough analysis of clinical genomes is needed to determine the prevalence of prophage mutations during infection.

The effect of *pf5r* mutations on native CRISPR is also an intriguing avenue of future study. While the prophage repressor normally confers resistance to exogenous Pf5, we have shown that Pf5 with *pf5r* mutations can superinfect cells already lysogenized by Pf5. The selection of

mutations in type IV pili suggests that resistance to phage is advantageous for *P. aeruginosa* in this environment. Therefore, it is feasible that other mechanisms of resistance to Pf5 may also be advantageous in the presence of Pf5 mutants, including CRISPR-mediated resistance. The PA14 strain of *P. aeruginosa* has two CRISPRs, CRISPR-1 and CRISPR-2, which flank *cas* genes (Zegans et al., 2009). Incorporation of a portion of the Pf5 genome into the CRISPR region to confer immunity to Pf5 would be detected by WGS as a new junction in the reference sequence and was not detected in any of the *pf5r* mutants described in this work (Appendix Table 3). However, it is possible that CRISPR-mediated immunity was simply not selected in these samples by chance, or that CRISPR-mediated immunity is advantageous, but less advantageous than resistance via mutations to type IV pili. Therefore, it would be useful to examine populations with Pf5 mutations at greater throughput to determine if CRISPR-mediated immunity evolves.

Populations with increased prophage induction also illustrate principles of evolutionary game theory which ought to be explored more thoroughly. Defectors use public goods produced by other members of their population (cooperators) without contributing public goods themselves. Therefore, the capsid deletion mutants identified in Chapter 4 likely represent viral defectors because they require the presence of genes encoded by cooperating viral genomes to produce virions (Turner and Chao, 1999). We detected the selection of five independent capsid deletion mutations at high frequencies over an extremely short period of time, suggesting that these mutations are highly advantageous for the phage, host, or both. However, will these mutations ever reach fixation? Defector fixation would render the prophage cryptic, because some prophage genes would remain in the genome but the PA14 strain would be unable to produce virions. Evolutionary game theory predicts that when the cost of defector fixation exceeds the cost to cooperators in the presence of defectors, cooperators and defectors should reach a polymorphic equilibrium (Turner

and Chao, 1999). In this instance, the defectors should be unable to replicate entirely without cooperators, so the cost of defector fixation to the phage is very high. Therefore, defectors should remain at an intermediate frequency within the population, but never fix. We propose using capsid deletions as a model system to test this principle by directly competing capsid deletions with ancestral phage. In theory, the viral defectors should never fix. However, it may be possible for defectors to fix following a transfer bottleneck if the defectors were at sufficiently high frequencies. This hypothesis is testable by performing transfers of varying bottleneck sizes for competitions of capsid deletion mutants versus the ancestral phage.

Another interesting possibility would be to perform fitness assays for capsid deletions with and without *pf5r* mutations. We observed that capsid deletions were selected in parallel shortly after the evolution of *pf5r* mutations. This finding is consistent with prior studies suggesting that viral defectors have a high fitness advantage at high multiplicity of infection (MOI), but less at low MOI (Turner and Chao, 1998). High multiplicity of infection results in increased competition between viruses within host cells, which is effectively produced by *pf5r* mutations. Therefore, *pf5r* mutations could be utilized to manipulate MOI to determine the impact on defector fitness.

Finally, we propose performing an evolution experiment of PA14 with mutant Pf5 to further identify the evolutionary outcomes of increased prophage induction. We have already detected two adaptations that are frequently identified in viral evolution experiments, namely the selection of putative viral defectors (capsid mutants) and putative phage-resistant hosts (type IV pili mutants). Evolution experiments would enable us to detect any additional mutations, including CRISPR-mediated immunity to mutant Pf5, that produce fitness advantages and to more precisely determine the order in which they occur. Also, while it is tempting to speculate the fate of Pf5 following the acquisition of Pf5 mutations, it is critical to acknowledge the speed at which

adaptations were subsequently selected in the host, thus may also play important roles in the fate of the population. For instance, the evolution of phage resistance through type IV pili mutations may influence the fitness of viral defectors, rendering the order of acquisition for these mutations critical to the fate of the population. These questions could be addressed with high throughput evolution experiments using *P. aeruginosa* strains with mutant Pf5 to identify the game-theoretical conditions and genetic mechanisms that promote exploitation by phage of their hosts or other phage, as well as the host genotypes that constrain mutant phage.

## 5.5 Limitations

While the frequent selection of mutations in genes known to acquire mutations during chronic infection implies that our experimental model recapitulates key aspects of the host environment, we acknowledge several limitations of our system in mimicking host conditions. First, the minimal medium used for the evolution experiments and several phenotypic assays described in this work was designed to roughly approximate nutrient levels in CF sputum (Palmer et al., 2007). This approach was chosen to enable findings which are more relevant to CF infection than experiments performed in standard laboratory media, but we note that the nutrient levels in our experimental medium do vary from those detected in CF sputum, as described in Chapter 3. Also, our medium does not incorporate mucins, thus the viscosity of CF sputum is not incorporated in our environment, unlike other studies (Schick and Kassen, 2018). In addition, several other aspects of the host environment are not represented in our model system, including the microbiome, immune cells, and certain classes of antibiotics. Our model therefore incompletely encompasses the host environment but was chosen in order to test the impact of specific aspects

of the host environment on evolution. We predict that incorporation of additional host factors into this experimental model may enable selection of additional mutations which are detected during infection. We do not aim to suggest that our model better recapitulates infections than other model systems that do include these factors, including mucins, growth in an aggregate lifestyle, or animal models; rather, our data suggest that the factors we investigated in this work may be sufficient for adaptations identified in more complex conditions.

The bead biofilm model used in these experiments enables selection of mutants which are adept at the entire biofilm lifecycle of attachment, biofilm growth, and dispersal. Its use was motivated by the ability to archive populations at various timepoints by freezing. However, there are also limitations to this model. For instance, this model produces strong selection for attachment to a polystyrene surface, but we acknowledge that other forms of biofilms, particularly those attached to biotic surfaces or growing within aggregates, may be more representative of the lifestyle of *P. aeruginosa* in the CF respiratory environment (Goltermann and Tolker-Nielsen, 2017; Jennings et al., 2021). Regardless, we found that mutations to the Wsp pathway, which are also frequently identified *in vivo* (Harrison et al., 2020), were a major target of selection in our model, suggesting that similar adaptations may be selected in both environments.

The absence of competing microbial species in our model also likely represents a limitation to this work. For instance, acquisition of antimicrobial resistance genes is a mechanism of antibiotic resistance for many bacterial strains, though this may be less relevant during CF infection (Hurley et al., 1995; MacLeod et al., 2000). In addition, recent findings from Marshall and Gloag et al. in which six strains of *P. aeruginosa* were competed in a porcine model of chronic infection suggest that prophage induction by competing strains can represent both a major mechanism of competition and evolution via active lysogeny *in vivo* (Gloag et al., 2019; Marshall

et al., 2021). Yet, our findings show that even in the absence of competing species, prophage induction can be a major driver and actor in the evolutionary diversification of bacterial populations.

## Appendix A Supplemental Material

### Appendix Table 1.

Tables of variants detected in evolved populations using the filtering parameters described in Chapter 2 are shown in SupplementaryData1.xlsx at <https://github.com/michellescribner/dissertation>.

### Appendix Table 2.

Tables of variants detected in evolved populations described in Chapters 3 and 4, which was generated from the same sequencing data as in Chapter 2 using different analysis parameters, can be viewed in SupplementaryData2.xlsx at <https://github.com/michellescribner/dissertation>. Detailed descriptions of the analysis parameters used for these chapters and rationale are provided in the methods section of Chapter 3.

### Appendix Table 3.

Tables of variants detected in sequenced clones described in Chapters 3 and 4 can be viewed in SupplementaryData3.xlsx at <https://github.com/michellescribner/dissertation>. Detailed descriptions of the analysis parameters used for these chapters and rationale are provided in the methods sections of Chapters 3 and 4.

## Appendix B List of Abbreviations

$\beta$  - beta

~ - approximately

$\Delta$  - deletion

$^{\circ}\text{C}$  – degrees Celsius

A – absorbance

AMR – Antimicrobial Resistance

ANOVA – Analysis of Variance

bp – base pair

cyclic-di-GMP – cyclic diguanylate monophosphate

cyclic-AMP – cyclic adenosine monophosphate

CF – Cystic Fibrosis

DNA – deoxyribonucleic acid

Kb – kilobases

*lacZ* – gene encoding  $\beta$ -galactosidase

mL – milliliter

mm – millimeter

mM – millimolar

OD – optical density

OD<sub>600</sub> – optical density at 600 nanometers

P – P value

PBS – phosphate buffered saline

PCR – polymerase chain reaction

pH – measurement of acidity/basicity

RNA – ribonucleic acid

SCFM – Synthetic Cystic Fibrosis Media

SD – standard deviation

TOB – tobramycin

X-gal - 5-bromo-4-chloro-3-indolyl- $\beta$ -D-galactopyranoside

$\mu$ g – microgram

$\mu$ L – microliter

$\mu$ M - micromolar

## Bibliography

- Abisado, R.G., Kimbrough, J.H., McKee, B.M., Craddock, V.D., Smalley, N.E., Dandekar, A.A., and Chandler, J.R. (2021). Tobramycin Adaptation Enhances Policing of Social Cheaters in *Pseudomonas aeruginosa*. *Appl Environ Microbiol* 87, e0002921.
- Adams, J., and Rosenzweig, F. (2014). Experimental microbial evolution: history and conceptual underpinnings. *Genomics* 104, 393–398.
- Ahmed, M.N., Porse, A., Sommer, M.O.A., Høiby, N., and Ciofu, O. (2018). Evolution of antibiotic resistance in biofilm and planktonic *P. aeruginosa* populations exposed to sub-inhibitory levels of ciprofloxacin. *Antimicrob. Agents Chemother.* AAC.00320-18.
- Ahmed, M.N., Abdelsamad, A., Wassermann, T., Porse, A., Becker, J., Sommer, M.O.A., Høiby, N., and Ciofu, O. (2020). The evolutionary trajectories of *P. aeruginosa* in biofilm and planktonic growth modes exposed to ciprofloxacin: beyond selection of antibiotic resistance. *Npj Biofilms Microbiomes* 6, 1–10.
- Andersson, D.I., and Hughes, D. (2010). Antibiotic resistance and its cost: is it possible to reverse resistance? *Nature Reviews Microbiology* 8, 260–271.
- Antonovics, J., and Kareiva, P. (1988). Frequency-dependent selection and competition: empirical approaches. *Philosophical Transactions of the Royal Society of London B, Biological Sciences* 319, 601–613.
- Armbruster, C.R., Lee, C.K., Parker-Gilham, J., de Anda, J., Xia, A., Zhao, K., Murakami, K., Tseng, B.S., Hoffman, L.R., Jin, F., et al. (2019). Heterogeneity in surface sensing suggests a division of labor in *Pseudomonas aeruginosa* populations. *ELife* 8, e45084.
- Armbruster, C.R., Marshall, C.W., Garber, A.I., Melvin, J.A., Zemke, A.C., Moore, J., Zamora, P.F., Li, K., Fritz, I.L., Manko, C.D., et al. (2021). Adaptation and genomic erosion in fragmented *Pseudomonas aeruginosa* populations in the sinuses of people with cystic fibrosis. *Cell Reports* 37.
- Azimi, S., Roberts, A.E.L., Peng, S., Weitz, J.S., McNally, A., Brown, S.P., and Diggle, S.P. (2020). Allelic polymorphism shapes community function in evolving *Pseudomonas aeruginosa* populations. *The ISME Journal* 14, 1929–1942.
- Bailey, S.F., Rodrigue, N., and Kassen, R. (2015). The Effect of Selection Environment on the Probability of Parallel Evolution. *Mol Biol Evol* 32, 1436–1448.
- Barbosa, C., Trebosc, V., Kemmer, C., Rosenstiel, P., Beardmore, R., Schulenburg, H., and Jansen, G. (2017). Alternative Evolutionary Paths to Bacterial Antibiotic Resistance Cause Distinct Collateral Effects. *Mol Biol Evol* 34, 2229–2244.

- Barrick, J.E., and Lenski, R.E. (2013). Genome dynamics during experimental evolution. *Nat Rev Genet* 14, 827–839.
- Barrick, J.E., Yu, D.S., Yoon, S.H., Jeong, H., Oh, T.K., Schneider, D., Lenski, R.E., and Kim, J.F. (2009). Genome evolution and adaptation in a long-term experiment with *Escherichia coli*. *Nature* 461, 1243–1247.
- Barth, A.L., and Pitt, T.L. (1996). The high amino-acid content of sputum from cystic fibrosis patients promotes growth of auxotrophic *Pseudomonas aeruginosa*. *Journal of Medical Microbiology*, 45, 110–119.
- Baumann, P., Doudoroff, M., and Stanier, R.Y. (1968). Study of the *Moraxella* Group I. Genus *Moraxella* and the *Neisseria catarrhalis* Group. *Journal of Bacteriology* 95, 58–73.
- Baym, M., Kryazhimskiy, S., Lieberman, T.D., Chung, H., Desai, M.M., and Kishony, R. (2015). Inexpensive Multiplexed Library Preparation for Megabase-Sized Genomes. *PLOS ONE* 10, e0128036.
- Baym, M., Lieberman, T.D., Kelsic, E.D., Chait, R., Gross, R., Yelin, I., and Kishony, R. (2016). Spatiotemporal microbial evolution on antibiotic landscapes. *Science* 353, 1147–1151.
- Belete, B., Lu, H., and Wozniak, D.J. (2008). *Pseudomonas aeruginosa* AlgR Regulates Type IV Pilus Biosynthesis by Activating Transcription of the *fimU-pilVWXYZ1Y2E* Operon. *Journal of Bacteriology* 190, 2023–2030.
- Berman, H.M., Westbrook, J., Feng, Z., Gilliland, G., Bhat, T.N., Weissig, H., Shindyalov, I.N., and Bourne, P.E. (2000). The Protein Data Bank. *Nucleic Acids Res* 28, 235–242.
- Berrazeg, M., Jeannot, K., Ntsogo Enguéné, V.Y., Broutin, I., Loeffert, S., Fournier, D., and Plésiat, P. (2015). Mutations in  $\beta$ -Lactamase AmpC Increase Resistance of *Pseudomonas aeruginosa* Isolates to Antipseudomonal Cephalosporins. *Antimicrobial Agents and Chemotherapy* 59, 6248–6255.
- Billings, N., Millan, M.R., Caldara, M., Rusconi, R., Tarasova, Y., Stocker, R., and Ribbeck, K. (2013). The Extracellular Matrix Component Psl Provides Fast-Acting Antibiotic Defense in *Pseudomonas aeruginosa* Biofilms. *PLOS Pathogens* 9, e1003526.
- Bjarnsholt, T. (2013). The role of bacterial biofilms in chronic infections. *APMIS Suppl.* 1–51.
- Blair, J.M.A., Webber, M.A., Baylay, A.J., Ogbolu, D.O., and Piddock, L.J.V. (2015). Molecular mechanisms of antibiotic resistance. *Nat Rev Microbiol* 13, 42–51.
- Blount, Z.D., Borland, C.Z., and Lenski, R.E. (2008). Historical contingency and the evolution of a key innovation in an experimental population of *Escherichia coli*. *Proc Natl Acad Sci U S A* 105, 7899–7906.
- Blundell, J.R., and Levy, S.F. (2014). Beyond genome sequencing: Lineage tracking with barcodes to study the dynamics of evolution, infection, and cancer. *Genomics* 104, 417–430.

- Bolard, A., Plesiat, P., and Jeannot, K. (2017). Mutations in gene *fusA1* as a novel mechanism of aminoglycoside resistance in clinical strains of *Pseudomonas aeruginosa*. *Antimicrob. Agents Chemother.* AAC.01835-17.
- Bolger, A.M., Lohse, M., and Usadel, B. (2014). Trimmomatic: a flexible trimmer for Illumina sequence data. *Bioinformatics* 30, 2114–2120.
- Bondy-Denomy, J., Qian, J., Westra, E.R., Buckling, A., Guttman, D.S., Davidson, A.R., and Maxwell, K.L. (2016). Prophages mediate defense against phage infection through diverse mechanisms. *ISME J* 10, 2854–2866.
- Borovinskaya, M.A., Pai, R.D., Zhang, W., Schuwirth, B.S., Holton, J.M., Hirokawa, G., Kaji, H., Kaji, A., and Cate, J.H.D. (2007). Structural basis for aminoglycoside inhibition of bacterial ribosome recycling. *Nature Structural & Molecular Biology* 14, 727–732.
- Boucher, J.C., Yu, H., Mudd, M.H., and Deretic, V. (1997). Mucoid *Pseudomonas aeruginosa* in cystic fibrosis: characterization of muc mutations in clinical isolates and analysis of clearance in a mouse model of respiratory infection. *Infect Immun* 65, 3838–3846.
- Bradley, P., Gordon, N.C., Walker, T.M., Dunn, L., Heys, S., Huang, B., Earle, S., Pankhurst, L.J., Anson, L., de Cesare, M., et al. (2015). Rapid antibiotic-resistance predictions from genome sequence data for *Staphylococcus aureus* and *Mycobacterium tuberculosis*. *Nature Communications* 6, 10063.
- Breen, M.S., Kemena, C., Vlasov, P.K., Notredame, C., and Kondrashov, F.A. (2012). Epistasis as the primary factor in molecular evolution. *Nature* 490, 535–538.
- Breidenstein, E.B.M., de la Fuente-Núñez, C., and Hancock, R.E.W. (2011). *Pseudomonas aeruginosa*: all roads lead to resistance. *Trends in Microbiology* 19, 419–426.
- Brockhurst, M.A. (2015). Experimental evolution can unravel the complex causes of natural selection in clinical infections. *Microbiology (Reading)* 161, 1175–1179.
- Brockhurst, M.A., Harrison, F., Veening, J.-W., Harrison, E., Blackwell, G., Iqbal, Z., and Maclean, C. (2019). Assessing evolutionary risks of resistance for new antimicrobial therapies. *Nature Ecology & Evolution* 3, 515–517.
- Bryan, L.E., and Kwan, S. (1983). Roles of ribosomal binding, membrane potential, and electron transport in bacterial uptake of streptomycin and gentamicin. *Antimicrob Agents Chemother* 23, 835–845.
- Bryan, L.E., O’Hara, K., and Wong, S. (1984). Lipopolysaccharide changes in impermeability-type aminoglycoside resistance in *Pseudomonas aeruginosa*. *Antimicrob Agents Chemother* 26, 250–255.
- Bulitta, J.B., Ly, N.S., Landersdorfer, C.B., Wanigaratne, N.A., Velkov, T., Yadav, R., Oliver, A., Martin, L., Shin, B.S., Forrest, A., et al. (2015). Two Mechanisms of Killing of *Pseudomonas*

aeruginosa by Tobramycin Assessed at Multiple Inocula via Mechanism-Based Modeling. *Antimicrob. Agents Chemother.* *59*, 2315–2327.

Burgener, E.B., Yacob, A.A., Bollyky, P., and Milla, C.E. (2017). 99 Pf bacteriophage (Pf) in *Pseudomonas aeruginosa* (Pa) biofilms is associated with increased elastase in the sputum of patients with cystic fibrosis (CF). *Journal of Cystic Fibrosis* *16*, S90.

Burgener, E.B., Sweere, J.M., Bach, M.S., Secor, P.R., Haddock, N., Jennings, L.K., Marvig, R.L., Johansen, H.K., Rossi, E., Cao, X., et al. (2019). Filamentous bacteriophages are associated with chronic *Pseudomonas* lung infections and antibiotic resistance in cystic fibrosis. *Science Translational Medicine* *11*.

Burns, J.L., Gibson, R.L., McNamara, S., Yim, D., Emerson, J., Rosenfeld, M., Hiatt, P., McCoy, K., Castile, R., Smith, A.L., et al. (2001). Longitudinal Assessment of *Pseudomonas aeruginosa* in Young Children with Cystic Fibrosis. *The Journal of Infectious Diseases* *183*, 444–452.

Burrows, L.L., Charter, D.F., and Lam, J.S. (1996). Molecular characterization of the *Pseudomonas aeruginosa* serotype O5 (PAO1) B-band lipopolysaccharide gene cluster. *Molecular Microbiology* *22*, 481–495.

Busby, B., Kristensen, D.M., and Koonin, E.V. (2013). Contribution of phage-derived genomic islands to the virulence of facultative bacterial pathogens. *Environmental Microbiology* *15*, 307–312.

Caballero, J.D., Clark, S.T., Coburn, B., Zhang, Y., Wang, P.W., Donaldson, S.L., Tullis, D.E., Yau, Y.C.W., Waters, V.J., Hwang, D.M., et al. (2015). Selective Sweeps and Parallel Pathoadaptation Drive *Pseudomonas aeruginosa* Evolution in the Cystic Fibrosis Lung. *MBio* *6*.

Caballero, J.D., Clark, S.T., Wang, P.W., Donaldson, S.L., Coburn, B., Tullis, D.E., Yau, Y.C.W., Waters, V.J., Hwang, D.M., and Guttman, D.S. (2018). A genome-wide association analysis reveals a potential role for recombination in the evolution of antimicrobial resistance in *Burkholderia multivorans*. *PLOS Pathogens* *14*, e1007453.

Cabot, G., Zamorano, L., Moyà, B., Juan, C., Navas, A., Blázquez, J., and Oliver, A. (2016). Evolution of *Pseudomonas aeruginosa* Antimicrobial Resistance and Fitness under Low and High Mutation Rates. *Antimicrobial Agents and Chemotherapy* *60*, 1767–1778.

Cao, H., Krishnan, G., Goumnerov, B., Tsongalis, J., Tompkins, R., and Rahme, L.G. (2001). A quorum sensing-associated virulence gene of *Pseudomonas aeruginosa* encodes a LysR-like transcription regulator with a unique self-regulatory mechanism. *PNAS* *98*, 14613–14618.

Card, K.J., Thomas, M.D., Graves, J.L., Barrick, J.E., and Lenski, R.E. (2021). Genomic evolution of antibiotic resistance is contingent on genetic background following a long-term experiment with *Escherichia coli*. *PNAS* *118*.

Carmody, L.A., Zhao, J., Murray, S., Young, V.B., Li, J.Z., and LiPuma, J.J. (2013). Changes in cystic fibrosis airway microbiota at pulmonary exacerbation. *Ann Am Thorac Soc* *10*, 179–187.

- Castang, S., and Dove, S.L. (2012). Basis for the Essentiality of H-NS Family Members in *Pseudomonas aeruginosa*. *Journal of Bacteriology* *194*, 5101–5109.
- Caverly, L.J., Zhao, J., and LiPuma, J.J. (2015). Cystic fibrosis lung microbiome: opportunities to reconsider management of airway infection. *Pediatr. Pulmonol.* *50 Suppl 40*, S31-38.
- Centers for Disease Control and Prevention (U.S.) (2019). Antibiotic resistance threats in the United States, 2019 (Centers for Disease Control and Prevention (U.S.)).
- Chang, C.-Y. (2018). Surface Sensing for Biofilm Formation in *Pseudomonas aeruginosa*. *Frontiers in Microbiology* *8*, 2671.
- Chen, R., Déziel, E., Groleau, M.-C., Schaefer, A.L., and Greenberg, E.P. (2019). Social cheating in a *Pseudomonas aeruginosa* quorum-sensing variant. *PNAS* *116*, 7021–7026.
- Cheng, K., Smyth, R.L., Govan, J.R., Doherty, C., Winstanley, C., Denning, N., Heaf, D.P., van Saene, H., and Hart, C.A. (1996). Spread of beta-lactam-resistant *Pseudomonas aeruginosa* in a cystic fibrosis clinic. *Lancet* *348*, 639–642.
- Chmiel, J.F., Aksamit, T.R., Chotirmall, S.H., Dasenbrook, E.C., Elborn, J.S., LiPuma, J.J., Ranganathan, S.C., Waters, V.J., and Ratjen, F.A. (2014). Antibiotic Management of Lung Infections in Cystic Fibrosis. I. The Microbiome, Methicillin-Resistant *Staphylococcus aureus*, Gram-Negative Bacteria, and Multiple Infections. *Annals ATS* *11*, 1120–1129.
- Choy, W.-K., Zhou, L., Syn, C.K.-C., Zhang, L.-H., and Swarup, S. (2004). MorA Defines a New Class of Regulators Affecting Flagellar Development and Biofilm Formation in Diverse *Pseudomonas* Species. *J Bacteriol* *186*, 7221–7228.
- Chung, J.C.S., Becq, J., Fraser, L., Schulz-Trieglaff, O., Bond, N.J., Foweraker, J., Bruce, K.D., Smith, G.P., and Welch, M. (2012). Genomic Variation among Contemporary *Pseudomonas aeruginosa* Isolates from Chronically Infected Cystic Fibrosis Patients. *J Bacteriol* *194*, 4857–4866.
- Ciofu, O., and Tolker-Nielsen, T. (2019). Tolerance and Resistance of *Pseudomonas aeruginosa* Biofilms to Antimicrobial Agents—How *P. aeruginosa* Can Escape Antibiotics. *Front. Microbiol.* *0*.
- Ciofu, O., Beveridge, T.J., Kadurugamuwa, J., Walther-Rasmussen, J., and Høiby, N. (2000). Chromosomal beta-lactamase is packaged into membrane vesicles and secreted from *Pseudomonas aeruginosa*. *J Antimicrob Chemother* *45*, 9–13.
- Ciofu, O., Tolker-Nielsen, T., Jensen, P.Ø., Wang, H., and Høiby, N. (2015). Antimicrobial resistance, respiratory tract infections and role of biofilms in lung infections in cystic fibrosis patients. *Adv Drug Deliv Rev* *85*, 7–23.
- Clark, S.T., Guttman, D.S., and Hwang, D.M. (2018). Diversification of *Pseudomonas aeruginosa* within the cystic fibrosis lung and its effects on antibiotic resistance. *FEMS Microbiology Letters* *365*.

- Clay, M.E., Hammond, J.H., Zhong, F., Chen, X., Kowalski, C.H., Lee, A.J., Porter, M.S., Hampton, T.H., Greene, C.S., Pletneva, E.V., et al. (2020). *Pseudomonas aeruginosa* lasR mutant fitness in microoxia is supported by an Anr-regulated oxygen-binding hemerythrin. *PNAS* *117*, 3167–3173.
- CLSI (2019). Performance Standards for Antimicrobial Susceptibility Testing (Wayne, PA: Clinical and Laboratory Standards Institute).
- Colvin, K.M., Gordon, V.D., Murakami, K., Borlee, B.R., Wozniak, D.J., Wong, G.C.L., and Parsek, M.R. (2011). The Pel Polysaccharide Can Serve a Structural and Protective Role in the Biofilm Matrix of *Pseudomonas aeruginosa*. *PLOS Pathogens* *7*, e1001264.
- Colvin, K.M., Irie, Y., Tart, C.S., Urbano, R., Whitney, J.C., Ryder, C., Howell, P.L., Wozniak, D.J., and Parsek, M.R. (2012). The Pel and Psl polysaccharides provide *Pseudomonas aeruginosa* structural redundancy within the biofilm matrix. *Environmental Microbiology* *14*, 1913–1928.
- Cooper, V.S. (2018). Experimental Evolution as a High-Throughput Screen for Genetic Adaptations. *MSphere* *3*, e00121-18.
- Cooper, T.F., Rozen, D.E., and Lenski, R.E. (2003). Parallel changes in gene expression after 20,000 generations of evolution in *Escherichia coli*. *Proc Natl Acad Sci U S A* *100*, 1072–1077.
- Cooper, V.S., Honsa, E., Rowe, H., Deitrick, C., Iverson, A.R., Whittall, J.J., Neville, S.L., McDevitt, C.A., Kietzman, C., and Rosch, J.W. (2020). Experimental Evolution In Vivo To Identify Selective Pressures during Pneumococcal Colonization. *MSystems* *5*, e00352-20.
- Cornforth, D.M., Diggle, F.L., Melvin, J.A., Bomberger, J.M., and Whiteley, M. (2020). Quantitative Framework for Model Evaluation in Microbiology Research Using *Pseudomonas aeruginosa* and Cystic Fibrosis Infection as a Test Case. *MBio* *11*.
- Costerton, J.W., Stewart, P.S., and Greenberg, E.P. (1999). Bacterial biofilms: a common cause of persistent infections. *Science* *284*, 1318–1322.
- Cramer, N., Klockgether, J., Wrasman, K., Schmidt, M., Davenport, C.F., and Tümmler, B. (2011). Microevolution of the major common *Pseudomonas aeruginosa* clones C and PA14 in cystic fibrosis lungs. *Environmental Microbiology* *13*, 1690–1704.
- Cutting, G.R. (2015). Cystic fibrosis genetics: from molecular understanding to clinical application. *Nat Rev Genet* *16*, 45–56.
- Cystic Fibrosis Patient Registry (2019). Cystic Fibrosis Patient Registry Annual Data Report. 92.
- Damper, P.D., and Epstein, W. (1981). Role of the membrane potential in bacterial resistance to aminoglycoside antibiotics. *Antimicrob Agents Chemother* *20*, 803–808.
- Dandekar, A.A., Chugani, S., and Greenberg, E.P. (2012). Bacterial Quorum Sensing and Metabolic Incentives to Cooperate. *Science* *338*, 264–266.

- D'Argenio, D.A., Wu, M., Hoffman, L.R., Kulasekara, H.D., Déziel, E., Smith, E.E., Nguyen, H., Ernst, R.K., Larson Freeman, T.J., Spencer, D.H., et al. (2007). Growth phenotypes of *Pseudomonas aeruginosa* lasR mutants adapted to the airways of cystic fibrosis patients. *Mol Microbiol* *64*, 512–533.
- Davies, E.V., James, C.E., Williams, D., O'Brien, S., Fothergill, J.L., Haldenby, S., Paterson, S., Winstanley, C., and Brockhurst, M.A. (2016). Temperate phages both mediate and drive adaptive evolution in pathogen biofilms. *PNAS* *113*, 8266–8271.
- Davies, E.V., James, C.E., Brockhurst, M.A., and Winstanley, C. (2017). Evolutionary diversification of *Pseudomonas aeruginosa* in an artificial sputum model. *BMC Microbiology* *17*, 3.
- Davis, B.M., Kimsey, H.H., Kane, A.V., and Waldor, M.K. (2002). A satellite phage-encoded antirepressor induces repressor aggregation and cholera toxin gene transfer. *EMBO J* *21*, 4240–4249.
- De Oliveira, D.M.P., Forde, B.M., Kidd, T.J., Harris, P.N.A., Schembri, M.A., Beatson, S.A., Paterson, D.L., and Walker, M.J. (2020). Antimicrobial Resistance in ESKAPE Pathogens. *Clinical Microbiology Reviews* *33*, e00181-19.
- Deatherage, D.E., and Barrick, J.E. (2014). Identification of mutations in laboratory-evolved microbes from next-generation sequencing data using breseq. *Methods Mol. Biol.* *1151*, 165–188.
- Dennehy, J.J., and Turner, P.E. (2004). Reduced fecundity is the cost of cheating in RNA virus  $\phi 6$ . *Proceedings of the Royal Society of London. Series B: Biological Sciences* *271*, 2275–2282.
- Desai, M.M., and Fisher, D.S. (2007). Beneficial Mutation–Selection Balance and the Effect of Linkage on Positive Selection. *Genetics* *176*, 1759–1798.
- Dettman, J.R., Sztepanacz, J.L., and Kassen, R. (2016). The properties of spontaneous mutations in the opportunistic pathogen *Pseudomonas aeruginosa*. *BMC Genomics* *17*.
- Déziel, E., Lépine, F., Milot, S., He, J., Mindrinos, M.N., Tompkins, R.G., and Rahme, L.G. (2004). Analysis of *Pseudomonas aeruginosa* 4-hydroxy-2-alkylquinolines (HAQs) reveals a role for 4-hydroxy-2-heptylquinoline in cell-to-cell communication. *Proc Natl Acad Sci U S A* *101*, 1339–1344.
- Dijk, T. van, Hwang, S., Krug, J., Visser, J.A.G.M. de, and Zwart, M.P. (2017). Mutation supply and the repeatability of selection for antibiotic resistance. *Phys. Biol.* *14*, 055005.
- Dillon, M.M., Sung, W., Lynch, M., and Cooper, V.S. (2015). The Rate and Molecular Spectrum of Spontaneous Mutations in the GC-Rich Multichromosome Genome of *Burkholderia cenocepacia*. *Genetics* *200*, 935–946.
- Doi, Y., Wachino, J., and Arakawa, Y. (2016). Aminoglycoside Resistance. *Infect Dis Clin North Am* *30*, 523–537.

- Dunai, A., Spohn, R., Farkas, Z., Lázár, V., Györkei, Á., Apjok, G., Boross, G., Szappanos, B., Grézal, G., Faragó, A., et al. (2019). Rapid decline of bacterial drug-resistance in an antibiotic-free environment through phenotypic reversion. *ELife* 8, e47088.
- Emerson, J., Rosenfeld, M., McNamara, S., Ramsey, B., and Gibson, R.L. (2002). *Pseudomonas aeruginosa* and other predictors of mortality and morbidity in young children with cystic fibrosis. *Pediatric Pulmonology* 34, 91–100.
- Eze, E.C., Chenia, H.Y., and Zowalaty, M.E.E. (2018). *Acinetobacter baumannii* biofilms: effects of physicochemical factors, virulence, antibiotic resistance determinants, gene regulation, and future antimicrobial treatments. *Infect Drug Resist* 11, 2277–2299.
- Fàbrega, A., Madurga, S., Giralt, E., and Vila, J. (2009). Mechanism of action of and resistance to quinolones. *Microb Biotechnol* 2, 40–61.
- Fang, Z., Zhang, L., Huang, Y., Qing, Y., Cao, K., Tian, G., and Huang, X. (2014). OprD mutations and inactivation in imipenem-resistant *Pseudomonas aeruginosa* isolates from China. *Infection, Genetics and Evolution* 21, 124–128.
- Fazli, M., Almblad, H., Rybtke, M.L., Givskov, M., Eberl, L., and Tolker-Nielsen, T. (2014). Regulation of biofilm formation in *Pseudomonas* and *Burkholderia* species. *Environmental Microbiology* 16, 1961–1981.
- Feigelman, R., Kahlert, C.R., Baty, F., Rassouli, F., Kleiner, R.L., Kohler, P., Brutsche, M.H., and von Mering, C. (2017). Sputum DNA sequencing in cystic fibrosis: non-invasive access to the lung microbiome and to pathogen details. *Microbiome* 5.
- Feliziani, S., Marvig, R.L., Luján, A.M., Moyano, A.J., Rienzo, J.A.D., Johansen, H.K., Molin, S., and Smania, A.M. (2014). Coexistence and Within-Host Evolution of Diversified Lineages of Hypermutable *Pseudomonas aeruginosa* in Long-term Cystic Fibrosis Infections. *PLOS Genetics* 10, e1004651.
- Feltner, J.B., Wolter, D.J., Pope, C.E., Groleau, M.-C., Smalley, N.E., Greenberg, E.P., Mayer-Hamblett, N., Burns, J., Déziel, E., Hoffman, L.R., et al. (2016). LasR Variant Cystic Fibrosis Isolates Reveal an Adaptable Quorum-Sensing Hierarchy in *Pseudomonas aeruginosa*. *MBio* 7, e01513-16.
- Feng, Y., Jonker, M.J., Moustakas, I., Brul, S., and ter Kuile, B.H. (2016). Dynamics of Mutations during Development of Resistance by *Pseudomonas aeruginosa* against Five Antibiotics. *Antimicrob Agents Chemother* 60, 4229–4236.
- Figuroa-Bossi, N., Uzzau, S., Maloriol, D., and Bossi, L. (2001). Variable assortment of prophages provides a transferable repertoire of pathogenic determinants in *Salmonella*. *Molecular Microbiology* 39, 260–272.
- Flynn, J.L., and Ohman, D.E. (1988). Cloning of genes from mucoid *Pseudomonas aeruginosa* which control spontaneous conversion to the alginate production phenotype. *Journal of Bacteriology* 170.

- Flynn, K.M., Dowell, G., Johnson, T.M., Koestler, B.J., Waters, C.M., and Cooper, V.S. (2016). Evolution of Ecological Diversity in Biofilms of *Pseudomonas aeruginosa* by Altered Cyclic Diguanylate Signaling. *Journal of Bacteriology* *198*, 2608–2618.
- Folsom, J.P., Richards, L., Pitts, B., Roe, F., Ehrlich, G.D., Parker, A., Mazurie, A., and Stewart, P.S. (2010). Physiology of *Pseudomonas aeruginosa* in biofilms as revealed by transcriptome analysis. *BMC Microbiology* *10*, 294.
- France, M.T., Cornea, A., Kehlet-Delgado, H., and Forney, L.J. (2019). Spatial structure facilitates the accumulation and persistence of antibiotic-resistant mutants in biofilms. *Evolutionary Applications* *12*, 498–507.
- Freschi, L., Vincent, A.T., Jeukens, J., Emond-Rheault, J.-G., Kukavica-Ibrulj, I., Dupont, M.-J., Charette, S.J., Boyle, B., and Levesque, R.C. (2019). The *Pseudomonas aeruginosa* Pan-Genome Provides New Insights on Its Population Structure, Horizontal Gene Transfer, and Pathogenicity. *Genome Biology and Evolution* *11*, 109–120.
- Friedman, L., and Kolter, R. (2004). Genes involved in matrix formation in *Pseudomonas aeruginosa* PA14 biofilms. *Molecular Microbiology* *51*, 675–690.
- Gabrielaite, M., Johansen, H.K., Molin, S., Nielsen, F.C., and Marvig, R.L. (2020). Gene Loss and Acquisition in Lineages of *Pseudomonas aeruginosa* Evolving in Cystic Fibrosis Patient Airways. *MBio* *11*, e02359-20.
- Gambello, M.J., and Iglewski, B.H. (1991). Cloning and characterization of the *Pseudomonas aeruginosa* lasR gene, a transcriptional activator of elastase expression. *Journal of Bacteriology* *173*, 3000–3009.
- Gambello, M.J., Kaye, S., and Iglewski, B.H. (1993). LasR of *Pseudomonas aeruginosa* is a transcriptional activator of the alkaline protease gene (apr) and an enhancer of exotoxin A expression. *Infection and Immunity* *61*, 1180–1184.
- Garneau-Tsodikova, S., and Labby, K.J. (2016). Mechanisms of Resistance to Aminoglycoside Antibiotics: Overview and Perspectives. *Medchemcomm* *7*, 11–27.
- Gatt, Y.E., and Margalit, H. (2021). Common Adaptive Strategies Underlie Within-Host Evolution of Bacterial Pathogens. *Molecular Biology and Evolution* *38*, 1101–1121.
- Gebhardt, M.J., and Shuman, H.A. (2017). GigA and GigB are Master Regulators of Antibiotic Resistance, Stress Responses, and Virulence in *Acinetobacter baumannii*. *J Bacteriol* *199*.
- Gifford, D.R., Furió, V., Papkou, A., Vogwill, T., Oliver, A., and MacLean, R.C. (2018). Identifying and exploiting genes that potentiate the evolution of antibiotic resistance. *Nature Ecology & Evolution* *2*, 1033.
- Gil, R., Silva, F.J., Peretó, J., and Moya, A. (2004). Determination of the Core of a Minimal Bacterial Gene Set. *Microbiol Mol Biol Rev* *68*, 518–537.

Gilbert, K.B., Kim, T.H., Gupta, R., Greenberg, E.P., and Schuster, M. (2009). Global position analysis of the *Pseudomonas aeruginosa* quorum-sensing transcription factor LasR. *Mol Microbiol* 73, 1072–1085.

Gilligan, P.H. (1991). Microbiology of airway disease in patients with cystic fibrosis. *Clinical Microbiology Reviews* 4, 35–51.

Gloag, E.S., Marshall, C.W., Snyder, D., Lewin, G.R., Harris, J.S., Santos-Lopez, A., Chaney, S.B., Whiteley, M., Cooper, V.S., and Wozniak, D.J. (2019). *Pseudomonas aeruginosa* Interstrain Dynamics and Selection of Hyperbiofilm Mutants during a Chronic Infection. *MBio* 10.

Goltermann, L., and Tolker-Nielsen, T. (2017). Importance of the Exopolysaccharide Matrix in Antimicrobial Tolerance of *Pseudomonas aeruginosa* Aggregates. *Antimicrob Agents Chemother* 61, e02696-16.

Good, B.H., McDonald, M.J., Barrick, J.E., Lenski, R.E., and Desai, M.M. (2017). The Dynamics of Molecular Evolution Over 60,000 Generations. *Nature* 551, 45–50.

Govan, J.R., and Deretic, V. (1996). Microbial pathogenesis in cystic fibrosis: mucoid *Pseudomonas aeruginosa* and *Burkholderia cepacia*. *Microbiol. Mol. Biol. Rev.* 60, 539–574.

Green, A.E., Howarth, D., Chaguza, C., Echlin, H., Langendonk, R.F., Munro, C., Barton, T.E., CD Hinton, J., Bentley, S.D., Rosch, J.W., et al. (2021). Pneumococcal colonisation and virulence factors identified via experimental evolution in infection models. *Mol Biol Evol.*

Greipel, L., Fischer, S., Klockgether, J., Dorda, M., Mielke, S., Wiehlmann, L., Cramer, N., and Tümmler, B. (2016). Molecular Epidemiology of Mutations in Antimicrobial Resistance Loci of *Pseudomonas aeruginosa* Isolates from Airways of Cystic Fibrosis Patients. *Antimicrob. Agents Chemother.* 60, 6726–6734.

Groleau, M.-C., Pereira, T. de O., Dekimpe, V., and Déziel, E. (2020). PqsE Is Essential for RhlR-Dependent Quorum Sensing Regulation in *Pseudomonas aeruginosa*. *MSystems* 5.

Gruger, T., Nitiss, J.L., Maxwell, A., Zechiedrich, E.L., Heisig, P., Seeber, S., Pommier, Y., and Strumberg, D. (2004). A Mutation in *Escherichia coli* DNA Gyrase Conferring Quinolone Resistance Results in Sensitivity to Drugs Targeting Eukaryotic Topoisomerase II. *Antimicrob Agents Chemother* 48, 4495–4504.

Gutierrez, B., Douthwaite, S., and Gonzalez-Zorn, B. (2013). Indigenous and acquired modifications in the aminoglycoside binding sites of *Pseudomonas aeruginosa* rRNAs. *RNA Biol* 10, 1324–1332.

Güvener, Z.T., and Harwood, C.S. (2007). Subcellular location characteristics of the *Pseudomonas aeruginosa* GGDEF protein, WspR, indicate that it produces cyclic-di-GMP in response to growth on surfaces. *Mol Microbiol* 66, 1459–1473.

Ha, D.-G., and O’Toole, G.A. (2015). c-di-GMP and its effects on biofilm formation and dispersion: a *Pseudomonas aeruginosa* review. *Microbiol Spectr* 3.

- Ha, D.-G., Richman, M.E., and O'Toole, G.A. (2014a). Deletion Mutant Library for Investigation of Functional Outputs of Cyclic Diguanylate Metabolism in *Pseudomonas aeruginosa* PA14. *Appl. Environ. Microbiol.* *80*, 3384–3393.
- Ha, D.-G., Kuchma, S.L., and O'Toole, G.A. (2014b). Plate-Based Assay for Swimming Motility in *Pseudomonas aeruginosa*. In *Pseudomonas Methods and Protocols*, A. Filloux, and J.-L. Ramos, eds. (New York, NY: Springer), pp. 59–65.
- Ha, D.-G., Kuchma, S.L., and O'Toole, G.A. (2014c). Plate-based assay for swarming motility in *Pseudomonas aeruginosa*. *Methods Mol Biol* *1149*, 67–72.
- Hall, C.W., and Mah, T.-F. (2017). Molecular mechanisms of biofilm-based antibiotic resistance and tolerance in pathogenic bacteria. *FEMS Microbiol Rev* *41*, 276–301.
- Hancock, R.E., Raffle, V.J., and Nicas, T.I. (1981). Involvement of the outer membrane in gentamicin and streptomycin uptake and killing in *Pseudomonas aeruginosa*. *Antimicrob Agents Chemother* *19*, 777–785.
- Hancock, R.E., Mutharia, L.M., Chan, L., Darveau, R.P., Speert, D.P., and Pier, G.B. (1983). *Pseudomonas aeruginosa* isolates from patients with cystic fibrosis: a class of serum-sensitive, nontypable strains deficient in lipopolysaccharide O side chains. *Infect Immun* *42*, 170–177.
- Harris, K.B., Flynn, K.M., and Cooper, V.S. (2021). Polygenic Adaptation and Clonal Interference Enable Sustained Diversity in Experimental *Pseudomonas aeruginosa* Populations. *Molecular Biology and Evolution*.
- Harrison, J.J., Almlblad, H., Irie, Y., Wolter, D.J., Eggleston, H.C., Randall, T.E., Kitzman, J.O., Stackhouse, B., Emerson, J.C., Mcnamara, S., et al. (2020). Elevated exopolysaccharide levels in *Pseudomonas aeruginosa* flagellar mutants have implications for biofilm growth and chronic infections. *PLOS Genetics* *16*, e1008848.
- Häussler, S., Tümmler, B., Weissbrodt, H., Rohde, M., and Steinmetz, I. (1999). Small-colony variants of *Pseudomonas aeruginosa* in cystic fibrosis. *Clin Infect Dis* *29*, 621–625.
- Hay, I.D., and Lithgow, T. (2019). Filamentous phages: masters of a microbial sharing economy. *EMBO Rep* *20*.
- He, J., Baldini, R.L., Déziel, E., Saucier, M., Zhang, Q., Liberati, N.T., Lee, D., Urbach, J., Goodman, H.M., and Rahme, L.G. (2004). The broad host range pathogen *Pseudomonas aeruginosa* strain PA14 carries two pathogenicity islands harboring plant and animal virulence genes. *PNAS* *101*, 2530–2535.
- Heilbron, K., Toll-Riera, M., Kojadinovic, M., and MacLean, R.C. (2014). Fitness Is Strongly Influenced by Rare Mutations of Large Effect in a Microbial Mutation Accumulation Experiment. *Genetics* *197*, 981–990.
- Hendrix, R.W. (2002). Bacteriophages: Evolution of the Majority. *Theoretical Population Biology* *61*, 471–480.

- Henry, R.L., Mellis, C.M., and Petrovic, L. (1992). Mucoïd *Pseudomonas aeruginosa* is a marker of poor survival in cystic fibrosis. *Pediatr Pulmonol* *12*, 158–161.
- Hernando-Amado, S., Sanz-García, F., and Martínez, J.L. (2019). Antibiotic Resistance Evolution Is Contingent on the Quorum-Sensing Response in *Pseudomonas aeruginosa*. *Mol Biol Evol* *36*, 2238–2251.
- Herron, M.D., and Doebeli, M. (2013). Parallel Evolutionary Dynamics of Adaptive Diversification in *Escherichia coli*. *PLoS Biol* *11*, e1001490.
- Heurlier, K., Dénervaud, V., Haenni, M., Guy, L., Krishnapillai, V., and Haas, D. (2005). Quorum-Sensing-Negative (*lasR*) Mutants of *Pseudomonas aeruginosa* Avoid Cell Lysis and Death. *Journal of Bacteriology* *187*, 4875–4883.
- Higashitani, A., Higashitani, N., and Horiuchi, K. (1997). Minus-strand origin of filamentous phage versus transcriptional promoters in recognition of RNA polymerase. *PNAS* *94*, 2909–2914.
- Higgins, S., Heeb, S., Rampioni, G., Fletcher, M.P., Williams, P., and Cámara, M. (2018). Differential Regulation of the Phenazine Biosynthetic Operons by Quorum Sensing in *Pseudomonas aeruginosa* PAO1-N. *Frontiers in Cellular and Infection Microbiology* *8*, 252.
- Hoffman, L.R., Kulasekara, H.D., Emerson, J., Houston, L.S., Burns, J.L., Ramsey, B.W., and Miller, S.I. (2009). *Pseudomonas aeruginosa lasR* mutants are associated with cystic fibrosis lung disease progression. *Journal of Cystic Fibrosis* *8*, 66–70.
- Hoffman, L.R., Richardson, A.R., Houston, L.S., Kulasekara, H.D., Martens-Habbena, W., Klausen, M., Burns, J.L., Stahl, D.A., Hassett, D.J., Fang, F.C., et al. (2010). Nutrient availability as a mechanism for selection of antibiotic tolerant *Pseudomonas aeruginosa* within the CF airway. *PLoS Pathog* *6*, e1000712.
- Høiby, N., Bjarnsholt, T., Givskov, M., Molin, S., and Ciofu, O. (2010). Antibiotic resistance of bacterial biofilms. *International Journal of Antimicrobial Agents* *35*, 322–332.
- Holloway, B.W.Y. 1955 (1955). Genetic Recombination in *Pseudomonas aeruginosa*. *Microbiology* *13*, 572–581.
- Horiuchi, K. (1983). Co-evolution of a filamentous bacteriophage and its defective interfering particles. *Journal of Molecular Biology* *169*, 389–407.
- Hughes, D., and Andersson, D.I. (2017). Evolutionary Trajectories to Antibiotic Resistance. *Annu. Rev. Microbiol.* *71*, 579–596.
- Hui, J.G.K., Mai-Prochnow, A., Kjelleberg, S., McDougald, D., and Rice, S.A. (2014). Environmental cues and genes involved in establishment of the superinfective Pf4 phage of *Pseudomonas aeruginosa*. *Front. Microbiol.* *5*.

Hurley, J.C., Miller, G.H., and Smith, A.L. (1995). Mechanism of amikacin resistance in *Pseudomonas aeruginosa* isolates from patients with cystic fibrosis. *Diagn Microbiol Infect Dis* 22, 331–336.

Ibacache-Quiroga, C., Oliveros, J.C., Couce, A., and Blázquez, J. (2018). Parallel Evolution of High-Level Aminoglycoside Resistance in *Escherichia coli* Under Low and High Mutation Supply Rates. *Front Microbiol* 9.

Imamovic, L., and Sommer, M.O.A. (2013). Use of Collateral Sensitivity Networks to Design Drug Cycling Protocols That Avoid Resistance Development. *Science Translational Medicine* 5, 204ra132–204ra132.

Ismail, M.H., Michie, K.A., Goh, Y.F., Noorian, P., Kjelleberg, S., Duggin, I.G., McDougald, D., and Rice, S.A. (2021). The Repressor C Protein, Pf4r, Controls Superinfection of *Pseudomonas aeruginosa* PAO1 by the Pf4 Filamentous Phage and Regulates Host Gene Expression. *Viruses* 13, 1614.

Jahn, L.J., Munck, C., Ellabaan, M.M.H., and Sommer, M.O.A. (2017). Adaptive Laboratory Evolution of Antibiotic Resistance Using Different Selection Regimes Lead to Similar Phenotypes and Genotypes. *Front Microbiol* 8.

Jahn, L.J., Porse, A., Munck, C., Simon, D., Volkova, S., and Sommer, M.O.A. (2018). Chromosomal barcoding as a tool for multiplexed phenotypic characterization of laboratory evolved lineages. *Sci Rep* 8, 6961.

Jain, M., Ramirez, D., Seshadri, R., Cullina, J.F., Powers, C.A., Schulert, G.S., Bar-Meir, M., Sullivan, C.L., McColley, S.A., and Hauser, A.R. (2004). Type III Secretion Phenotypes of *Pseudomonas aeruginosa* Strains Change during Infection of Individuals with Cystic Fibrosis. *J Clin Microbiol* 42, 5229–5237.

James, C.E., Davies, E.V., Fothergill, J.L., Walshaw, M.J., Beale, C.M., Brockhurst, M.A., and Winstanley, C. (2015). Lytic activity by temperate phages of *Pseudomonas aeruginosa* in long-term cystic fibrosis chronic lung infections. *ISME J* 9, 1391–1398.

Jansen, G., Mahrt, N., Tueffers, L., Barbosa, C., Harjes, M., Adolph, G., Friedrichs, A., Krenz-Weinreich, A., Rosenstiel, P., and Schulenburg, H. (2016). Association between clinical antibiotic resistance and susceptibility of *Pseudomonas* in the cystic fibrosis lung. *Evol Med Public Health* 2016, 182–194.

Jenal, U., Reinders, A., and Lori, C. (2017). Cyclic di-GMP: second messenger extraordinaire. *Nature Reviews Microbiology* 15, 271–284.

Jennings, L.K., Dreifus, J.E., Reichhardt, C., Storek, K.M., Secor, P.R., Wozniak, D.J., Hisert, K.B., and Parsek, M.R. (2021). *Pseudomonas aeruginosa* aggregates in cystic fibrosis sputum produce exopolysaccharides that likely impede current therapies. *Cell Reports* 34.

Johanson, U., and Hughes, D. (1994). Fusidic acid-resistant mutants define three regions in elongation factor G of *Salmonella typhimurium*. *Gene* 143, 55–59.

- Jones, A.K., Woods, A.L., Takeoka, K.T., Shen, X., Wei, J.-R., Caughlan, R.E., and Dean, C.R. (2017). Determinants of Antibacterial Spectrum and Resistance Potential of the Elongation Factor G Inhibitor Argyrin B in Key Gram-Negative Pathogens. *Antimicrobial Agents and Chemotherapy* 61, e02400-16.
- Jorth, P., Staudinger, B.J., Wu, X., Hisert, K., Hayden, H., Garudathri, J., Harding, C., Radey, M.C., Rezayat, A., Bautista, G., et al. (2015). Regional Isolation Drives Bacterial Diversification within Cystic Fibrosis Lungs. *Cell Host Microbe* 18, 307–319.
- Jorth, P., McLean, K., Ratjen, A., Secor, P.R., Bautista, G.E., Ravishankar, S., Rezayat, A., Garudathri, J., Harrison, J.J., Harwood, R.A., et al. (2017). Evolved Aztreonam Resistance Is Multifactorial and Can Produce Hypervirulence in *Pseudomonas aeruginosa*. *MBio* 8, e00517-17.
- Kadurugamuwa, J.L., Lam, J.S., and Beveridge, T.J. (1993). Interaction of gentamicin with the A band and B band lipopolysaccharides of *Pseudomonas aeruginosa* and its possible lethal effect. *Antimicrob Agents Chemother* 37, 715–721.
- Karlowsky, J.A., Hoban, D.J., Zelenitsky, S.A., and Zhanel, G.G. (1997). Altered denA and anr gene expression in aminoglycoside adaptive resistance in *Pseudomonas aeruginosa*. *J Antimicrob Chemother* 40, 371–376.
- Kasetty, S., Katharios-Lanwermeyer, S., O’Toole, G.A., and Nadell, C.D. (2021). Differential Surface Competition and Biofilm Invasion Strategies of *Pseudomonas aeruginosa* PA14 and PAO1. *Journal of Bacteriology* 203, e00265-21.
- Katharios-Lanwermeyer, S., Whitfield, G.B., Howell, P.L., and O’Toole, G.A. (2021). *Pseudomonas aeruginosa* Uses c-di-GMP Phosphodiesterases RmcA and MorA To Regulate Biofilm Maintenance. *MBio* 12.
- Kim, S., Lieberman, T.D., and Kishony, R. (2014). Alternating antibiotic treatments constrain evolutionary paths to multidrug resistance. *Proceedings of the National Academy of Sciences* 111, 14494–14499.
- Klockgether, J., Cramer, N., Fischer, S., Wiehlmann, L., and Tümmler, B. (2018). Long-Term Microevolution of *Pseudomonas aeruginosa* Differs between Mildly and Severely Affected Cystic Fibrosis Lungs. *Am J Respir Cell Mol Biol* 59, 246–256.
- Knopp, M., and Andersson, D.I. (2018). Predictable Phenotypes of Antibiotic Resistance Mutations. *MBio* 9, e00770-18.
- Kohanski, M.A., Dwyer, D.J., and Collins, J.J. (2010). How antibiotics kill bacteria: from targets to networks. *Nat Rev Microbiol* 8, 423–435.
- Koskella, B., and Brockhurst, M.A. (2014). Bacteria–phage coevolution as a driver of ecological and evolutionary processes in microbial communities. *FEMS Microbiology Reviews* 38, 916–931.

- Kosorok, M.R., Zeng, L., West, S.E., Rock, M.J., Splaingard, M.L., Laxova, A., Green, C.G., Collins, J., and Farrell, P.M. (2001). Acceleration of lung disease in children with cystic fibrosis after *Pseudomonas aeruginosa* acquisition. *Pediatr Pulmonol* 32, 277–287.
- Kostylev, M., Kim, D.Y., Smalley, N.E., Salukhe, I., Greenberg, E.P., and Dandekar, A.A. (2019). Evolution of the *Pseudomonas aeruginosa* quorum-sensing hierarchy. *PNAS* 116, 7027–7032.
- Krause, K.M., Serio, A.W., Kane, T.R., and Connolly, L.E. (2016). Aminoglycosides: An Overview. *Cold Spring Harb Perspect Med* 6.
- Kryazhimskiy, S., Rice, D.P., Jerison, E.R., and Desai, M.M. (2014). Global epistasis makes adaptation predictable despite sequence-level stochasticity. *Science* 344, 1519–1522.
- Kulesekara, H., Lee, V., Brencic, A., Liberati, N., Urbach, J., Miyata, S., Lee, D.G., Neely, A.N., Hyodo, M., Hayakawa, Y., et al. (2006). Analysis of *Pseudomonas aeruginosa* diguanylate cyclases and phosphodiesterases reveals a role for bis-(3'-5')-cyclic-GMP in virulence. *PNAS* 103, 2839–2844.
- La Rosa, R., Johansen, H.K., and Molin, S. (2018). Convergent Metabolic Specialization through Distinct Evolutionary Paths in *Pseudomonas aeruginosa*. *MBio* 9.
- Lang, G.I., Rice, D.P., Hickman, M.J., Sodergren, E., Weinstock, G.M., Botstein, D., and Desai, M.M. (2013). Pervasive Genetic Hitchhiking and Clonal Interference in 40 Evolving Yeast Populations. *Nature* 500, 571–574.
- Lässig, M., Mustonen, V., and Walczak, A.M. (2017). Predicting evolution. *Nature Ecology & Evolution* 1, 0077.
- Lee, C.K., Vachier, J., Anda, J. de, Zhao, K., Baker, A.E., Bennett, R.R., Armbruster, C.R., Lewis, K.A., Tarnopol, R.L., Lomba, C.J., et al. (2020). Social Cooperativity of Bacteria during Reversible Surface Attachment in Young Biofilms: a Quantitative Comparison of *Pseudomonas aeruginosa* PA14 and PAO1. *MBio* 11.
- Lee, D.G., Urbach, J.M., Wu, G., Liberati, N.T., Feinbaum, R.L., Miyata, S., Diggins, L.T., He, J., Saucier, M., Déziel, E., et al. (2006). Genomic analysis reveals that *Pseudomonas aeruginosa* virulence is combinatorial. *Genome Biol* 7, R90.
- Lee, Y., Song, S., Sheng, L., Zhu, L., Kim, J.-S., and Wood, T.K. (2018). Substrate Binding Protein DppA1 of ABC Transporter DppBCDF Increases Biofilm Formation in *Pseudomonas aeruginosa* by Inhibiting Pf5 Prophage Lysis. *Front. Microbiol.* 9.
- Lenski, R.E. (2017). Experimental evolution and the dynamics of adaptation and genome evolution in microbial populations. *ISME J* 11, 2181–2194.
- Lenski, R.E., Rose, M.R., Simpson, S.C., and Tadler, S.C. (1991). Long-Term Experimental Evolution in *Escherichia coli*. I. Adaptation and Divergence During 2,000 Generations. *The American Naturalist* 138, 1315–1341.

- Letarov, A., and Kulikov, E. (2009). The bacteriophages in human- and animal body-associated microbial communities. *Journal of Applied Microbiology* *107*, 1–13.
- Li, C., Wally, H., Miller, S.J., and Lu, C.-D. (2009a). The Multifaceted Proteins MvaT and MvaU, Members of the H-NS Family, Control Arginine Metabolism, Pyocyanin Synthesis, and Prophage Activation in *Pseudomonas aeruginosa* PAO1. *J Bacteriol* *191*, 6211–6218.
- Li, H., Handsaker, B., Wysoker, A., Fennell, T., Ruan, J., Homer, N., Marth, G., Abecasis, G., and Durbin, R. (2009b). The Sequence Alignment/Map format and SAMtools. *Bioinformatics* *25*, 2078–2079.
- Li, Y., Liu, X., Tang, K., Wang, P., Zeng, Z., Guo, Y., and Wang, X. (2019). Excisionase in Pf filamentous prophage controls lysis-lysogeny decision-making in *Pseudomonas aeruginosa*. *Molecular Microbiology* *111*, 495–513.
- Lieberman, T.D., Flett, K.B., Yelin, I., Martin, T.R., McAdam, A.J., Priebe, G.P., and Kishony, R. (2014). Genetic variation of a bacterial pathogen within individuals with cystic fibrosis provides a record of selective pressures. *Nature Genetics* *46*, 82–87.
- LiPuma, J.J. (2010). The Changing Microbial Epidemiology in Cystic Fibrosis. *Clinical Microbiology Reviews* *23*, 299–323.
- Long, H., Sung, W., Miller, S.F., Ackerman, M.S., Doak, T.G., and Lynch, M. (2014). Mutation Rate, Spectrum, Topology, and Context-Dependency in the DNA Mismatch Repair-Deficient *Pseudomonas fluorescens* ATCC948. *Genome Biol Evol* *7*, 262–271.
- López-Causapé, C., Sommer, L.M., Cabot, G., Rubio, R., Ocampo-Sosa, A.A., Johansen, H.K., Figuerola, J., Cantón, R., Kidd, T.J., Molin, S., et al. (2017). Evolution of the *Pseudomonas aeruginosa* mutational resistome in an international Cystic Fibrosis clone. *Sci Rep* *7*.
- López-Causapé, C., Rubio, R., Cabot, G., and Oliver, A. (2018). Evolution of the *Pseudomonas aeruginosa* Aminoglycoside Mutational Resistome In Vitro and in the Cystic Fibrosis Setting. *Antimicrob. Agents Chemother.* *62*, e02583-17.
- Lukačičinová, M., Fernando, B., and Bollenbach, T. (2020). Highly parallel lab evolution reveals that epistasis can curb the evolution of antibiotic resistance. *Nature Communications* *11*, 3105.
- Luo, Y., Zhao, K., Baker, A.E., Kuchma, S.L., Coggan, K.A., Wolfgang, M.C., Wong, G.C.L., and O’Toole, G.A. (2015). A Hierarchical Cascade of Second Messengers Regulates *Pseudomonas aeruginosa* Surface Behaviors. *MBio* *6*, e02456-14.
- Lythgoe, K.A., and Chao, L. (2003). Mechanisms of coexistence of a bacteria and a bacteriophage in a spatially homogeneous environment. *Ecology Letters* *6*, 326–334.
- Ma, L., Conover, M., Lu, H., Parsek, M.R., Bayles, K., and Wozniak, D.J. (2009). Assembly and Development of the *Pseudomonas aeruginosa* Biofilm Matrix. *PLoS Pathog* *5*, e1000354.

- MacLean, R.C., and Buckling, A. (2009). The Distribution of Fitness Effects of Beneficial Mutations in *Pseudomonas aeruginosa*. *PLoS Genetics* 5, e1000406.
- MacLean, R.C., and San Millan, A. (2019). The evolution of antibiotic resistance. *Science* 365, 1082–1083.
- MacLean, R.C., Perron, G.G., and Gardner, A. (2010). Diminishing Returns From Beneficial Mutations and Pervasive Epistasis Shape the Fitness Landscape for Rifampicin Resistance in *Pseudomonas aeruginosa*. *Genetics* 186, 1345–1354.
- MacLeod, D.L., Nelson, L.E., Shawar, R.M., Lin, B.B., Lockwood, L.G., Dirk, J.E., Miller, G.H., Burns, J.L., and Garber, R.L. (2000). Aminoglycoside-resistance mechanisms for cystic fibrosis *Pseudomonas aeruginosa* isolates are unchanged by long-term, intermittent, inhaled tobramycin treatment. *J Infect Dis* 181, 1180–1184.
- Mah, T.-F.C., and O’Toole, G.A. (2001). Mechanisms of biofilm resistance to antimicrobial agents. *Trends in Microbiology* 9, 34–39.
- Mahenthiralingam, E., Campbell, M.E., and Speert, D.P. (1994). Nonmotility and phagocytic resistance of *Pseudomonas aeruginosa* isolates from chronically colonized patients with cystic fibrosis. *Infect Immun* 62, 596–605.
- Mai-Prochnow, A., Hui, J.G.K., Kjelleberg, S., Rakonjac, J., McDougald, D., and Rice, S.A. (2015). ‘Big things in small packages: the genetics of filamentous phage and effects on fitness of their host.’ *FEMS Microbiol Rev* 39, 465–487.
- Malhotra, S., Hayes, D., and Wozniak, D.J. (2019). Cystic Fibrosis and *Pseudomonas aeruginosa*: the Host-Microbe Interface. *Clinical Microbiology Reviews* 32, e00138-18.
- Malone, J.G. (2015). Role of small colony variants in persistence of *Pseudomonas aeruginosa* infections in cystic fibrosis lungs. *Infect Drug Resist* 8, 237–247.
- Markussen, T., Marvig, R.L., Gómez-Lozano, M., Aanæs, K., Burleigh, A.E., Høiby, N., Johansen, H.K., Molin, S., and Jelsbak, L. (2014). Environmental Heterogeneity Drives Within-Host Diversification and Evolution of *Pseudomonas aeruginosa*. *MBio* 5, e01592-14.
- Marshall, C.W., Gloag, E.S., Lim, C., Wozniak, D.J., and Cooper, V.S. (2021). Rampant prophage movement among transient competitors drives rapid adaptation during infection. *Science Advances* 7, eabh1489.
- Martínez, E., and Campos-Gómez, J. (2016). Pf Filamentous Phage Requires UvrD for Replication in *Pseudomonas aeruginosa*. *MSphere* 1, e00104-15.
- Marvig, R.L., Johansen, H.K., Molin, S., and Jelsbak, L. (2013). Genome Analysis of a Transmissible Lineage of *Pseudomonas aeruginosa* Reveals Pathoadaptive Mutations and Distinct Evolutionary Paths of Hypermutators. *PLOS Genetics* 9, e1003741.

- Marvig, R.L., Sommer, L.M., Molin, S., and Johansen, H.K. (2015). Convergent evolution and adaptation of *Pseudomonas aeruginosa* within patients with cystic fibrosis. *Nat Genet* 47, 57–64.
- Maselli, D.J., Keyt, H., and Restrepo, M.I. (2017). Inhaled Antibiotic Therapy in Chronic Respiratory Diseases. *International Journal of Molecular Sciences* 18, 1062.
- Mathee, K., Narasimhan, G., Valdes, C., Qiu, X., Matewish, J.M., Koehrsen, M., Rokas, A., Yandava, C.N., Engels, R., Zeng, E., et al. (2008). Dynamics of *Pseudomonas aeruginosa* genome evolution. *Proc Natl Acad Sci U S A* 105, 3100–3105.
- McCall, I.C., Shah, N., Govindan, A., Baquero, F., and Levin, B.R. (2019). Antibiotic Killing of Diversely Generated Populations of Nonreplicating Bacteria. *Antimicrobial Agents and Chemotherapy* 63, e02360-18.
- McDonald, M.J. (2019). Microbial Experimental Evolution – a proving ground for evolutionary theory and a tool for discovery. *EMBO Rep* 20, e46992.
- McDonald, M.J., Gehrig, S.M., Meintjes, P.L., Zhang, X.-X., and Rainey, P.B. (2009). Adaptive Divergence in Experimental Populations of *Pseudomonas fluorescens*. IV. Genetic Constraints Guide Evolutionary Trajectories in a Parallel Adaptive Radiation. *Genetics* 183, 1041–1053.
- McElroy, K.E., Hui, J.G.K., Woo, J.K.K., Luk, A.W.S., Webb, J.S., Kjelleberg, S., Rice, S.A., and Thomas, T. (2014). Strain-specific parallel evolution drives short-term diversification during *Pseudomonas aeruginosa* biofilm formation. *PNAS* 111, E1419–E1427.
- Meir, M., Harel, N., Miller, D., Gelbart, M., Eldar, A., Gophna, U., and Stern, A. (2020). Competition between social cheater viruses is driven by mechanistically different cheating strategies. *Science Advances* 6, eabb7990.
- Melnyk, A.H., Wong, A., and Kassen, R. (2015). The fitness costs of antibiotic resistance mutations. *Evol Appl* 8, 273–283.
- Melnyk, A.H., McCloskey, N., Hinz, A.J., Dettman, J., and Kassen, R. (2017). Evolution of Cost-Free Resistance under Fluctuating Drug Selection in *Pseudomonas aeruginosa*. *MSphere* 2, e00158-17.
- Mena, A., Smith, E.E., Burns, J.L., Speert, D.P., Moskowitz, S.M., Perez, J.L., and Oliver, A. (2008). Genetic Adaptation of *Pseudomonas aeruginosa* to the Airways of Cystic Fibrosis Patients Is Catalyzed by Hypermutation. *Journal of Bacteriology* 190, 7910–7917.
- Mhatre, E., Snyder, D.J., Sileo, E., Turner, C.B., Buskirk, S.W., Fernandez, N.L., Neiditch, M.B., Waters, C.M., and Cooper, V.S. (2020). One gene, multiple ecological strategies: A biofilm regulator is a capacitor for sustainable diversity. *PNAS* 117, 21647–21657.
- Mistry, J., Chuguransky, S., Williams, L., Qureshi, M., Salazar, G.A., Sonnhammer, E.L.L., Tosatto, S.C.E., Paladin, L., Raj, S., Richardson, L.J., et al. (2021). Pfam: The protein families database in 2021. *Nucleic Acids Research* 49, D412–D419.

- Modi, S.R., Lee, H.H., Spina, C.S., and Collins, J.J. (2013). Antibiotic treatment expands the resistance reservoir and ecological network of the phage metagenome. *Nature* 499, 219–222.
- Mogre, A., Sengupta, T., Veetil, R.T., Ravi, P., and Seshasayee, A.S.N. (2014). Genomic Analysis Reveals Distinct Concentration-Dependent Evolutionary Trajectories for Antibiotic Resistance in *Escherichia coli*. *DNA Res* 21, 711–726.
- Mooij, M.J., Drenkard, E., Llamas, M.A., Vandenbroucke-Grauls, C.M.J.E., Savelkoul, P.H.M., Ausubel, F.M., and Bitter, W. (2007). Characterization of the integrated filamentous phage Pf5 and its involvement in small-colony formation. *Microbiology* 153, 1790–1798.
- Moradali, M.F., Ghods, S., and Rehm, B.H.A. (2017). *Pseudomonas aeruginosa* Lifestyle: A Paradigm for Adaptation, Survival, and Persistence. *Front Cell Infect Microbiol* 7.
- Moskowitz, S.M., Brannon, M.K., Dasgupta, N., Pier, M., Sgambati, N., Miller, A.K., Selgrade, S.E., Miller, S.I., Denton, M., Conway, S.P., et al. (2012). PmrB Mutations Promote Polymyxin Resistance of *Pseudomonas aeruginosa* Isolated from Colistin-Treated Cystic Fibrosis Patients. *Antimicrob. Agents Chemother.* 56, 1019–1030.
- Mould, D.L., Botelho, N.J., and Hogan, D.A. (2020). Intraspecies Signaling between Common Variants of *Pseudomonas aeruginosa* Increases Production of Quorum-Sensing-Controlled Virulence Factors. *MBio* 11.
- Moyá, B., Beceiro, A., Cabot, G., Juan, C., Zamorano, L., Alberti, S., and Oliver, A. (2012). Pan- $\beta$ -Lactam Resistance Development in *Pseudomonas aeruginosa* Clinical Strains: Molecular Mechanisms, Penicillin-Binding Protein Profiles, and Binding Affinities. *Antimicrobial Agents and Chemotherapy* 56, 4771–4778.
- Muhlebach, M.S., Zorn, B.T., Esther, C.R., Hatch, J.E., Murray, C.P., Turkovic, L., Ranganathan, S.C., Boucher, R.C., Stick, S.M., and Wolfgang, M.C. (2018). Initial acquisition and succession of the cystic fibrosis lung microbiome is associated with disease progression in infants and preschool children. *PLoS Pathog* 14, e1006798.
- Mukherjee, S., Moustafa, D.A., Stergioula, V., Smith, C.D., Goldberg, J.B., and Bassler, B.L. (2018). The PqsE and RhIR proteins are an autoinducer synthase–receptor pair that control virulence and biofilm development in *Pseudomonas aeruginosa*. *PNAS* 115, E9411–E9418.
- Mulcahy, L.R., Isabella, V.M., and Lewis, K. (2014). *Pseudomonas aeruginosa* biofilms in disease. *Microb Ecol* 68, 1–12.
- Nguyen, A.T., O'Neill, M.J., Watts, A.M., Robson, C.L., Lamont, I.L., Wilks, A., and Oglesby-Sherrouse, A.G. (2014). Adaptation of Iron Homeostasis Pathways by a *Pseudomonas aeruginosa* Pyoverdine Mutant in the Cystic Fibrosis Lung. *J Bacteriol* 196, 2265–2276.
- Nixon, G.M., Armstrong, D.S., Carzino, R., Carlin, J.B., Olinsky, A., Robertson, C.F., and Grimwood, K. (2001). Clinical outcome after early *Pseudomonas aeruginosa* infection in cystic fibrosis. *The Journal of Pediatrics* 138, 699–704.

- Norström, T., Lannergård, J., and Hughes, D. (2007). Genetic and Phenotypic Identification of Fusidic Acid-Resistant Mutants with the Small-Colony-Variant Phenotype in *Staphylococcus aureus*. *Antimicrob Agents Chemother* 51, 4438–4446.
- Nyfelner, B., Hoepfner, D., Palestrant, D., Kirby, C.A., Whitehead, L., Yu, R., Deng, G., Caughlan, R.E., Woods, A.L., Jones, A.K., et al. (2012). Identification of Elongation Factor G as the Conserved Cellular Target of Argyrin B. *PLOS ONE* 7, e42657.
- O'Connor, J.R., Kuwada, N.J., Huangyutitham, V., Wiggins, P.A., and Harwood, C.S. (2012). Surface sensing and lateral subcellular localization of WspA, the receptor in a chemosensory-like system leading to c-di-GMP production. *Molecular Microbiology* 86, 720–729.
- Oliver, A., Cantón, R., Campo, P., Baquero, F., and Blázquez, J. (2000). High frequency of hypermutable *Pseudomonas aeruginosa* in cystic fibrosis lung infection. *Science* 288, 1251–1254.
- O'Toole, G.A. (2011). Microtiter Dish Biofilm Formation Assay. *J Vis Exp*.
- O'Toole, G.A., and Kolter, R. (1998). Flagellar and twitching motility are necessary for *Pseudomonas aeruginosa* biofilm development. *Molecular Microbiology* 30, 295–304.
- Ozer, E.A., Nnah, E., Didelot, X., Whitaker, R.J., and Hauser, A.R. (2019). The Population Structure of *Pseudomonas aeruginosa* Is Characterized by Genetic Isolation of *exoU*<sup>+</sup> and *exoS*<sup>+</sup> Lineages. *Genome Biology and Evolution* 11, 1780–1796.
- Palmer, A.C., and Kishony, R. (2013). Understanding, predicting and manipulating the genotypic evolution of antibiotic resistance. *Nat Rev Genet* 14, 243–248.
- Palmer, K.L., Mashburn, L.M., Singh, P.K., and Whiteley, M. (2005). Cystic Fibrosis Sputum Supports Growth and Cues Key Aspects of *Pseudomonas aeruginosa* Physiology. *J Bacteriol* 187, 5267–5277.
- Palmer, K.L., Aye, L.M., and Whiteley, M. (2007). Nutritional Cues Control *Pseudomonas aeruginosa* Multicellular Behavior in Cystic Fibrosis Sputum. *J. Bacteriol.* 189, 8079–8087.
- Palmer, S.O., Rangel, E.Y., Hu, Y., Tran, A.T., and Bullard, J.M. (2013). Two Homologous EF-G Proteins from *Pseudomonas aeruginosa* Exhibit Distinct Functions. *PLOS ONE* 8, e80252.
- Pang, Z., Raudonis, R., Glick, B.R., Lin, T.-J., and Cheng, Z. (2019). Antibiotic resistance in *Pseudomonas aeruginosa*: mechanisms and alternative therapeutic strategies. *Biotechnology Advances* 37, 177–192.
- Papenfort, K., and Bassler, B.L. (2016). Quorum sensing signal-response systems in Gram-negative bacteria. *Nat Rev Microbiol* 14, 576–588.
- Papp, B., Notebaart, R.A., and Pál, C. (2011). Systems-biology approaches for predicting genomic evolution. *Nature Reviews Genetics* 12, 591–602.

- Passador, L., Cook, J.M., Gambello, M.J., Rust, L., and Iglewski, B.H. (1993). Expression of *Pseudomonas aeruginosa* virulence genes requires cell-to-cell communication. *Science* *260*, 1127–1130.
- Pearson, J.P., Passador, L., Iglewski, B.H., and Greenberg, E.P. (1995). A second N-acylhomoserine lactone signal produced by *Pseudomonas aeruginosa*. *PNAS* *92*, 1490–1494.
- Pearson, J.P., Pesci, E.C., and Iglewski, B.H. (1997). Roles of *Pseudomonas aeruginosa* las and rhl quorum-sensing systems in control of elastase and rhamnolipid biosynthesis genes. *Journal of Bacteriology* *179*, 5756–5767.
- Pesci, E.C., Pearson, J.P., Seed, P.C., and Iglewski, B.H. (1997). Regulation of las and rhl quorum sensing in *Pseudomonas aeruginosa*. *J Bacteriol* *179*, 3127–3132.
- Pesci, E.C., Milbank, J.B.J., Pearson, J.P., McKnight, S., Kende, A.S., Greenberg, E.P., and Iglewski, B.H. (1999). Quinolone signaling in the cell-to-cell communication system of *Pseudomonas aeruginosa*. *PNAS* *96*, 11229–11234.
- Pessi, G., and Haas, D. (2000). Transcriptional Control of the Hydrogen Cyanide Biosynthetic Genes hcnABC by the Anaerobic Regulator ANR and the Quorum-Sensing Regulators LasR and RhlR in *Pseudomonas aeruginosa*. *Journal of Bacteriology* *182*, 6940–6949.
- Pesttrak, M.J., Chaney, S.B., Eggleston, H.C., Dellos-Nolan, S., Dixit, S., Mathew-Steiner, S.S., Roy, S., Parsek, M.R., Sen, C.K., and Wozniak, D.J. (2018). *Pseudomonas aeruginosa* rugose small-colony variants evade host clearance, are hyper-inflammatory, and persist in multiple host environments. *PLOS Pathogens* *14*, e1006842.
- Peterson, A.A., Hancock, R.E., and McGroarty, E.J. (1985). Binding of polycationic antibiotics and polyamines to lipopolysaccharides of *Pseudomonas aeruginosa*.
- Pettersen, E.F., Goddard, T.D., Huang, C.C., Couch, G.S., Greenblatt, D.M., Meng, E.C., and Ferrin, T.E. (2004). UCSF Chimera--a visualization system for exploratory research and analysis. *J Comput Chem* *25*, 1605–1612.
- Phippen, C.W., Mikolajek, H., Schlaefli, H.G., Keevil, C.W., Webb, J.S., and Tews, I. (2014). Formation and dimerization of the phosphodiesterase active site of the *Pseudomonas aeruginosa* MorA, a bi-functional c-di-GMP regulator. *FEBS Letters* *588*, 4631–4636.
- Piechaud, M., and Second, L. (1951). [Studies of 26 strains of *Moraxella Iwoffii*]. *Ann Inst Pasteur (Paris)* *80*, 97–99.
- Platt, M.D., Schurr, M.J., Sauer, K., Vazquez, G., Kukavica-Ibrulj, I., Potvin, E., Levesque, R.C., Fedynak, A., Brinkman, F.S.L., Schurr, J., et al. (2008). Proteomic, Microarray, and Signature-Tagged Mutagenesis Analyses of Anaerobic *Pseudomonas aeruginosa* at pH 6.5, Likely Representing Chronic, Late-Stage Cystic Fibrosis Airway Conditions. *J Bacteriol* *190*, 2739–2758.
- Poltak, S.R., and Cooper, V.S. (2011). Ecological succession in long-term experimentally evolved biofilms produces synergistic communities. *ISME J* *5*, 369–378.

- Poole, K. (2005). Aminoglycoside Resistance in *Pseudomonas aeruginosa*. *Antimicrobial Agents and Chemotherapy* 49, 479–487.
- Popat, R., Crusz, S.A., Messina, M., Williams, P., West, S.A., and Diggle, S.P. (2012). Quorum-sensing and cheating in bacterial biofilms. *Proc Biol Sci* 279, 4765–4771.
- Poulsen, B.E., Yang, R., Clatworthy, A.E., White, T., Osmulski, S.J., Li, L., Penaranda, C., Lander, E.S., Shoresh, N., and Hung, D.T. (2019). Defining the core essential genome of *Pseudomonas aeruginosa*. *PNAS* 116, 10072–10080.
- Prickett, M.H., Hauser, A.R., McColley, S.A., Cullina, J., Potter, E., Powers, C., and Jain, M. (2017). Aminoglycoside resistance of *Pseudomonas aeruginosa* in cystic fibrosis results from convergent evolution in the *mexZ* gene. *Thorax* 72, 40–47.
- Qi, Q., Preston, G.M., and MacLean, R.C. (2014). Linking System-Wide Impacts of RNA Polymerase Mutations to the Fitness Cost of Rifampin Resistance in *Pseudomonas aeruginosa*. *MBio* 5.
- R Core Team (2021). R: A language and environment for statistical computing.
- Rahme, L.G., Stevens, E.J., Wolfort, S.F., Shao, J., Tompkins, R.G., and Ausubel, F.M. (1995). Common virulence factors for bacterial pathogenicity in plants and animals. *Science* 268, 1899–1902.
- Rainey, P.B., and Travisano, M. (1998). Adaptive radiation in a heterogeneous environment. *Nature* 394, 69–72.
- Ramsey, B.W., Pepe, M.S., Quan, J.M., Otto, K.L., Montgomery, A.B., Williams-Warren, J., Vasiljev-K, M., Borowitz, D., Bowman, C.M., Marshall, B.C., et al. (1999). Intermittent Administration of Inhaled Tobramycin in Patients with Cystic Fibrosis. *New England Journal of Medicine* 340, 23–30.
- Reichhardt, C., Jacobs, H.M., Matwichuk, M., Wong, C., Wozniak, D.J., and Parsek, M.R. (2020). The Versatile *Pseudomonas aeruginosa* Biofilm Matrix Protein CdrA Promotes Aggregation through Different Extracellular Exopolysaccharide Interactions. *J Bacteriol* 202, e00216-20.
- Rice, S.A., Tan, C.H., Mikkelsen, P.J., Kung, V., Woo, J., Tay, M., Hauser, A., McDougald, D., Webb, J.S., and Kjelleberg, S. (2009). The biofilm life cycle and virulence of *Pseudomonas aeruginosa* are dependent on a filamentous prophage. *ISME J* 3, 271–282.
- Riechmann, L., and Holliger, P. (1997). The C-terminal domain of TolA is the coreceptor for filamentous phage infection of *E. coli*. *Cell* 90, 351–360.
- Rocchetta, H.L., Burrows, L.L., and Lam, J.S. (1999). Genetics of O-Antigen Biosynthesis in *Pseudomonas aeruginosa*. *Microbiol. Mol. Biol. Rev.* 63, 523–553.
- Rohmer, L., Hocquet, D., and Miller, S.I. (2011). Are pathogenic bacteria just looking for food? Metabolism and microbial pathogenesis. *Trends in Microbiology* 19, 341–348.

- Rossi, E., La Rosa, R., Bartell, J.A., Marvig, R.L., Haagensen, J.A.J., Sommer, L.M., Molin, S., and Johansen, H.K. (2020). *Pseudomonas aeruginosa* adaptation and evolution in patients with cystic fibrosis. *Nature Reviews Microbiology* 1–12.
- Roux, S., Krupovic, M., Daly, R.A., Borges, A.L., Nayfach, S., Schulz, F., Sharrar, A., Matheus Carnevali, P.B., Cheng, J.-F., Ivanova, N.N., et al. (2019). Cryptic inoviruses revealed as pervasive in bacteria and archaea across Earth's biomes. *Nat Microbiol* 4, 1895–1906.
- Rust, L., Pesci, E.C., and Iglewski, B.H. (1996). Analysis of the *Pseudomonas aeruginosa* elastase (lasB) regulatory region. *J Bacteriol* 178, 1134–1140.
- Ryder, C., Byrd, M., and Wozniak, D.J. (2007). Role of polysaccharides in *Pseudomonas aeruginosa* biofilm development. *Current Opinion in Microbiology* 10, 644–648.
- Saiman, L., Mehar, F., Niu, W.W., Neu, H.C., Shaw, K.J., Miller, G., and Prince, A. (1996). Antibiotic susceptibility of multiply resistant *Pseudomonas aeruginosa* isolated from patients with cystic fibrosis, including candidates for transplantation. *Clin Infect Dis* 23, 532–537.
- Salunkhe, P., Smart, C.H.M., Morgan, J.A.W., Panagea, S., Walshaw, M.J., Hart, C.A., Geffers, R., Tümmler, B., and Winstanley, C. (2005). A Cystic Fibrosis Epidemic Strain of *Pseudomonas aeruginosa* Displays Enhanced Virulence and Antimicrobial Resistance. *Journal of Bacteriology* 187, 4908–4920.
- Sandoz, K.M., Mitzimberg, S.M., and Schuster, M. (2007). Social cheating in *Pseudomonas aeruginosa* quorum sensing. *Proceedings of the National Academy of Sciences* 104, 15876–15881.
- Santajit, S., and Indrawattana, N. (2016). Mechanisms of Antimicrobial Resistance in ESKAPE Pathogens. *Biomed Res Int* 2016.
- Santos-Lopez, A., Marshall, C.W., Scribner, M.R., Snyder, D.J., and Cooper, V.S. (2019). Evolutionary pathways to antibiotic resistance are dependent upon environmental structure and bacterial lifestyle. *ELife* 8, e47612.
- Santos-Lopez, A., Marshall, C.W., Haas, A.L., Turner, C., Rasero, J., and Cooper, V.S. (2021). The roles of history, chance, and natural selection in the evolution of antibiotic resistance. *ELife* 10, e70676.
- Sanz-García, F., Hernando-Amado, S., and Martínez, J.L. (2018). Mutational Evolution of *Pseudomonas aeruginosa* Resistance to Ribosome-Targeting Antibiotics. *Front Genet* 9.
- Savelsbergh, A., Rodnina, M.V., and Wintermeyer, W. (2009). Distinct functions of elongation factor G in ribosome recycling and translocation. *RNA* 15, 772–780.
- Schick, A., and Kassen, R. (2018). Rapid diversification of *Pseudomonas aeruginosa* in cystic fibrosis lung-like conditions. *PNAS* 115, 10714–10719.
- Schick, A., and Kassen, R. (2020). Genomics of experimental diversification of *Pseudomonas aeruginosa* in cystic fibrosis lung-like conditions. *BioRxiv* 2020.04.14.041954.

- Schroth, M.N., Cho, J.J., Green, S.K., Kominos, S.D., and Microbiology Society Publishing, null (2018). Epidemiology of *Pseudomonas aeruginosa* in agricultural areas. *J Med Microbiol* 67, 1191–1201.
- Schurek, K.N., Marr, A.K., Taylor, P.K., Wiegand, I., Semene, L., Khaira, B.K., and Hancock, R.E.W. (2008). Novel Genetic Determinants of Low-Level Aminoglycoside Resistance in *Pseudomonas aeruginosa*. *Antimicrob Agents Chemother* 52, 4213–4219.
- Schuster, M., Lostroh, C.P., Ogi, T., and Greenberg, E.P. (2003). Identification, Timing, and Signal Specificity of *Pseudomonas aeruginosa* Quorum-Controlled Genes: a Transcriptome Analysis. *Journal of Bacteriology* 185, 2066–2079.
- Schuster, M., Sexton, D.J., Diggle, S.P., and Greenberg, E.P. (2013). Acyl-homoserine lactone quorum sensing: from evolution to application. *Annu Rev Microbiol* 67, 43–63.
- Scribner, M.R., Santos-Lopez, A., Marshall, C.W., Deitrick, C., and Cooper, V.S. (2020). Parallel Evolution of Tobramycin Resistance across Species and Environments. *MBio* 11, e00932-20.
- Scribner, M.R., Stephens, A.C., Huong, J.L., Richardson, A.R., and Cooper, V.S. (2021). The nutritional environment is sufficient to select coexisting biofilm and quorum-sensing mutants of *Pseudomonas aeruginosa*.
- Secor, P.R., Sweere, J.M., Michaels, L.A., Malkovskiy, A.V., Lazzareschi, D., Katznelson, E., Rajadas, J., Birnbaum, M.E., Arrigoni, A., Braun, K.R., et al. (2015). Filamentous Bacteriophage Promote Biofilm Assembly and Function. *Cell Host & Microbe* 18, 549–559.
- Secor, P.R., Michaels, L.A., Smigiel, K.S., Rohani, M.G., Jennings, L.K., Hisert, K.B., Arrigoni, A., Braun, K.R., Birkland, T.P., Lai, Y., et al. (2016). Filamentous Bacteriophage Produced by *Pseudomonas aeruginosa* Alters the Inflammatory Response and Promotes Noninvasive Infection In Vivo. *Infect Immun* 85.
- Secor, P.R., Burgener, E.B., Kinnersley, M., Jennings, L.K., Roman-Cruz, V., Popescu, M., Van Belleghem, J.D., Haddock, N., Copeland, C., Michaels, L.A., et al. (2020). Pf Bacteriophage and Their Impact on *Pseudomonas* Virulence, Mammalian Immunity, and Chronic Infections. *Front. Immunol.* 11.
- Shapiro, J.W., Williams, E.S.C.P., and Turner, P.E. (2016). Evolution of parasitism and mutualism between filamentous phage M13 and *Escherichia coli*. *PeerJ* 4, e2060.
- Sherrard, L.J., Tunney, M.M., and Elborn, J.S. (2014). Antimicrobial resistance in the respiratory microbiota of people with cystic fibrosis. *Lancet* 384, 703–713.
- Slowikowski, K., Schep, A., Hughes, S., Dang, T.K., Lukauskas, S., Irisson, J.-O., Kamvar, Z.N., Ryan, T., Christophe, D., Hiroaki, Y., et al. (2021). ggrepel: Automatically Position Non-Overlapping Text Labels with “ggplot2.”
- Smith, P., and Schuster, M. (2019). Public goods and cheating in microbes. *Current Biology* 29, R442–R447.

- Smith, E.E., Buckley, D.G., Wu, Z., Saenphimmachak, C., Hoffman, L.R., D'Argenio, D.A., Miller, S.I., Ramsey, B.W., Speert, D.P., Moskowitz, S.M., et al. (2006). Genetic adaptation by *Pseudomonas aeruginosa* to the airways of cystic fibrosis patients. *PNAS* *103*, 8487–8492.
- Sniegowski, P.D., Gerrish, P.J., and Lenski, R.E. (1997). Evolution of high mutation rates in experimental populations of *E. coli*. *Nature* *387*, 703–705.
- Sprouffske, K., and Wagner, A. (2016). Growthcurver: an R package for obtaining interpretable metrics from microbial growth curves. *BMC Bioinformatics* *17*, 172.
- Starkey, M., Hickman, J.H., Ma, L., Zhang, N., De Long, S., Hinz, A., Palacios, S., Manoil, C., Kirisits, M.J., Starner, T.D., et al. (2009). *Pseudomonas aeruginosa* rugose small-colony variants have adaptations that likely promote persistence in the cystic fibrosis lung. *J Bacteriol* *191*, 3492–3503.
- Steenackers, H.P., Parijs, I., Foster, K.R., and Vanderleyden, J. (2016). Experimental evolution in biofilm populations. *FEMS Microbiology Reviews* *40*, 373–397.
- Stover, C.K., Pham, X.Q., Erwin, A.L., Mizoguchi, S.D., Warrenner, P., Hickey, M.J., Brinkman, F.S.L., Hufnagle, W.O., Kowalik, D.J., Lagrou, M., et al. (2000). Complete genome sequence of *Pseudomonas aeruginosa* PAO1, an opportunistic pathogen. *Nature* *406*, 959–964.
- Suttle, C.A. (2007). Marine viruses--major players in the global ecosystem. *Nat Rev Microbiol* *5*, 801–812.
- Takeya, K., and Amako, K. (1966). A rod-shaped *Pseudomonas* phage. *Virology* *28*, 163–165.
- Tamma, P.D., Fan, Y., Bergman, Y., Perteza, G., Kazmi, A.Q., Lewis, S., Carroll, K.C., Schatz, M.C., Timp, W., and Simner, P.J. (2019). Applying Rapid Whole-Genome Sequencing To Predict Phenotypic Antimicrobial Susceptibility Testing Results among Carbapenem-Resistant *Klebsiella pneumoniae* Clinical Isolates. *Antimicrobial Agents and Chemotherapy* *63*, e01923-18.
- Tognon, M., Köhler, T., Gdaniec, B.G., Hao, Y., Lam, J.S., Beaume, M., Luscher, A., Buckling, A., and van Delden, C. (2017). Co-evolution with *Staphylococcus aureus* leads to lipopolysaccharide alterations in *Pseudomonas aeruginosa*. *ISME J* *11*, 2233–2243.
- Touchon, M., Bernheim, A., and Rocha, E.P. (2016). Genetic and life-history traits associated with the distribution of prophages in bacteria. *ISME J* *10*, 2744–2754.
- Trampani, E., Holden, E.R., Wickham, G.J., Ravi, A., Prischi, F., de Oliveira Martins, L., Savva, G.M., Bavro, V.N., and Webber, M.A. (2019). Antibiotics select for novel pathways of resistance in biofilms. *BioRxiv*.
- Traverse, C.C., Mayo-Smith, L.M., Poltak, S.R., and Cooper, V.S. (2013). Tangled bank of experimentally evolved *Burkholderia* biofilms reflects selection during chronic infections. *Proc Natl Acad Sci U S A* *110*, E250–E259.

- Travisano, M., Mongold, J.A., Bennett, A.F., and Lenski, R.E. (1995). Experimental tests of the roles of adaptation, chance, and history in evolution. *Science* 267, 87–90.
- Tseng, B.S., Zhang, W., Harrison, J.J., Quach, T.P., Song, J.L., Penterman, J., Singh, P.K., Chopp, D.L., Packman, A.I., and Parsek, M.R. (2013). The extracellular matrix protects *Pseudomonas aeruginosa* biofilms by limiting the penetration of tobramycin. *Environ Microbiol* 15, 2865–2878.
- Turner, P.E., and Chao, L. (1998). Sex and the evolution of intrahost competition in RNA virus phi6. *Genetics* 150, 523–532.
- Turner, P.E., and Chao, L. (1999). Prisoner’s dilemma in an RNA virus. *Nature* 398, 441–443.
- Turner, C.B., Marshall, C.W., and Cooper, V.S. (2018). Parallel genetic adaptation across environments differing in mode of growth or resource availability. *Evolution Letters* 2, 355–367.
- Turner, C.B., Buskirk, S.W., Harris, K.B., and Cooper, V.S. (2020). Negative frequency-dependent selection maintains coexisting genotypes during fluctuating selection. *Molecular Ecology* 29, 138–148.
- Vázquez-Espinosa, E., Girón, R.M., Gómez-Punter, R.M., García-Castillo, E., Valenzuela, C., Cisneros, C., Zamora, E., García-Pérez, F.J., and Ancochea, J. (2015). Long-term safety and efficacy of tobramycin in the management of cystic fibrosis. *Ther Clin Risk Manag* 11, 407–415.
- Ventura, M., Canchaya, C., Pridmore, D., Berger, B., and Brüßow, H. (2003). Integration and distribution of *Lactobacillus johnsonii* prophages. *J Bacteriol* 185, 4603–4608.
- Vestergaard, M., Paulander, W., Marvig, R.L., Clasen, J., Jochumsen, N., Molin, S., Jelsbak, L., Ingmer, H., and Folkesson, A. (2016). Antibiotic combination therapy can select for broad-spectrum multidrug resistance in *Pseudomonas aeruginosa*. *International Journal of Antimicrobial Agents* 47, 48–55.
- Vogwill, T., Kojadinovic, M., Furió, V., and MacLean, R.C. (2014). Testing the Role of Genetic Background in Parallel Evolution Using the Comparative Experimental Evolution of Antibiotic Resistance. *Mol Biol Evol* 31, 3314–3323.
- Vogwill, T., Kojadinovic, M., and MacLean, R.C. (2016). Epistasis between antibiotic resistance mutations and genetic background shape the fitness effect of resistance across species of *Pseudomonas*. *Proc. Biol. Sci.* 283.
- Waldor, M.K., and Friedman, D.I. (2005). Phage regulatory circuits and virulence gene expression. *Curr Opin Microbiol* 8, 459–465.
- Walters, M.C., Roe, F., Bugnicourt, A., Franklin, M.J., and Stewart, P.S. (2003). Contributions of Antibiotic Penetration, Oxygen Limitation, and Low Metabolic Activity to Tolerance of *Pseudomonas aeruginosa* Biofilms to Ciprofloxacin and Tobramycin. *Antimicrob Agents Chemother* 47, 317–323.

- Ward, H., Perron, G.G., and Maclean, R.C. (2009). The cost of multiple drug resistance in *Pseudomonas aeruginosa*. *Journal of Evolutionary Biology* 22, 997–1003.
- Wardell, S.J.T., Rehman, A., Martin, L.W., Winstanley, C., Patrick, W.M., and Lamont, I.L. (2019). A Large-Scale Whole-Genome Comparison Shows that Experimental Evolution in Response to Antibiotics Predicts Changes in Naturally Evolved Clinical *Pseudomonas aeruginosa*. *Antimicrobial Agents and Chemotherapy* 63.
- Waters, C.M., and Bassler, B.L. (2005). Quorum sensing: cell-to-cell communication in bacteria. *Annu Rev Cell Dev Biol* 21, 319–346.
- Wattam, A.R., Davis, J.J., Assaf, R., Boisvert, S., Brettin, T., Bun, C., Conrad, N., Dietrich, E.M., Disz, T., Gabbard, J.L., et al. (2017). Improvements to PATRIC, the all-bacterial Bioinformatics Database and Analysis Resource Center. *Nucleic Acids Res.* 45, D535–D542.
- Webb, J.S., Thompson, L.S., James, S., Charlton, T., Tolker-Nielsen, T., Koch, B., Givskov, M., and Kjelleberg, S. (2003). Cell Death in *Pseudomonas aeruginosa* Biofilm Development. *Journal of Bacteriology* 185, 4585–4592.
- Webb, J.S., Lau, M., and Kjelleberg, S. (2004). Bacteriophage and Phenotypic Variation in *Pseudomonas aeruginosa* Biofilm Development. *J Bacteriol* 186, 8066–8073.
- Wei, Q., Le Minh, P.N., Dötsch, A., Hildebrand, F., Panmanee, W., Elfarash, A., Schulz, S., Plaisance, S., Charlier, D., Hassett, D., et al. (2012). Global regulation of gene expression by OxyR in an important human opportunistic pathogen. *Nucleic Acids Research* 40, 4320–4333.
- Werner, E., Roe, F., Bugnicourt, A., Franklin, M.J., Heydorn, A., Molin, S., Pitts, B., and Stewart, P.S. (2004). Stratified Growth in *Pseudomonas aeruginosa* Biofilms. *Applied and Environmental Microbiology* 70, 6188–6196.
- Whitchurch, C.B., Tolker-Nielsen, T., Ragas, P.C., and Mattick, J.S. (2002). Extracellular DNA Required for Bacterial Biofilm Formation. *Science* 295, 1487–1487.
- Whiteley, M., Lee, K.M., and Greenberg, E.P. (1999). Identification of genes controlled by quorum sensing in *Pseudomonas aeruginosa*. *PNAS* 96, 13904–13909.
- Whiteley, M., Banger, M.G., Bumgarner, R.E., Parsek, M.R., Teitzel, G.M., Lory, S., and Greenberg, E.P. (2001). Gene expression in *Pseudomonas aeruginosa* biofilms. *Nature* 413, 860–864.
- Wickham, H., Averick, M., Bryan, J., Chang, W., McGowan, L.D., François, R., Grolemond, G., Hayes, A., Henry, L., Hester, J., et al. (2019). Welcome to the Tidyverse. *Journal of Open Source Software* 4, 1686.
- Wihlmann, L., Wagner, G., Cramer, N., Siebert, B., Gudowius, P., Morales, G., Köhler, T., van Delden, C., Weinel, C., Slickers, P., et al. (2007). Population structure of *Pseudomonas aeruginosa*. *Proc Natl Acad Sci U S A* 104, 8101–8106.

- Wilder, C.N., Allada, G., and Schuster, M. (2009). Instantaneous Within-Patient Diversity of *Pseudomonas aeruginosa* Quorum-Sensing Populations from Cystic Fibrosis Lung Infections. *Infect Immun* 77, 5631–5639.
- Wilder, C.N., Diggle, S.P., and Schuster, M. (2011). Cooperation and cheating in *Pseudomonas aeruginosa* : the roles of the *las*, *rhl* and *pqs* quorum-sensing systems. *The ISME Journal* 5, 1332–1343.
- Winsor, G.L., Griffiths, E.J., Lo, R., Dhillon, B.K., Shay, J.A., and Brinkman, F.S.L. (2016). Enhanced annotations and features for comparing thousands of *Pseudomonas* genomes in the *Pseudomonas* genome database. *Nucleic Acids Res* 44, D646-653.
- Winstanley, C., and Fothergill, J.L. (2009). The role of quorum sensing in chronic cystic fibrosis *Pseudomonas aeruginosa* infections. *FEMS Microbiol Lett* 290, 1–9.
- Winstanley, C., O’Brien, S., and Brockhurst, M.A. (2016). *Pseudomonas aeruginosa* Evolutionary Adaptation and Diversification in Cystic Fibrosis Chronic Lung Infections. *Trends Microbiol.* 24, 327–337.
- Wiser, M.J., Ribeck, N., and Lenski, R.E. (2013). Long-term dynamics of adaptation in asexual populations. *Science* 342, 1364–1367.
- Wistrand-Yuen, E., Knopp, M., Hjort, K., Koskiniemi, S., Berg, O.G., and Andersson, D.I. (2018). Evolution of high-level resistance during low-level antibiotic exposure. *Nature Communications* 9, 1599.
- Wong, A., and Kassen, R. (2011). Parallel evolution and local differentiation in quinolone resistance in *Pseudomonas aeruginosa*. *Microbiology* 157, 937–944.
- Wong, A., Rodrigue, N., and Kassen, R. (2012). Genomics of Adaptation during Experimental Evolution of the Opportunistic Pathogen *Pseudomonas aeruginosa*. *PLOS Genetics* 8, e1002928.
- Wright, E.A., Fothergill, J.L., Paterson, S., Brockhurst, M.A., and Winstanley, C. (2013). Sub-inhibitory concentrations of some antibiotics can drive diversification of *Pseudomonas aeruginosa* populations in artificial sputum medium. *BMC Microbiol* 13, 170.
- Yang, L., Haagensen, J.A.J., Jelsbak, L., Johansen, H.K., Sternberg, C., Høiby, N., and Molin, S. (2008). In Situ Growth Rates and Biofilm Development of *Pseudomonas aeruginosa* Populations in Chronic Lung Infections. *Journal of Bacteriology* 190, 2767–2776.
- Yang, L., Jelsbak, L., Marvig, R.L., Damkiær, S., Workman, C.T., Rau, M.H., Hansen, S.K., Folkesson, A., Johansen, H.K., Ciofu, O., et al. (2011). Evolutionary dynamics of bacteria in a human host environment. *Proc Natl Acad Sci U S A* 108, 7481–7486.
- Yen, P., and Papin, J.A. (2017). History of antibiotic adaptation influences microbial evolutionary dynamics during subsequent treatment. *PLOS Biology* 15, e2001586.

Zegans, M.E., Wagner, J.C., Cady, K.C., Murphy, D.M., Hammond, J.H., and O'Toole, G.A. (2009). Interaction between Bacteriophage DMS3 and Host CRISPR Region Inhibits Group Behaviors of *Pseudomonas aeruginosa*. *J Bacteriol* *191*, 210–219.

Zhao, M., Wang, Q., Wang, Q., Jia, P., and Zhao, Z. (2013). Computational tools for copy number variation (CNV) detection using next-generation sequencing data: features and perspectives. *BMC Bioinformatics* *14*, S1.

Zheng, M., Åslund, F., and Storz, G. (1998). Activation of the OxyR Transcription Factor by Reversible Disulfide Bond Formation. *Science* *279*, 1718–1722.